IMPACT OF TRANSLUCENT WATER-BASED ACRYLIC PAINT ON THE THERMAL PERFORMANCE OF A LOW COST HOUSE

University of Fort Hare
Together in Excellence

A dissertation submitted in fulfilment of the requirements for the degree of

MASTERS OF SCIENCE

By

OVEREN OCHUKO KELVIN

In the Faculty of Science and Agriculture at the University of Fort Hare

Promoters: Professor E L Meyer

Doctor G Makaka

June 2014

DECLARATION

I, the undersigned, hereby declare that the work contained in this dissertation is my own original work and that I have not previously in its entirety or part submitted it at any other University for a degree.

Overen O.K.

Name

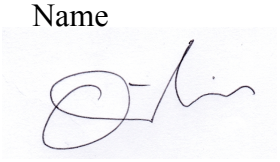

26-09-14

Signed Date

To my late father; Mr. Overen Alfred
"...Always be the best in whatever you are doing..."

ACKNOWLEDGEMENTS

My overwhelming gratitude to:

- My promoters, Prof. E. L. Meyer and Dr. G. Makaka for their unceasing motivation and guidance throughout the project.
- The occupants and owner of the building used in the project, Miss N. Nkcubeko and her children for their tremendous cooperation during the period of monitoring the building.
- The staff and my colleagues at Fort Hare Institute of Technology and the department of Physics for their assistance and encouragement.
- To my beloved girlfriend, Miss N. Z. Manzi and son, Mr. O. M. Overen. Also, to my family back in Nigeria for their profound love, advice and encouragement.
- The sponsors GMRDC and THRIP for their financial support.
- Lastly and most importantly, God almighty for keeping me alive and strengthen me to fulfil this project.

SUMMARY

Insulation materials are selected based on their R-value, which is a measure of the thermal resistance of a material. Therefore, the higher the R-value of a material, the better its thermal insulation performance. There are two major groups of insulation materials: bulk and reflective insulation (or combine bulk and reflective). Bulk insulation is design to resist heat transfer due to conduction and convection. Reflective insulation resists radiant heat flow due to its high reflectivity and low emissivity. Insulation materials are not restricted to these materials only. Other low thermal conductive materials can be used as long as the primary aim of thermal insulation, which is increasing thermal resistance, is achieved. Hence, the aim of the project is to investigate the insulation ability of Translucent Water-based Acrylic Paint (TWAP) on the thermal performance of Low Cost Housing (LCH). To achieve the aim of the study, the inner surfaces of the external walls of LCH was coated with TWAP.

Before the inner surfaces of the external walls were coated, the following techniques were used to characterised the paint; Scanning Electron Microscopy/ Energy Dispersive X-ray spectroscopy (SEM/EDX), Fourier Transform Infra-Red (FTIR) and IR thermography. SEM/EDX was adapted to view the surface morphology and to detect the elemental composition responsible for the thermal resistance of the TWAP. FTIR spectroscopy was used to determine the functional group and organic molecular composition of the paint. The heat resistance of TWAP was analyzed using IR thermography technique. A low cost house located in the Golf Course settlement in Alice, Eastern Cape, South Africa under the Nkonkobe Municipality Eastern Cape was used as a case study in this research. The house is facing geographical N16°E, It comprises a bedroom, toilet and an open plan living room and kitchen. The house has a floor dimension of 7.20 m x 5.70 m, giving

an approximate area of 41 m^2. The roof is made of galvanized corrugated iron sheets with no ceiling or any form of roof insulation. The walls of the buildings are made of the M6 (0.39 m x 0.19 m x 0.14 m) hollow concrete blocks, with no plaster or insulation. The following meteorological parameters were measured: temperature, relative humidity, solar irradiance, wind speed and wind direction. Eleven type-K thermocouples were used to measure the indoor temperature, inner and outer surfaces temperature of the building walls. Two sets of HMP50 humidity sensors were used to measure the indoor and outdoor relative humidity as well as the ambient temperature. The indoor temperature and relative humidity were measured at a height of 1.80 m so as to have good indoor parameter variation patterns that are not influenced by the roof temperature. The outdoor relative humidity sensor together with a 03001 wind sentry anemometer/vane and Li-Cor pyranometer were installed at a height of 0.44 m above the roof of the building. Wind speed and direction were measured by the 03001 wind sentry anemometer/vane, while solar radiation was measured by the Li-Cor pyranometer. The entire set of sensors was connected to a CR1000 data logger from which data are stored and retrieved following a setup program.

The SEM image shows that TWAP is transparent in its dry state. EDX spectrum reveals the presence of Al in the paint, which is present as Al_2O_3. Due to the refractive index (1.73) of Al_2O_3, it is used as IR reflective pigment in reflective paints. Other elements like Si were also identified as SiO_2 that contributes to the thermal resistance of the paint. The functional groups that made up the different molecular bonding of the paint were clearly shown by the FTIR spectrum. These include O–H, CH_2, Si–H, C═C and others. From the IR thermography, average decrement factor of 0.54

and 1.04 were found for the coated and uncoated, respectively. This implies that the coated surface has more heat reduction than the uncoated surface.

The indoor temperature was observed to be influenced by the temperature of the building envelope in both summer and winter seasons. In summer, it was observed that the indoor temperature variation closely follow the external wall temperature. On a typical summer hot day, the average maximum heating rate of the North, West and South walls were 5.93 W, 5,07 W and 2.24 W, respectively. It was found that the indoor temperature was mostly higher than the outdoor temperature. Also, that the indoor temperature was within the comfort zone for only 46% of the time. The indoor relative humidity was within the comfort zone throughout the day. A time lag of 2.5 hours was observed between the time the solar radiation and indoor temperature were at their maximum value.

In the winter season, it was found that the indoor temperature is influenced more by the middle and external walls temperature. On a typical cold winter day, the average cooling rate for the North, West and South walls were found to be 0.89 W, 8.27 W and 0.30 W, respectively. The indoor and outdoor temperatures were seen to be completely below the comfort zone. On the other hand, the indoor relative humidity was found at the upper region of the comfort zone, ranging from 55% to 65%. It was found that the wind speed experienced in winter was 12% higher than the maximum wind speed in the summer season.

After coating, the thermal performance of the building showed significant improvement. The amount of cooling and heating degree hour required by the inner space of the house to maintain

thermal comfort, decreased by an average of 50% and 41%, respectively, in both winter and summer periods. Finally, the house was found to save an average of 37% of cooling and cooling energy demand after coating.

The model developed shows that all components of the building envelope contributed positively to the indoor temperature, in the summer. Indoor, outdoor relative humidity and winter speed contribute negatively to the indoor temperature. In the winter, it was observed that the floor and South walls contributed negatively to the indoor temperature, as well as the wind speed and indoor relative humidity. In both seasons, the measured and predicted indoor temperatures showed a best fit with approximately 99% of the response data set perfectly on the predicted temperature. This proves that the predictors are the parameter that can serve as the basis for indoor temperature

TABLE OF CONTENTS

LIST OF TABLES

LIST OF FIGURES

NOMENCLATURE

T_{in}	Indoor air temperature (°C)
T_{out}	Ambient air temperature (°C)
RH_{-in}	Indoor relative humidity (%)
RH_{-out}	Ambient relative humidity (%)
RH	Relative humidity (%)
IR	Infrared radiation
M	Metabolic rate (Wm^{-2})
w	External work (Wm^{-2})
q	Rate of heat flow (W)
η	Cooling or heating energy demand (kWh)
α	Radiation absorbed
ρ	Radiation reflected
τ	Radiation transmitted
σ	Stefan-Boltzmann constant $\left(5.67\times10^{-8}Wm^{-2}K^{-4}\right)$
ε	Emissivity
W	Total emissive power (W/m^2)
P_a	Partial water pressure (Pa)
t_a	Air temperature (°C)
f_{cl}	Ratio of clothed surface to nude surface area
UA	Overall heat loss coefficient (kWK^{-1})
t_r	Mean radiant temperature
h_c	Convective heat transfer coefficient (Wm^2K)

k	Thermal conductivity ($Wm^{-1}K^{-1}$)
R	Thermal resistance ($m^2K^{-1}W^{-1}$)
A	Surface area (m^2)
l	Thickness (m)
PMV	Predicted Mean Vote)
PPD	Predicted Percentage of Dissatisfied (%)
TWAP	Translucent water-based acrylic paint
RDP	Reconstruction and development programme
LCH	Low cost housing
Al_2O_3	Aluminum oxide
SiO_2	Silicon dioxide
CDH	Cooling degree-hours
HDH	Heating degree-hours

CHAPTER 1

INTRODUCTION

1.1 BACKGROUND

The thermal properties and the heat flow dynamics of a building determine the thermal performance of a building. Basically, heat is transferred by means of radiation, conduction and convection. With respect to thermal energy of a building, heat from the sun gets to the surrounding of a building by means of radiation. The heat is then transferred into the building through the building envelope (walls) by means of conduction. The heat is circulated around the house by convectional currents. At night, a reverse process of conduction and convection takes place. Warm air from one end of the house drift to a cold area, the walls at that area absorbs heat from the warm air and transfers to the building surrounding [Dilavore, 1984: 97]. This process continues until the indoor and outdoor temperature difference is at its minimum. According to the second law of thermal dynamics (entropy), heat will naturally flow from warmer side to cooler. Since it is impossible to completely stop heat transfer, the best solution is to reduce the rate of heat transfer. The rate of heat transfer through a building wall is given by the Fourier's law:

$$q = kA\frac{\Delta T}{\Delta l} \qquad [1.1]$$

Where q is the rate of heat flow, A (m^2) is the surface area of the wall, k is the thermal conductivity of the ($Wm^{-1}K^{-1}$). In a building, Δl (m) is the thickness of the wall and ΔT (°C) is the difference

between the inner and outer surface temperature of the wall. From Equation [1.1], the rate of heat transfer will increase as the difference between the indoor and outdoor surface temperature increases. It can be reduced by increasing the thickness of the wall. To increase the thickness of the walls, a low thermal conductive material is required. Such material is known as thermal insulator. Insulation materials are selected based on their R-value; which is a measure of the thermal resistance of a material. Therefore, the higher the R-value of a material the better its thermal insulation performance.

There are two major groups of insulation materials; bulk and reflective insulation (or combine bulk and reflective). Bulk insulation is design to resist heat transfer due to conduction and convection. Examples of bulk insulation are cellulose, fiber glass, mineral wool, extruded polystyrene foam (XPS), expanded polystyrene foam (EPS) or bead board and polyurethane foam. Reflective insulation on the other hand, resists radiant heat flow due to its high reflectivity and low emissivity. A typical example of reflective insulation is aluminum foil [Downton and Reardon, 2010: 102]. Insulation materials are not restricted to these materials only. Other low thermal conductive materials are used as long as the primary aim of thermal insulation which is, increasing thermal resistance is achieved. Hence, in this study, a thermal reflective paint known as Translucent Water-based Acrylic Paint (TWAP) was used as the insulation material to improve the thermal performance of low cost housing (LCH)

LCH previously known as RDP housing were first introduced in South Africa in 1994 by the democratically elected government. The government introduced a white paper on Reconstruction and Development Program (RDP) in November 1994. One of the agenda of the RDP is to provide

decent housing to the homeless and low income earning people of South Africa. Studies [Knight, 2004, klunne, 2002, *et al*] have shown that, the good intentions of the government to produce decent houses for the homeless and low income earning people of South Africa have been overshadowed by the poor quality of the houses. Most of the LCH were constructed without thermal efficiency considerations. The occupants of these houses find their home freezing in winter and overheating in summer, spending their limited resources on electrical energy to achieve thermal comfort [Holm *et al*, 2008].

1.2 PROBLEM STATEMENT

Considering the total surface of the inner space enclosed by the building envelope from the outside of the house, the total surface wall area is 31%, the total surface area of the roof and floor is 64%, while the total surface area of the doors and windows is only 5%, and because of this, the walls influences the thermal performance of the building. In most cases, the walls of LCH are not plastered nor insulated on either inner or outer surfaces, resulting in high rate of heat transfer through the building walls. Due to the poor insulation of the LCH, the indoor temperature closely follows the variation of the outdoor temperature. Thus the occupants of LCH consume excess energy in space heating or cooling to maintain the indoor environment within the thermal comfort level. Majority of LCH occupants cannot afford electric heating or cooling appliance. Hence, occupants resort to using coal or paraffin for space heating, thus leading to the increase of CO_2 emissions which are hazardous to human health [Klunne, 2002]. Statistics from the International Energy Agency (IEA) show that, South Africa moved from the 18^{th} largest national emitter of CO_2 in 2007 to the 15^{th} position in 2009 [IEA, 2011: 56].

1.3 AIM AND OBJECTIVES

The aim of this research project is to investigate the insulation ability of TWAP on the thermal performance of a low cost house. Insulating the walls of the building reduce heat transfer between the habitable space and the surrounding of a building through the walls, thus reducing the cooling and heating energy demands required to achieve indoor thermal comfort. To achieve the aim of the research the following objectives will be considered:

- To characterize the paint (TWAP) using the following techniques:
  - Scanning Electron Microscopy (SEM) and Energy Dispersive X-ray spectroscopy (EDX).
  - Fourier Transform Infra-red spectroscopy (FTIR).
  - Thermography analysis.
- To monitor the thermal performance of the house before coating.
- To monitor the thermal influence of TWAP on the thermal performance of the house after coating.
- To develop prediction models for the indoor temperature of a LCH with the inner surfaces of walls coated with TWAP.

1.4 RESEARCH QUESTION

i. What are the insulation materials that are commonly used in building insulation?
ii. What are the thermal properties that made the TWAP an insulation material?
iii. What is the thermal performance of the house without thermal insulation?

iv. What is the impact of TWAP on the thermal performance of the building after coating?

1.5 RESEARCH METHODOLOGY

The characterization of TWAP was aimed to determine the constituents of the paint that attributes its insulation properties. Based on that, SEM/EDX technique was used to analyze the surface morphology and elemental composition of the paint. FTIR spectroscopy was also used to determine the functional groups and organic molecular composition of the paint. The heat resistance of TWAP was examined using IR thermography technique. Selection of the LCH used in this study was done. A house location in Golf Course, Alice in the Eastern Cape of South Africa was used as a case study. The house was selected based on its orientation, N16°E; which is the recommended orientation for a passive solar design [Klunne, 2002]. Meteorological parameters such as; temperature, relative humidity, wind speed and direction and solar radiation were monitored to establish the thermal performance baseline of the building. The weather parameters were monitored using the following sensors: thermocouples, temperature relative humidity probes, anemometer/vane and pyranometer. All sensors were connected to a data logger and multiplexer, from which data was recorded and retrieved using PC400 in a computer system. The monitoring stretched from early summer season to mid-winter. At mid-winter the inner surfaces of the external walls of the house was coated with TWAP. Thereafter, the second stage of meteorological monitoring commenced. The final results were based on the comparison of the thermal performance of the house before and after coating.

1.6 RATIONALE OF THE STUDY

Heating and cooling loads of a house are mostly due to heat through the building envelope especially the roof and to a lesser extent to the walls. From energy viewpoint, the most effective way of reducing heating and cooling loads is by applying thermal insulation to the building envelope [Ozel, 2011]. Introducing energy efficient initiative will in future perfect the LCH already built and thus create a healthy home as well as minimize energy consumption for space heating which will eventually reduce the emission of greenhouse gases. This initiative is known as retrofitting. The introduction of the concept of retrofitting on LCH can be an immediate and long-term solution to the problem of housing and energy in South Africa [Klunne, 2003]. This retrofit can be through retrofitting energy lighting in houses, through the use of photovoltaic system as the primary or secondary electricity source and improving thermal performance of the houses through thermal insulation.

1.7 DELINEATION AND LIMITATION

According to Thermal Insulation Association of South Africa (TIASA) approximately 24% of heat is lost through walls in an un-insulated home. Apart from the roof, heat is transferred more through the walls than any other components of the building envelop [TIASA, 2010]. Also, due to the materials available during the course of the research; this study specifically focused on reducing the rate of heat transfer through the building walls to improve the indoor thermal comfort.

1.8 DEFINITION OF TERMS

The following terms should be used and understood as defined in this section unless the context suggests otherwise:

After coating: the period after the inner surfaces of the building external walls were coated with translucent water-based acrylic paint.

Before coating: the period before the inner surfaces of the building external walls were coated with translucent water-based acrylic paint.

Building envelope refers to those components of the building enclosing the habitable space from the building surrounding. These include walls, floor, roof, external doors and windows.

External walls: refers to those walls that enclose the inner space of the building from the weather factors.

Heat transfer is the flow of heat as a result of change in temperature.

Low Cost House (LCH) is one of the agendas of Reconstruction and Development Program (RDP) in 1994. It is aimed to provide subsidized houses to the homeless and low income earning people of South Africa.

Retrofitting in this case, it is the process of making an already existing building more thermal efficient.

Thermal energy is the energy associated with the temperature of an object.

Thermal performance is used to describe the thermal influence in the building envelope on the indoor temperature.

Thermal comfort is achieved when the indoor air temperature the building is between 20°C and 28°C while relative humidity is 30% and 60%.

Thermal conductance is the rate of heat flow between two surfaces of unit area separated by unit distance when the temperature difference between them is minimal.

Thermal insulation these are materials or combination of material used to resist the flow of heat due to their thermal properties (high R-value).

Thermal resistance (R-value) is the reciprocal of thermal conductance; it's a measure of the heat flow resistivity of a material.

1.9 ENVISAGED OUTCOMES

The following outcomes are expected:

i. Chemical composition and IR imaging of the insulation material, highlighting its thermal insulation properties.
ii. The thermal performance baseline of a LCH in winter and summer season. It includes the thermal influence of the external walls on the indoor temperature.
iii. The thermal influence of translucent water-based acrylic paint on the thermal performance of the building after coating.
iv. Multiple linear regression models that predict the baseline indoor temperature of a LCH with the inner surfaces of the walls coated with TWAP.

1.10 LAYOUT OF THESIS

This thesis is divided into seven chapters. Chapter 2 presents a theoretical review of indoor thermal comfort and heat transfer in building. The various modes of heat transfer and effect in a building are discussed. Chapter 3 presents the experimental setup and procedure used in the characterization

of translucent water-based acrylic paint (TWAP). Also, the methods and procedures used in measuring the surface temperatures of the various components of the building envelope and the weather factor are discussed. The details of the house and its location used as a case study are also present. It also includes the various procedures used in the data analysis.

Chapter 4 details the characterization of the TWAP. It also includes an experimental heat resistance analysis of TWAP, using IR thermography techniques. The thermal baseline of the building is presented in chapter 5. This includes the thermal influence of the building envelope and weather factors on the indoor temperature.

In chapter 6, the thermal influence of TWAP on the thermal performance of the building using cooling and heating degree-hours is discussed. Summary, conclusion and recommendations are presented in chapter 7.

CHAPTER 2

THERMAL COMFORT AND HEAT TRANSFER IN BUILDINGS

2.1 INTRODUCTION

The human body can be considered as a thermodynamic machine, which uses food and oxygen as fuel. As it is known, in thermal machines, some of the energy is converted into mechanical work while some are transformed into other forms of energy such as heat. The human body converts energy into heat by a chemical process known as metabolism [Kaynakli and Kilic, 2004]. In order for the human body to achieve optimum functionality, it has to maintain constant internal temperature. Thus a regular exchange of heat between the body and its environment is required [Butera, 1998]. The branch of building physics that deals with human thermal sensation and level of satisfaction of its environment is known as thermal comfort. For research purpose, the factors affecting the indoor thermal comfort of a building can be examined in two main groups: personal and environmental. Personal factors are clothing and personal activities/conditions. Environmental factors include air temperature, air velocity, relative humidity and thermal radiation [Kaynakli and Kilic, 2004]. Building heat transfer plays an important role in the indoor thermal comfort as highlighted by the environmental factors of thermal comfort. Whenever there is a temperature difference between the indoor space of a building and outdoor ambient, heat transfer takes place. This always occurs through the building envelope (walls, roof, floor, etc.) or opening around external doors and windows (infiltration or exfiltration) [ASHRAE, 1997]. Basically, heat is transferred by means of radiation, conduction and convection. On a sunny day, the sun heats up the external walls of a building by means of radiation. The heat on the external walls of the building is transferred to the inner surface by conduction. The amount and time taken for the heat to be

transferred through the walls of the building depends on the solar irradiance at that particular time and the thermophysical properties of the wall. Heat on the wall inner surface is distributed in the indoor space of the building by mean of convection. At night, a reverse process of conduction and convection takes place. Warm air from one end of the house drift to cold areas, the walls around that area transfers the energy (heat) of the warm air back to the surrounding [Dilavore, 1984: 97].

This chapter considers theoretical review of thermal comfort and heat transfer in a building. In order to improve the indoor thermal comfort level of a building, a minimum and controlled heat transfer between the indoor space and its surrounding is required. It also includes some of the basic concept that is involved in the heat transfer in buildings.

2.2 THERMAL COMFORT

The definition and control of indoor thermal comfort in buildings are hard to be established, due to the variations in the parameter involved [Freire, Oliveira and Mendes, 2007]. Commonly, thermal comfort is defined as the condition of mind in which satisfaction is expressed with the thermal environment [AHRAE, 2004]. Dissatisfaction may be caused by the body warm or cool as a whole. Thermal dissatisfaction may also be caused by an unwanted heating or cooling of one particular part of the body [Butera, 1998]. Extensive investigations and experiments involving numerous subjects have resulted in methods for predicting the degree of thermal discomfort of people exposed to a still thermal environment. The most well-known and widely accepted methods are Fanger's Predicted Mean Vote (PMV), Predicted Percentage of Dissatisfied (PPD) and adaptation model [Djongyang, Tchinda and Njomo, 2010]. The PMV – PPD uses data from climate chamber studies to support its theory while the adaptive model uses data from field studies

of people in a building [Alison *et al*, 2010]. The PMV – PPD model of thermal comfort has been a path breaking contribution to the theory of thermal comfort and to the evaluation of indoor thermal environments in buildings. It is widely used and accepted for design and field assessment of thermal comfort [Lin and Deng, 2008].

2.2.1 The predicted mean vote

The human perception of thermal comfort analysis conducted by Fanger in 1982, shows that the sensation of thermal comfort was most significantly determined by narrow ranges of skin temperature and sweat evaporation rate, depending on activity level. More active people were comfortable at low skin temperatures and higher evaporation rates. By combining this information with the ASHRAE thermal sensation scale, shown in the table below, he (Fanger) developed a comfort index called PMV [Brandemuehl, 2005].

Table 2.1: ASHRAE thermal sensation scale [Adopted from Brandemuehl, 2005]

+	3	Hot
+	2	Warm
+	1	Slightly warm
	0	Neutral
–	1	Slightly cool
–	2	Cool
–	3	Cold

PMV is an index that predicts the mean value of the votes of a large group of persons on a seven-point thermal sensation scale [Lin and Deng, 2008], indicated in Table 2.1. The PMV index can be determined when the activity (metabolic rate) and the clothing (thermal resistance) are estimated,

and the following environmental parameters are measured: air temperature, mean radiant temperature, relative air velocity and partial water vapour pressure. The PMV is given by the equation [Markov, 2006];

$$PMV = (0.303e^{-0.036M} + 0.028)\{(M - W) - 3.05\times10^{-3}[5733 - 6.99(M - W) - 0.42[(M - w) - 5815] \\ -1.7\times10^{-5}(5867 - P_a) - 0.0014M(34 - t_a) - 3.96\times10^{-8} f_{cl}[(t_r + 273)^4] - f_{cl}h_c(t_{cl} - t_a)\} \quad [2.1]$$

Where M = Metabolic rate (W/m^2)

w = External work (W/m^2)

P_a = Partial water pressure (Pa)

t_a = Air temperature

f_{cl} = Ratio of clothed surface to nude surface area

t_r = Mean radiant temperature

h_c = Convective heat transfer coefficient (Wm^2K)

In the PMV index the physiological response of the thermoregulatory system has been related statistically to thermal sensation votes collected from approximately 4000 subjects. The PMV index is derived for steady state conditions, but can be applied with good approximation during minor fluctuations of one or more of the variables, provided that time-weighted averages of the variables are applied [Butera, 1998].

2.2.2 Predicted percentage dissatisfied

PPD is a predicted value calculated from PMV. It predicts the percentage of people dissatisfied with the thermal conditions of their surroundings [ISO 7730, 2005]. People who felt more than slightly warm or slightly cold (i.e. the percentage of the people who inclined to complain about the environment). Using the thermal sensation scale in table 2.1, Fanger postulated: people who responded to ±2 and ±3 are declared uncomfortable. Those who responded to ±1 and 0 are declared comfortable. The relationship between PPD and PMV is given by equation 2.2 and figure 2.1 [Fanger, 1972];

$$PPD = 100 - 95e^{-\left(0.03353\,PMV^4 + 0.2179\,PMV^2\right)} \qquad [2.2]$$

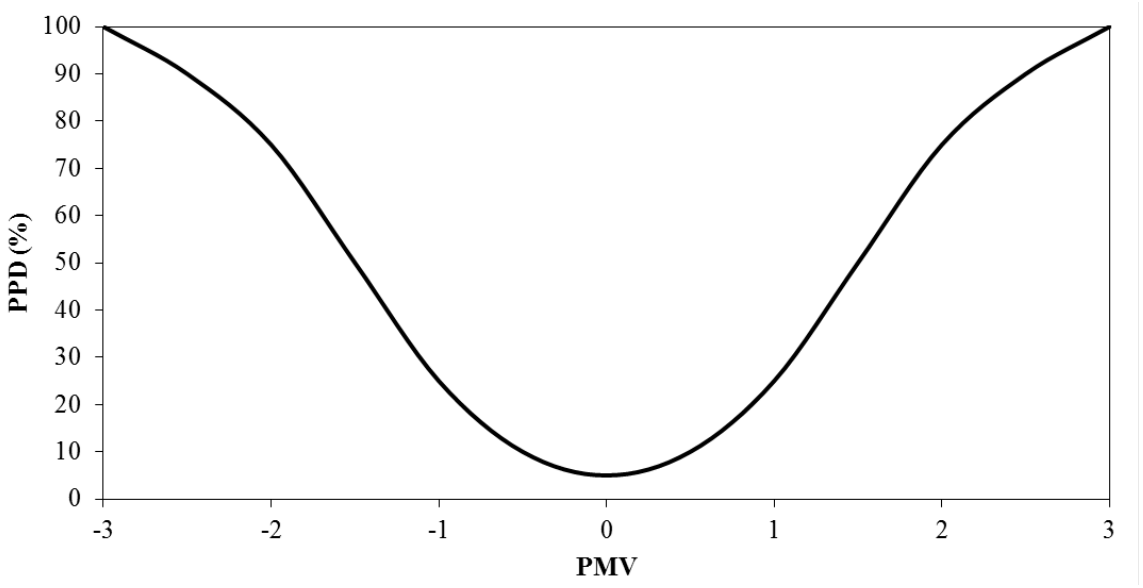

Figure 2.1: Relationship between PMV and PPD [Adopted from Fanger, 1972]

Owing to individual differences, it is impossible to specify a thermal environment that will satisfy everybody. This is highlighted in Fig. 2.1, where it is shown that even if the PMV is zero, 5% of people are dissatisfied. It is possible, however, to specify environment known to be acceptable by a certain percentage of the occupants. The ISO standard 7730, for example, recommends that the PPD should be lower than 10%, i.e. PMV within the range $-0.5 \div \pm 0.5$ [ISO 7730, 1984].

2.2.3 Adaptation model

Adaptive model derives from field studies, having the purpose of analysing the real acceptability of thermal environment, which strongly depends on the context, the behaviour of occupants and their expectations [De Dear, 2004]. The adaptive principle is explained as: if a change occurs such as to produce discomfort, people react in ways which tend to restore their comfort [Nicol and Humphreys, 2002]. This model is also based on the notion that occupants expecting 'thermal constancy' in their indoor environment will tend to be more sensitive to even slight deviation from the optimum conditions [De Dear, 2007]. In a real environment, people utilize various adaptive approaches freely according to their own thermal preference to achieve thermal comfort. People adapt by changing the physical parameters (environment), their physiology or activity level, their clothing, their expectations and the way they use rating scales [Halawaa and Hoof, 2012]. There are three main types of adaptations: physiological, psychological and behavioural [Yao *et al*, 2009].

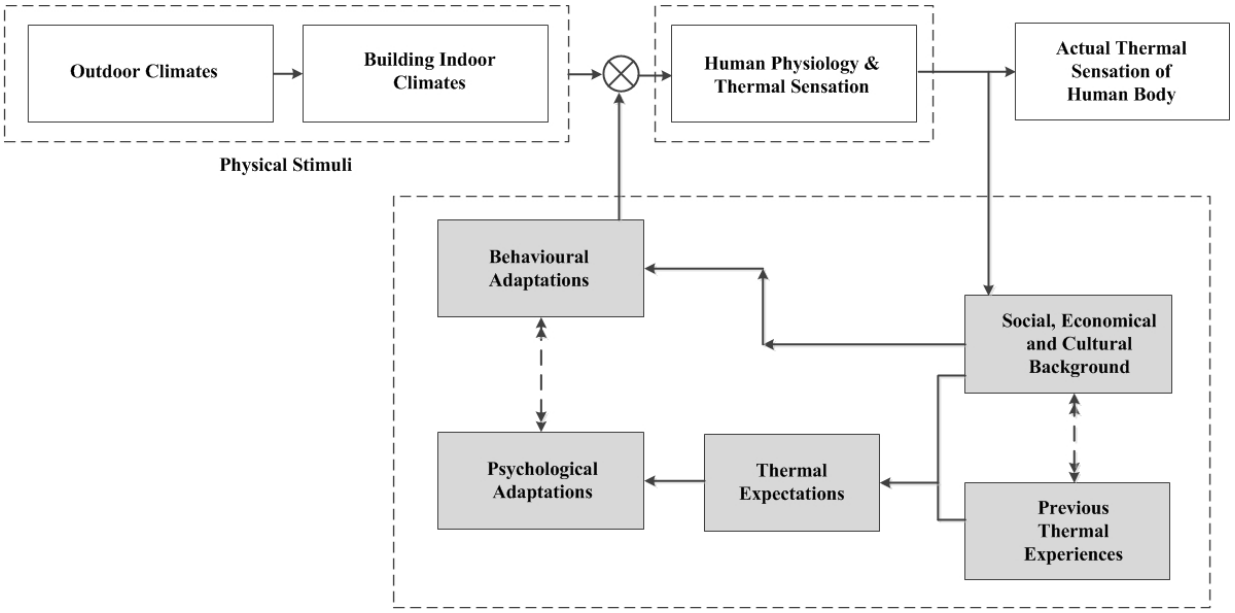

Figure 2.2: The thermal comfort adaptive model mechanism [Adopted from Yao *et al*, 2009]

The adaptive comfort approach may take credit for widening the range of acceptable comfort temperature, which makes it possible to claim more energy savings in buildings designed using this approach than those design using PMV/PPD approach. However, in the long run, this may prove unsustainable. Early results from adopting the adaptive approach to the design of a number of buildings have found that green buildings are 'much colder' in winter and 'much warmer' in summer [Leaman, Thomas and Vandenberg, 2007]. This is not to be expected if one recalls adaptive approach's claim that the building occupants actually can tolerate much wider temperature range than that permitted by Fanger's PMV/PPD formulation. 'Much colder' and 'much warmer' sensations fall just on the boundary between 'acceptable' and 'unacceptable' before they cross to 'too cold' and 'too hot' sensations [Halawaa and Hoof, 2012].

2.3 HEAT TRANSFER IN BUILDINGS

2.3.1 Conduction

This is the transfer of heat energy from one place to another through a substance without the movement of the substance as whole. In a building, heat is transferred by conduction through the walls, roof, floor and even through the frame of the windows. The rate of heat flow through a material at steady state is given by the Fourier's law:

$$q = -kA\frac{\Delta T}{\Delta l} \qquad [2.3]$$

Where q is the rate of heat flow, A is the area normal to the direction of the heat flow, k is the thermal conductivity coefficient. The thermal conductivity coefficient is defined as the rate of heat flow between two surfaces of unit area separated by unit distance when the temperature difference between them is minimal ($Wm^{-1}K^{-1}$). In a building, Δl is the thickness of the building envelope (walls) and ΔT is the difference between the internal and external temperature. When the outdoor temperature of the building is greater than the indoor temperature, $\Delta T = T_{out} - T_{in}$; which usually occurs on a sunny day. At this period heat is being generated in the building. A reverse process takes place on a cold day, $\Delta T = T_{in} - T_{out}$; where the outdoor temperature is greater than the indoor temperature, resulting in the extraction of heat from the building.

When dealing with building heat transfer, building walls is often designed with several materials. This is a thermal insulation measures, designed to increase the thermal resistance of the wall.

Thermal resistance is also known as the R-value, it indicates the resistance that a material offers to heat flow. Thermal resistance is the reciprocal of thermal conductance from the equation [2.3], q can be redefined:

$$q = \frac{\Delta T}{R} \qquad [2.4]$$

Where $R = \frac{l}{kA}$, is thermal resistance. As the thickness of the material increases, the thermal conductivity decreases and the thermal resistance increases. The unit of thermal resistance is $W^{-1}m^2K^{-1}$. When a wall is composed of several different layouts of materials, the resultant resistance (R) is the sum of the resistance materials. Figure 2.3 shows a composite wall with $T_{out} > T_{in}$, where (a) and (c) are insulation materials and (b) represents a building wall.

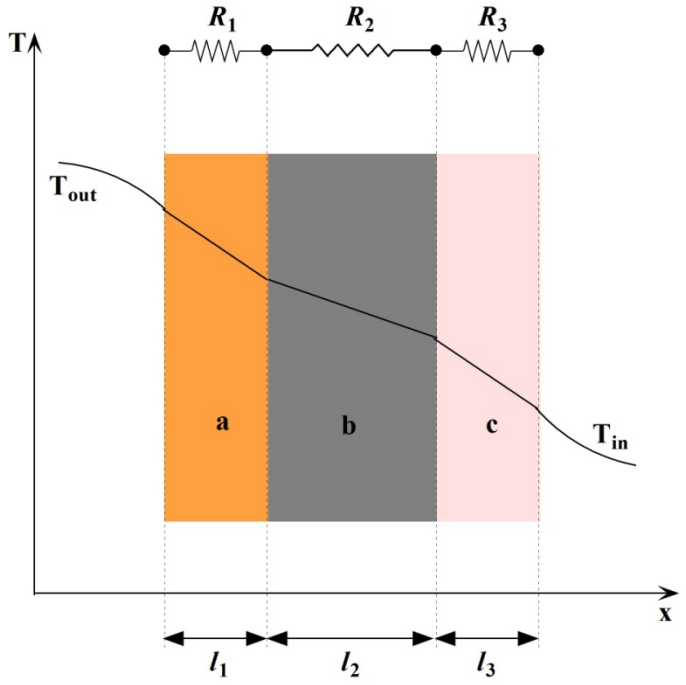

Figure 2.3: Heat transfer through an insulated wall (composite wall)

The resultant resistance is given by:

$$R = R_1 + R_2 + R_3 = \frac{l_1}{k_1 A_1} + \frac{l_2}{k_2 A_2} + \frac{l_3}{k_3 A_3} \quad [2.5]$$

The overall heat transfer rate is expressed by

$$q = \frac{T_{out} - T_{in}}{R} = \frac{T_{out} - T_{in}}{R_1 + R_2 + R_3} \quad [2.6]$$

The analysis above is applicable to all components of the building envelope such as windows, doors, floor among others.

2.3.2 Convection

Convection involves the transfer of heat between a surface at a given temperature and a fluid at bulk temperature. Natural convection takes place when motion and mixing of the fluid macroscopic particles is caused by density variations which result from temperature differences in the fluid. On the other hand forced convection occurs when fluid motion and mixing is caused by an external force such as a pump. The rate of heat transfer by convection is obtained from Newton's law of cooling as [Cengel and Boles, 1994]:

$$q = h_c A(T_s - T_f) \quad [2.7]$$

Where h_c is the convective heat transfer coefficient, T_s is the surface temperature and T_f is the fluid temperature. The transfer of heat from warm air around the building wall to inside or outside of a building occurs by the combination of conduction and convection. Figure 2.4 shows the configuration.

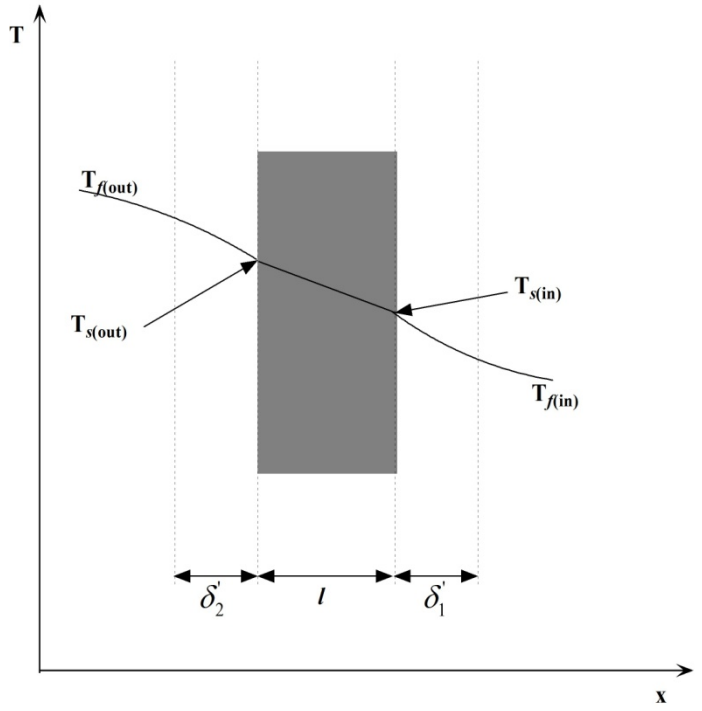

Figure 2.4: Building wall with convectional heat transfer

Where δ_1 is fluid 1 (indoor air) and δ_2 is fluid 2 (outdoor air). The heat transfer in fluid (1) is given by,

$$\frac{q}{A} = h_{in}(T_{s(in)} - T_{f(in)}) \qquad [2.8]$$

Which is the heat transfer per unit area to the fluid. The heat transfer in fluid (2) is similarly given by

$$\frac{q}{A} = h_{out}(T_{f(out)} - T_{s(out)}) \qquad [2.9]$$

Across the wall, heat transfer per unit area is expressed as:

$$\frac{q}{A} = \frac{k}{l}(T_{s(out)} - T_{s(in)}) \qquad [2.10]$$

The quantity $\frac{q}{A}$ is the same in all of these expressions. Putting them all together to write the overall temperature drop yields a relation between heat transfer and overall temperature drop, $T_{f(out)} - T_{f(in)}$:

$$T_{f(out)} - T_{f(in)} = (T_{f(out)} - T_{s(out)}) + (T_{s(out)} - T_{s(in)}) + (T_{s(in)} - T_{f(in)}) = \frac{q}{A}\left[\frac{1}{h_{(in)}} + \frac{l}{k} + \frac{1}{h_{(out)}}\right] \qquad [2.11]$$

Thermal resistance R, can be redefined, as in equation [2.6]

$$q = \frac{T_{f(out)} - T_{s(in)}}{R}$$

Where R is given by

$$R = \frac{1}{h_{in}A} + \frac{l}{Ak} + \frac{1}{h_{out}A} \qquad [2.12]$$

Equation [2.12] is the thermal resistance for solid wall with convection heat transfer on each side.

2.3.3 Radiation

This is the transfer of heat by electromagnetic radiation that arises due to the temperature of an object. When thermal radiation reaches a surface, it may be absorbed, reflected or transmitted. Figure 2.5 shows these processes graphically. The behavior of a surface with radiation incident upon it can be described by the following quantities:

α = absorptance fraction of incident radiation absorbed.

ρ = reflection fraction of incident radiation reflected.

τ = transmittance fraction of incident radiation transmitted.

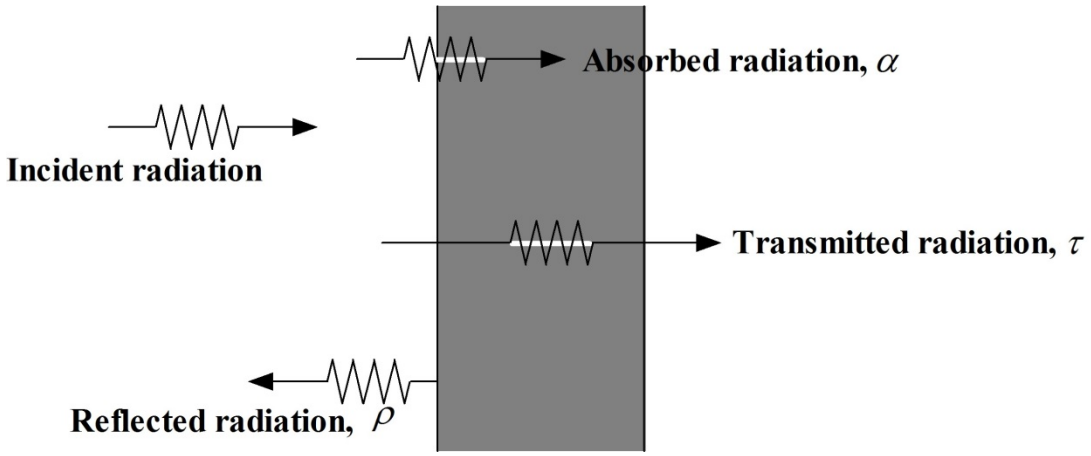

Figure 2.5: Radiation surface properties

From energy considerations the three coefficients must be equal to unity [Anapolkaya and Gandin, 1990]:

$$\alpha + \rho + \tau = 1 \qquad [2.13]$$

A body that emits the maximum amount of heat energy at its absolute temperature is called a blackbody radiator. Radiant heat transfer from a black body to its surroundings is given by the Stefan-Boltzmann law as:

$$q = \sigma T^4 \qquad [2.14]$$

Where σ is Stefan-Boltzmann constant (5.67×10^{-8} W/m^2 K^{-4}) and T is absolute temperature in kelvin. The net radiation from a wall with emissivity ε and at temperature T_a to another body at temperature T_b is given as [Duffie and Beckman, 2006]:

$$q = \varepsilon A \sigma (T_a^4 - T_b^4) \qquad [2.15]$$

Equation [2.15] can also be used to deduce the net radiation from a building wall to the outside or the sky.

2.4 CONCEPT OF HEAT TRANSFER IN BUILDINGS

2.4.1 Decrement factor and time lag

Decrement factor (f) is the ratio of heat transferred out of a material to the heat transferred into the material. Time lag (τ) on the other hand, is the time taken (in hour) for heat energy to be conducted through a material. Basically, time lag and decrement factor are used to quantify the thermal storage capacity of a building wall. The higher the storage capacity of the wall, the longer it takes the heat on the outer surface to propagate to the inner surface. Also the smaller the amount of heat transferred to the inner surface. Thus walls with high storage capacity will have a high time lag and small decrement factor. Figure 2.6 shows the schematic of time lag and decrement factor of a wall [Asan, 2005].

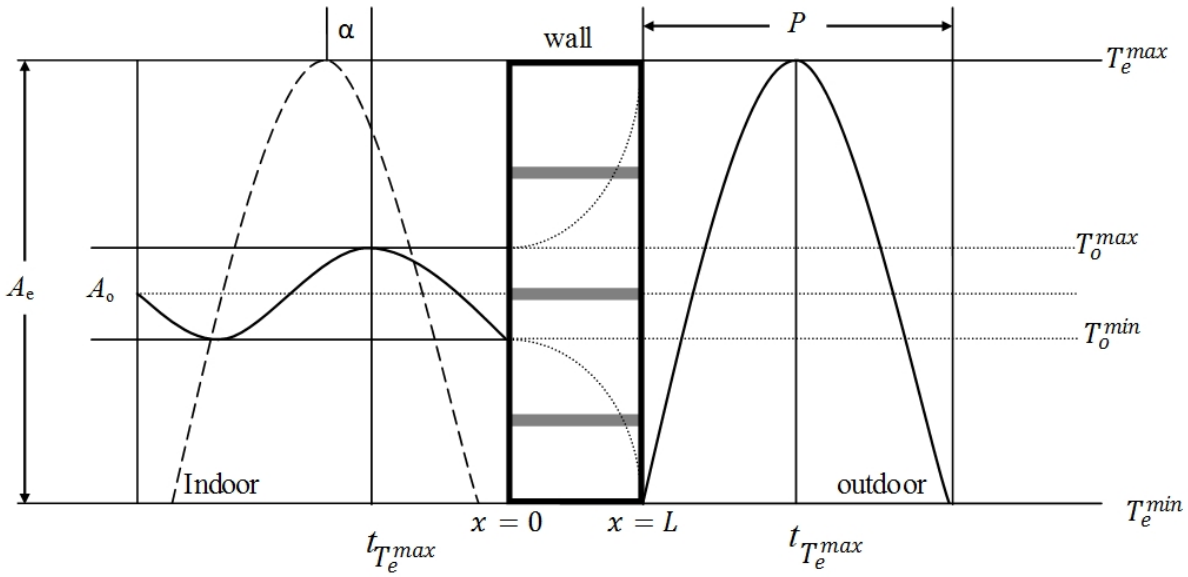

Figure 2.6: Schematic of time lag and decrement factor of a wall [Adopted from Asan, 2005]

Decrement factor (f) is given by:

$$f = \frac{\mathrm{A_o}}{\mathrm{A_e}} = \frac{T_{\mathrm{o}}^{\max} - T_{\mathrm{o}}^{\min}}{T_{\mathrm{e}}^{\max} - T_{\mathrm{e}}^{\min}} \quad [2.16]$$

Where $\mathrm{A_o}$ and $\mathrm{A_e}$ are the amplitudes of the heat wave in the inner and outer surfaces of the wall respectively. $T_{\mathrm{o}}^{\max}$ and $T_{\mathrm{o}}^{\min}$ are maximum and minimum inner surface temperature of the wall. $T_e^{\max}$ and $T_e^{\min}$ represents the maximum and minimum outer surface temperature of the wall. Decrement factor lies between 0 and 1, with 1 representing no reduction or attenuation of imposed heat gain transmitted to or from the inside of the building. The decrement factor of a wall depends on the thermal conductivity, specific heat capacity and density of a wall.

2.4.2 Rate of temperature change

The rate of temperature change is the sum of the temperature difference between the outer and inner surface of a wall over a period of time. It is given as

$$\frac{\sum \Delta T}{dt} \quad [2.17]$$

Where ΔT is the temperature difference between the outer and inner surface. A positive ($+\Delta T$) implies rate of temperature increase while a ($-\Delta T$) implies rate of temperature decrease. The positive and negative values of ΔT are summed separately to obtain $\sum \Delta T$. In a rare situation, the

ΔT is equal to zero. This suggests that the outer and inner temperatures are equal. Hence, the higher the rates of temperature change, the higher the temperature difference between the outer and the inner surface.

2.4.3 Cooling and heating degree day

Degree-days also known as degree-hour are essentially the summation of temperature differences over time, and hence they capture both extremity and duration of outdoor temperatures. The temperature difference is between a reference temperature and the outdoor temperature. The reference temperature is known as the base temperature $\left(T_b\right)$, for buildings, is a balance point temperature, i.e. the outdoor temperature at which the heating (or cooling) systems do not need to run in order to maintain comfort conditions. When the outdoor temperature is below the base temperature, the heating system needs to provide heat. Since heat loss from a building is directly proportional to the indoor-to-outdoor, temperature difference follows that the energy consumption of a heated building over a period of time that should be related to the sum of these temperature differences over this period. The usual time period is 24 hours, hence the term degree-days, but it is possible to work with degree-hours. Degree-days are in fact mean degree-hours, or degree-hours divided by 24 [Day, 2006: 1–6]. Monthly degree-hours are simply the sum of daily degree-hours over the number of days in the month. Likewise, yearly degree-hours are sum of monthly degree-hours over the 12 months of the year. Therefore, the number of cooling degree hours (CDH) and heating degree hours (HDH) in a day are given as [Assawamartbunlue, 2013]:

$$CDH = \sum_{i=1}^{N} (T_i - T_b)^+ \qquad [2.18]$$

$$HDH = \sum_{i=1}^{N} (T_b - T_i)^+ \qquad [2.19]$$

Where N is the number of hours in the day and the"+" superscript indicates that only positive values of the bracketed quantity are taken into account in the sum. T_b is the base temperature to which the degree-days are calculated, and T_i is the average hourly temperature. The base temperatures vary from country to country. For example, in the UK heating degree days are based on an outside dry bulb temperature of 15.5°C, whereas Australia uses 18°C and United States uses 18.3°C. Either way, the result is a value which represents the amount of time that the temperature was at least one degree lower or higher than the base [Ecotect, WIKI, 2012].

There are number of ways of interpreting the degree –days concept with respect to simplify the heating analysis, it include energy demand. As discussed by Hitchin and Hyde, 1979, these are all predicated on the notion that heating energy demand is directly proportional to the indoor-to-outdoor temperature difference, such that:

$$\eta = UA \times DD \times 24 \qquad [2.20]$$

Where η is heating or cooling energy demand (kWh), DD is the total degree days (°C day) in a year and the "24" is included to convert from days to hours. UA is the overall heat loss coefficient (kWK^{-1}) of the building. The overall heat loss coefficient (UA) is the sum of the U-value of all components of the building envelope that experience ΔT from one side to the other multiplied by

their surface area A. Table 2.2 shows the thermal properties of the major components of building envelope [Ecotect, 2012, Giancoli, 1998 and Al-Jabri, 2004].

Table 2.2: Properties of building material

Material (Descriptions)	**Density** ρ (kg/m^3)	**Specific heat capacity** c (J/kg/K)	**Thermal conductivity** k (W/m/K)	**Thickness** *l* (mm)
Concrete block (6inches, hollow)	1400	1000	0.51	140
Floor (medium concrete)	3800	656.9	0.753	110
Door (pine wood)	650	1200	0.14	42
Roof (corrugated iron sheet)	7000	390	43	0.3
Window (single pane glass)	2600	840	0.94	6

2.5 SUMMARY

Thermal comfort defined by Fanger, sets boundaries at which a person will feel comfortable or uncomfortable by using mathematical model. Adoptive approach proposes that a person reacts to the environmental condition, in order to achieve thermal comfort. In all approach, the human body requires a constant internal temperature to achieve thermal comfort. The human body loses or gains temperature due to the surrounding temperature fluctuation, resulting in thermal discomfort. The indoor temperature fluctuation is as a result of uncontrolled heat transfer between the inner and outer space of the building. This heat transfer could be in the form of conduction, convection and radiation. To reduce the heat transfer between the inner space of the building and its surrounding, high thermal resistance materials is required for the component of the building envelope.

CHAPTER 3

METHODOLOGY

3.1 INTRODUCTION

Two major analyses were used to investigate the thermal effect of translucent water based acrylic paint (TWAP) on the thermal performance of low cost house; chemical analysis of the paint and thermal performance of the building. Chemical analysis involves inorganic and organic analyses. Organic analysis deals with the molecular properties of a material that has to do with the various carbon bonding. Inorganic analysis reveals the elemental constituent of a material that is responsible for the physical properties of the material. Thermal performance of a building describes the response of the building envelope to the weather condition. The response of the building envelope influences the indoor temperature.

This chapter focuses on the various techniques adopted in analyzing the paint (TWAP). It also involves an overview of the house and the location used as a case study. Sensors and methods used in the data acquisition were discussed in detail. This chapter also highlights the various steps and precautions taken while applying the insulation material to the inner surface of the building walls. It also presents methods and steps used to analyse the thermal performance baseline and thermal performance of the house after coating. At the end, the design and development of indoor temperature models was discussed.

3.2 CHARACTERISATION OF TRANSLUCENT WATER-BASED ACRYLIC PAINT

Before the Translucent water–base acrylic latex paint (TWAP) was applied to the building, the following analyses were performed; Scanning Electron Microscopy/ Energy Dispersive X-ray spectroscopy (SEM/EDX), Fourier Transform Infra-Red (FTIR) and IR thermography. Studies by [Hanlan, 1975 and Mantler *et al*, 2000] have shown that SEM/EDX provides information about surface morphology and the elemental composition of paint's pigment. This technique (SEM/EDX) was adapted to determine the surface morphology and the elemental composition that is responsible for the thermal resistance of the TWAP. FTIR spectroscopy was used to determine the functional group and organic molecular composition of the paint. IR thermography technique was used to establish the heat resistance of the TWAP.

SEM is a type of electron microscope that images the sample surface by scanning it with a high energy beam of electrons in a raster scan pattern. The electrons interact with the atoms that made up the sample producing signals that contain information about the sample's surface morphology, composition and other properties such as electrical conductivity [Goldstein, 1981]. The combination of the scanning electron microscope and the X-ray spectrometer allows the surface scan of the sample with the use of an electron beam and the measurement of characteristic X-rays to form elemental maps [Kaszowska *et al*, 2012]. Figure 3.1 shows a photo of the sample (insulation material) preparation for SEM analysis.

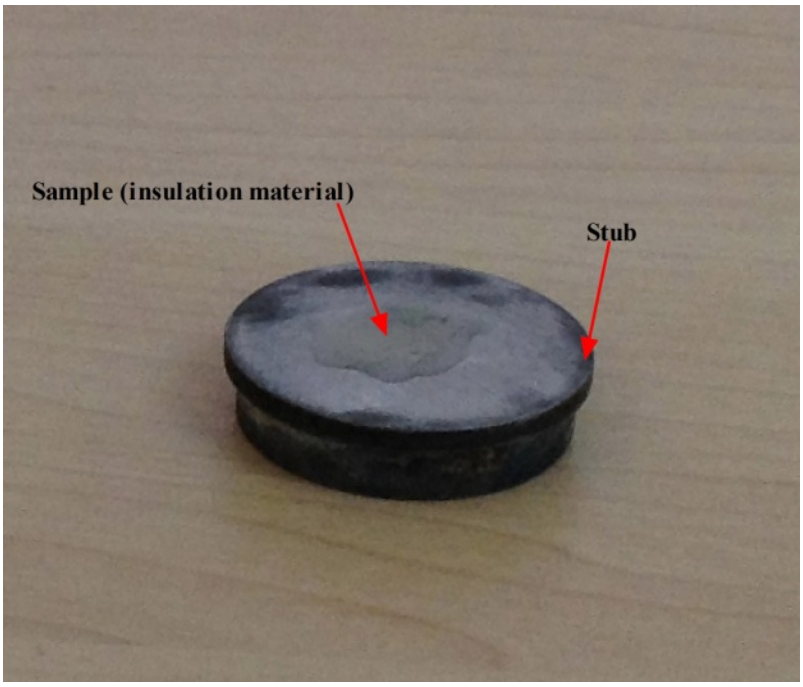

Figure 3.1: Sample (TWAP) preparation for SEM analysis

A drop of TWAP was spread on a stub, where it was allowed to dry for a period of 24 hours. The sample was then coated with gold palladium (Au–Pd) to increase its conductivity because dry paints are electrically non-conductive. After which, the stub was placed on a stage and inserted into the electron microscope for scanning. A JEOL (JSM-6390LV) scanning electron microscope was used to perform the SEM analysis. Electron beam current and potential were varied for optimal imaging. The SEM images were produced in three different magnifications (1600X, 3700X, & 9500X). The elemental content in weight (%) was measured.

FTIR is the most preferred and common method of infrared spectroscopy. IR spectroscopy or IR spectra is the absorption or transmission measurement of different IR frequencies of a sample positioned in the path of an IR beam [Settle, 1997: 249]. IR is typically operated in the Mid-IR

range between 4000-400 cm^{-1} (2.5-25 μm) when it is used for compound identification purposes. IR in either the Far-IR range between 400-10 cm^{-1}(25-1000 μm) or the Near-IR 14000-4000 cm^{-1} (0.71-2.5 μm) is typically carried out for special purposes. FTIR analytical methods are adopted in the analysis of a wide range of different materials. These include; monomeric materials for purity, and to identify polymers (polyethylene, polyester, nylon, etc.) and their compositions [Razumovskiy, 2007]. In this study, FTIR is used to identify the molecular composition of the insulation material. Every organic molecule gives rise to complex IR spectra. Both the complexity and the wave numbers of the peaks in the spectra give information about the molecule. The information is interpreted by comparing the peaks of the molecule with that of a well-known spectrum [Faist, 2002]. During the sample preparation, the insulation material was mixed with non-reactive oil before it was placed in the IR spectrometer. The sample was scanned for 5 minutes, after which the spectra were obtained. FTIR deals with the analysis of organic substance (binding media) of the insulation material, whereas SEM/EDX is used for identification of inorganic substance.

Infrared thermography is a non-intrusive testing technology that can be used to determine the superficial temperature of objects. Thermal cameras collect infrared radiation emitted by the surface, convert it into electrical signals by the imaging sensor (microbolometer) in the thermal camera and display a thermal image of the body's superficial temperature distribution [NEC San-EI Instruments Ltd, 1991]. The thermal image contains a series of colours (or shades of grey) which correspond to various temperature levels of the surface (target) on which it is focused [Eads, Epperly, and Snell, 2000]. The use of infrared thermography in building monitoring is found to be extensive. It has been used successfully for more than 25 years in building diagnostics concerning,

historical buildings and sites, monuments, modern structures [Avedelidis, 2002]. It can also be used to evaluate the building performance. According to Hart (1991), thermography can be used to detect insulation defect, air leakage, heat loss through windows, dampness and ‘‘hidden details’’ (subsurface pipes, flues, ducts, wall ties, etc.) [Hart, 1991]. Thermography is based on the principle that all objects radiate energy that is transported in the form of electromagnetic waves, travelling at the speed of light. The quantity of energy leaving a unit surface area (A) as radiant heat is proportional to emissivity (ε) and the fourth power of its absolute temperature given by

$$W = \varepsilon \sigma A T^4 \qquad [3.1]$$

Where W is the total emissive power (radiated watts per unit area, W/m^2), σ the Stefan-Boltzmann constant, ε is the total emissivity of the surface ($0 < \varepsilon < 1$) and T is the surface absolute temperature (K). The emissivity of the surface depends on the temperature of a surface, which is a measure of how efficient it radiates heat energy [Balaras and Argiriou, 2002]. According to Kirchhoff’s law, for an opaque material, the spectral emissivity and spectral absorbance of the material are equal at any specified temperature and wavelength; that is $\varepsilon = \alpha$. Thus, equation 2.13 can be rewritten as;

$$\alpha + \rho = 1 \qquad [3.2]$$

Therefore the quantity of heat energy emitted by the surface of a building wall depends on absorbed radiation $(\alpha)$and reflected radiation (ρ). The application of TWAP on the wall surface

will reduce the quantity of absorbed heat transferred to the surface of the wall; thereby reducing the emissivity of the wall.

In this study, the surface temperatures of a coated and un-coated wall sample were monitored simultaneously using IR thermograph and thermocouples. The experiment was performed on the East wall of the building. During the period (December) when the experiment was performed, the East wall was exposed to direct sun rays from 7h00 to 12h00, mid-day. As a result of the over-hanging roof at the north elevation of the building, more than half of the surface area of the north wall was shaded from direct sun rays all through the day. The west wall was only exposed to direct sun rays at 17h00 to 19h00, ±2 hours of the day. Owing to this, the East wall was the only wall which demonstrates a typical building heat transfer process. The inner surface of a building wall was divided into two areas which measured 41 cm x 62 cm each. The chosen dimensions have no significance in the experiment, since the measurement is taken at any spot in the areas. The most important factor considered while choosing the dimension was that each area should contain at least the entire surface area of a block. Figure 3.2 shows the samples of the wall surface.

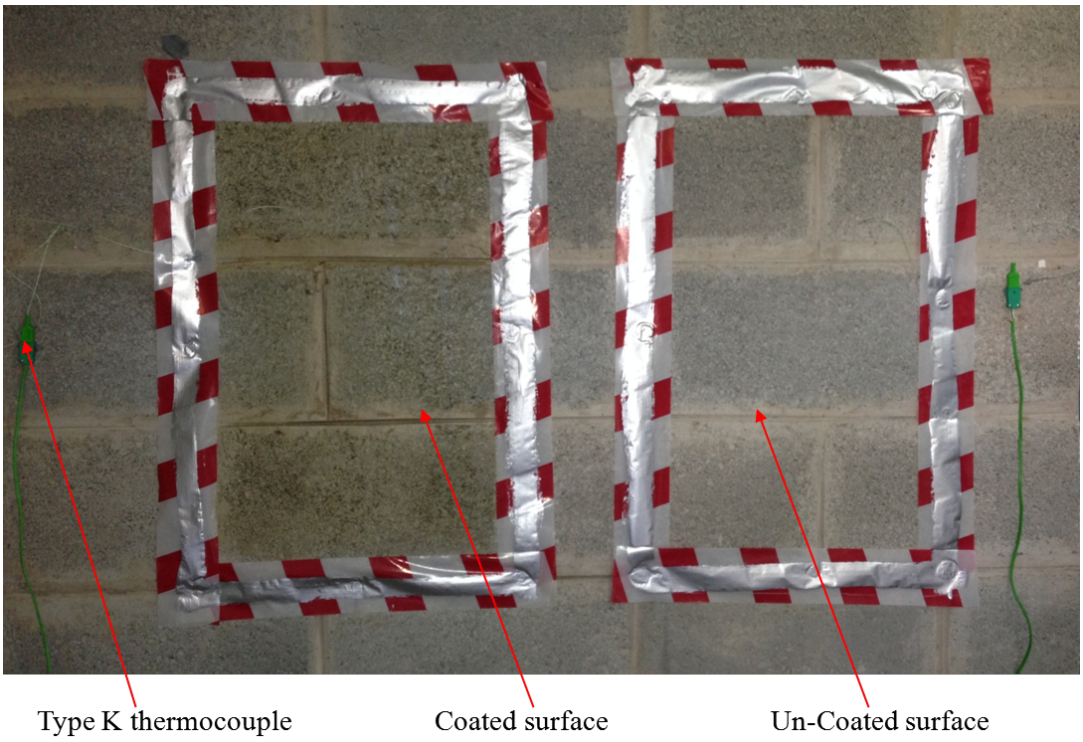

Figure 3.2: Wall samples of coated and uncoated surface

One of the areas was coated with 3 coats of TWAP on the inner surface of the wall, whereas the other area was left un-coated. The inner surface was coated only to allow the free flow of heat from the outer surface, in order to determine the quantity of heat reduced by the film of the paint at the inner surface. Dock tapes used to demarcate the insulated and un-insulated surface has no contribution to the results of the experiment. It was used to clearly show the demarcated area in the thermography. Type-K thermocouples were used to measure the inner/outer surface temperature of both sections of the wall, as well as the outer ambient temperature. The indoor air temperature and relative humidity were measured with a temperature relative humidity probe, suspended approximately 1.8 m from the floor of the room. All sensors were connected to a Campbell Scientific CR1000 data logger and readings were recorded at 30 minutes intervals. Figure 3.3 shows the data acquisition system.

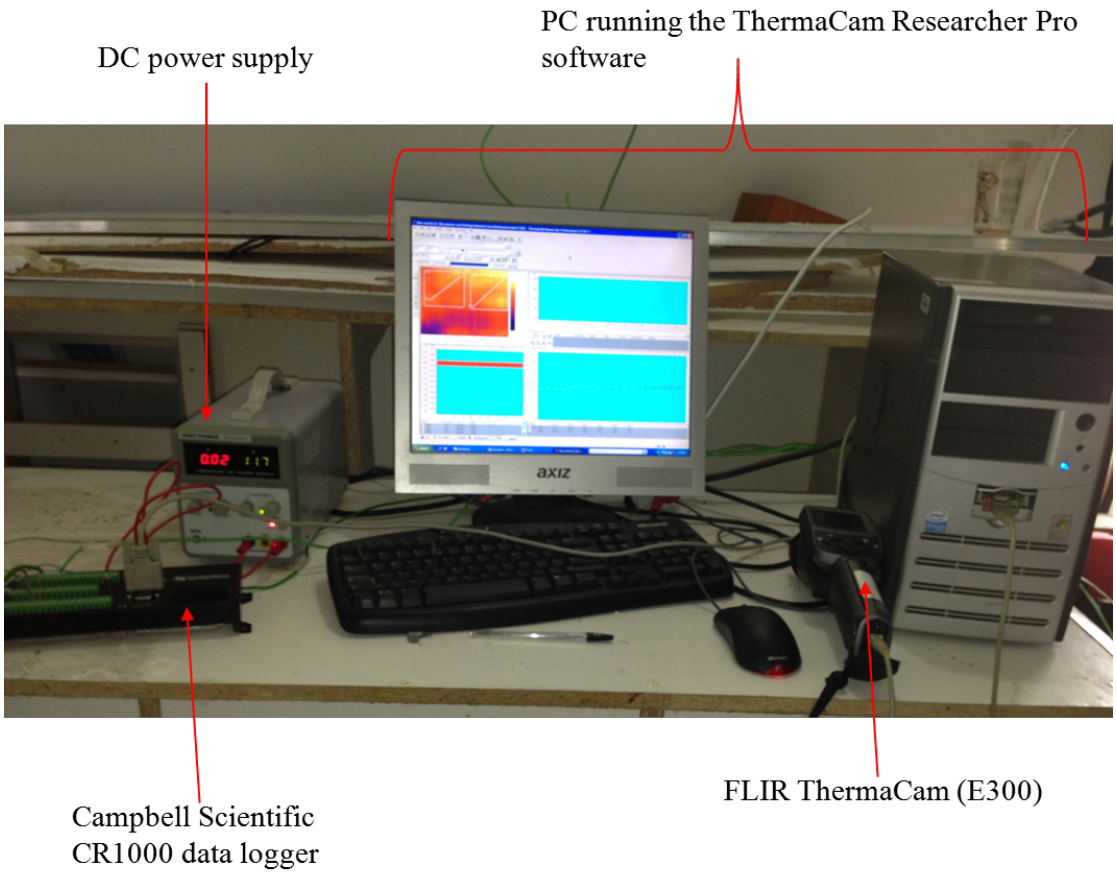

Figure 3.3: Data acquisition system for IR thermography analysis

The IR imaging of the wall surface was done manually. The day of the experiment was divided into three periods; before sunrise (5h00 to 6h30), mid-day (12h30 to 14h00) and after sunset (18h30 to 2h00). In each period, the IR image of the wall was taken at 30 minutes intervals, each intervals represent a phase of the temperature distribution of the wall surface. Decrement factor and time lag are used to portray the thermal resistance of the TWAP.

3.3 SELECTION OF HOUSE

A Low cost house (LCH) located at the Golf Course settlement in Alice under the Nkonkobe Municipality Eastern Cape was used as a case study in this research. Figure 3.4 shows an aerial photograph of the settlement and a photo of the LCH used.

Figure 3.4: Google earth of Golf Course settlement and low cost house

Golf Course is located at 32°S latitude and 26°E longitude at an altitude of 493 m; in the temperate interior (Zone 2) climate of South Africa [TIASA, 2010: 17]. Golf Course has an average summer temperature of 18°C to 26°C, with a relatively mild winter of an average temperature between 7°C to 20°C. The east wind is predominant in summer while the winter is dominated by the west wind. A moderate wind speed of an average of 2.5 m/s is experienced in Golf Course throughout the year. Like most LCH settlements in the country, Golf Course is a rural settlement primarily occupied by senior citizens, children and low income earners. As observed in the aerial photograph, some regions of the settlement are laid out with no particular consideration for

geographical north (red circled regions). The geographical orientation of the house was the basic criteria used to select the house. Figure 3.5 shows the floor plan of a typical LCH.

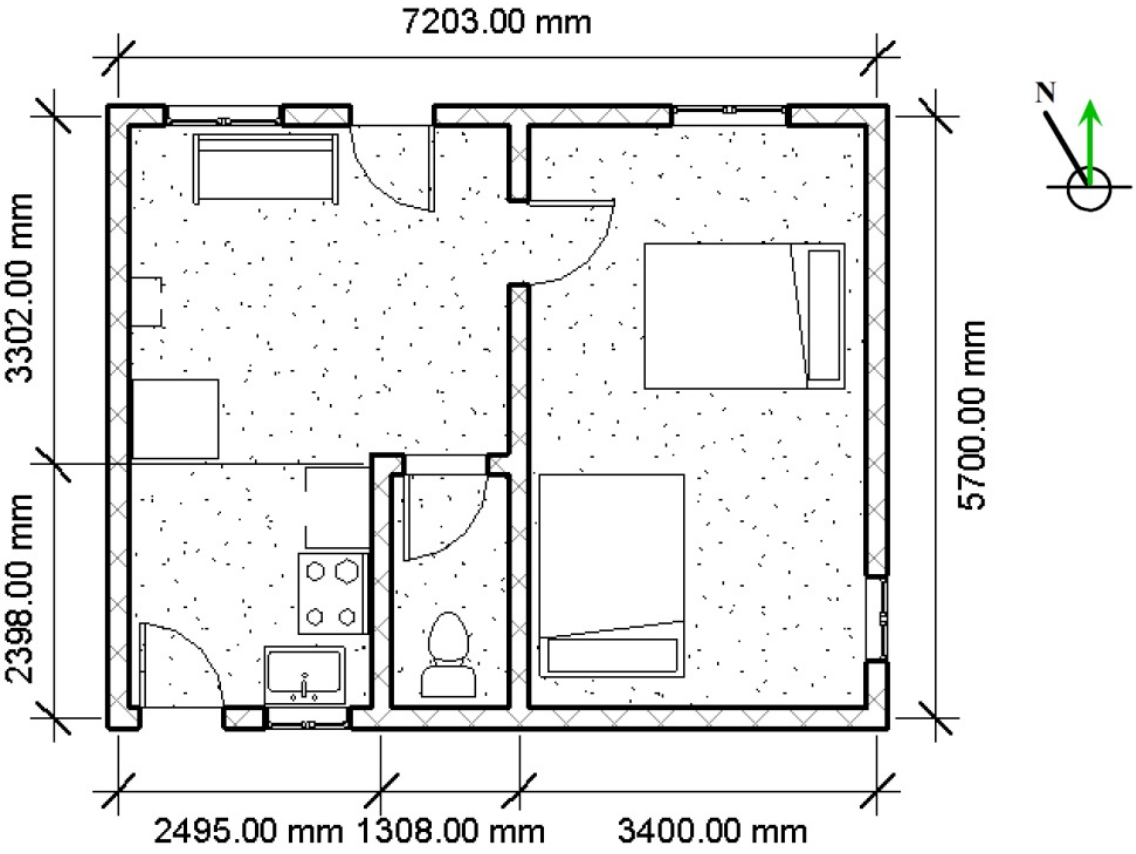

Figure 3.5: A typical floor plan of LCH

The house used is facing N16°E. It comprises of a bedroom, toilet and an open plan living room and kitchen. It has a floor dimension of 7.20 m x 5.70 m, giving an approximate area of 41 m^2. The roof is made of galvanized, corrugated iron sheets with no ceiling or any form of roof insulation. The walls of the buildings are made of the M6 (0.39 x 0.19 x 0.14 m) hollow concrete blocks, with no plaster or insulation. Thus the thickness of the walls assumed the width (0.14 mm) of the

blocks. More than 97% of the buildings in this settlement share the same design. Figure 3.6 shows the elevations of a typical LCH.

Figure 3.6: Typical buildings elevation of LCH

Although these elevations are not directly lined- up with North, East, South or West; the labels are used for simplicity and thus imply the closest geographical direction to the said elevations. The building façade (North wall) has two large (1.10 x 1.00 m) windows (single glazing). These windows allow the penetration of low angle winter sun rays into the building as well as the window in East wall, at the east elevation of the building; that provides access for the early morning sun rays. As seen in Figure 3.6, the West wall at the west elevation has no windows, as a result, increase the thermal mass of the West wall at the west elevation of the building.

Thermal mass is a term used to describe the thermal storage ability of building materials. Such materials absorb and store heat with low temperature change. When the air temperature around the thermal mass material drops, heat stored is released into the surrounding. Thermal mass is a function of the density and specific heat capacity of a material, the denser the material, the higher its thermal mass capacity [Gregory *et al*, 2007]. For efficient use, thermal mass should be insulated from the external environment, i.e. it should be located within insulated walls [Victoria, 2005]. The West wall in this case, has a low storage capacity due to the thickness and the material (hollow concrete block) used in the wall. Furthermore, it has a high heat absorption rate; since the wall is made of material of the same thermal properties. Therefore, when the outdoor air temperature drops; wall 3 absorbs and transfers heat from the inside of the building to the outside.

3.4 METEOROLOGICAL DATA MEASUREMENT

The thermal influence of the building envelope (external walls, floor, roof, windows and doors enclosing the indoor space of a building) on indoor temperature before and after coating were analyzed. Thus, the building was monitored for a period covering summer, autumn and winter seasons. The following meteorological parameters were measured; temperature, relative humidity, solar irradiance, wind speed and direction. A number of sensors were installed to measure the above listed parameters; these include: Thirteen type-K thermocouples, which were used to measure the indoor temperature and the inner and outer surfaces of the building walls temperatures. The thermocouples measuring the wall surface temperature were mounted such that their sentry terminals are in a direct contact with the walls. Two set of HMP50 humidity sensors were used to measure the indoor and outdoor relative humidity and ambient temperature. Figure 3.7 shows the meteorological sensor map of the building.

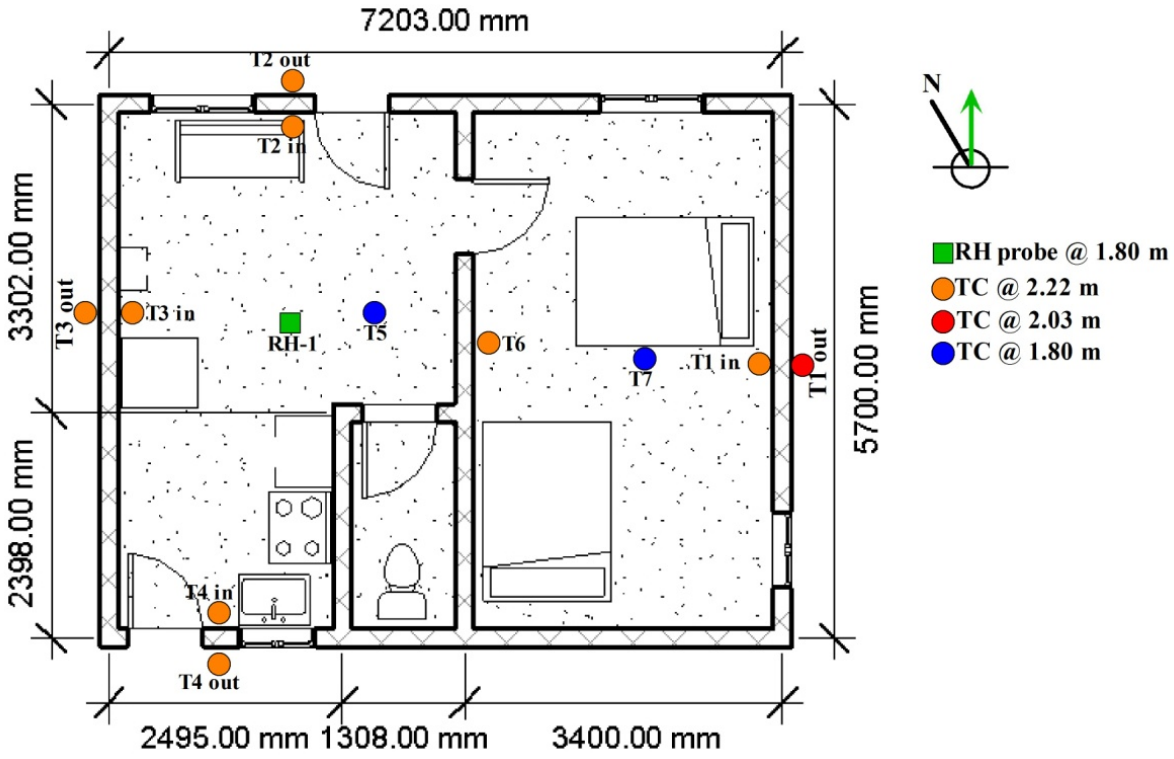

Figure 3.7: Meteorological sensor map

These type-K thermocouples are denoted $T_{\text{N-in}}$ and $T_{N\text{-out}}$, where $N = 1, 2, 3, 4\ldots$n. The temperature measurement of the walls is a spot measurement, targeted to measure the temperature felt by the occupants in the building. During the period of measurement, the building was used by a single mother, teenage daughter and a toddler. Sensors were placed in such a way that they do not disturb the family activities. Thermocouples $T_{5\text{-in}}$, $T_{7\text{-in}}$ were placed at a height of 1.80 m, as well as the indoor relative humidity sensor. So as to have a good indoor parameter variation patterns that is not influenced by the roof temperature. The 03001 wind sentry anemometer/vane and Li-Cor pyranometer together with the outdoor relative humidity sensor were installed at a height of 0.44 m above the roof of the building. Figure 3.8 shows the outdoor meteorological sensors.

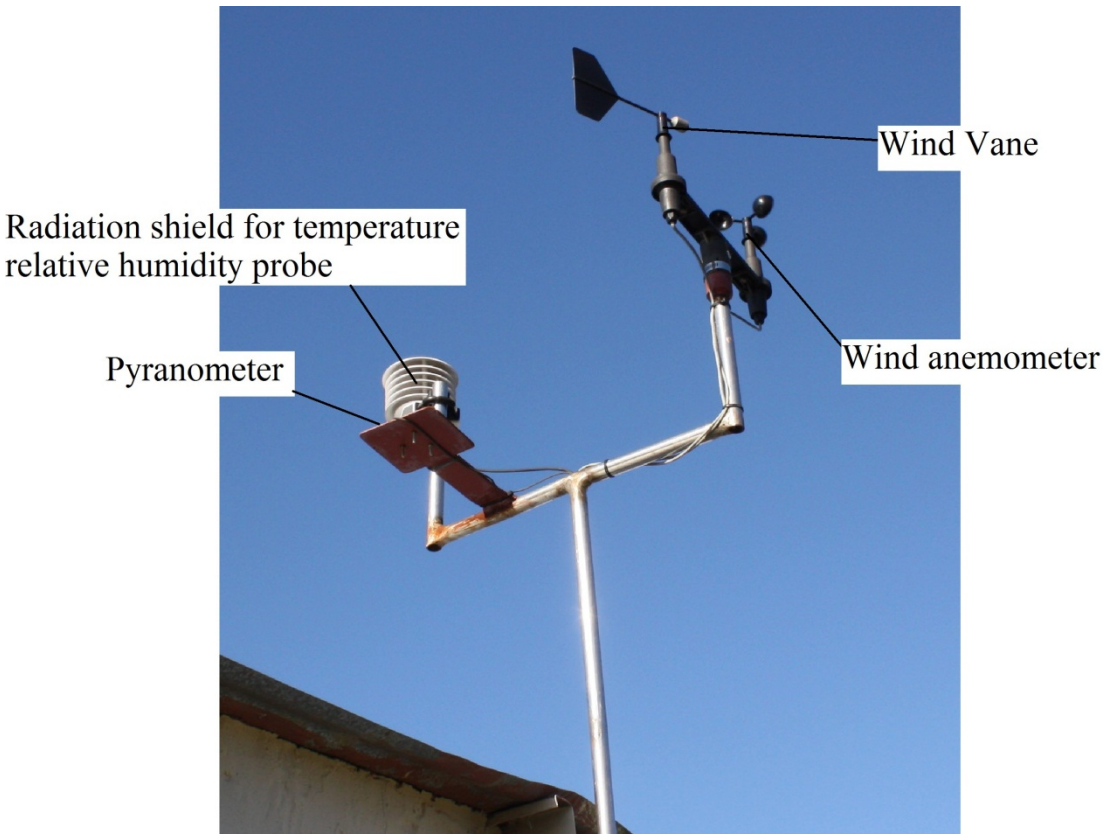

Figure 3.8: Outdoor meteorological sensors

The wind sentry anemometer and vane is place at sure height to prevent obstruction of the wind by other buildings. The sensors (anemometer and vane) measure the horizontal wind speed and wind direction. The pyranometer was mounted horizontally above the roof to measure the true global solar radiation. At the same time, the pyranometer was placed such that the shadows of other sensors do not fall on it. The outdoor relative humidity sensor was housed in a solar radiation shield to precisely measure the ambient humidity and temperature. The entire set of sensors was connected to a CR1000 data logger. Figure 3.9 shows the schematic diagram of the data acquisition system (DAS).

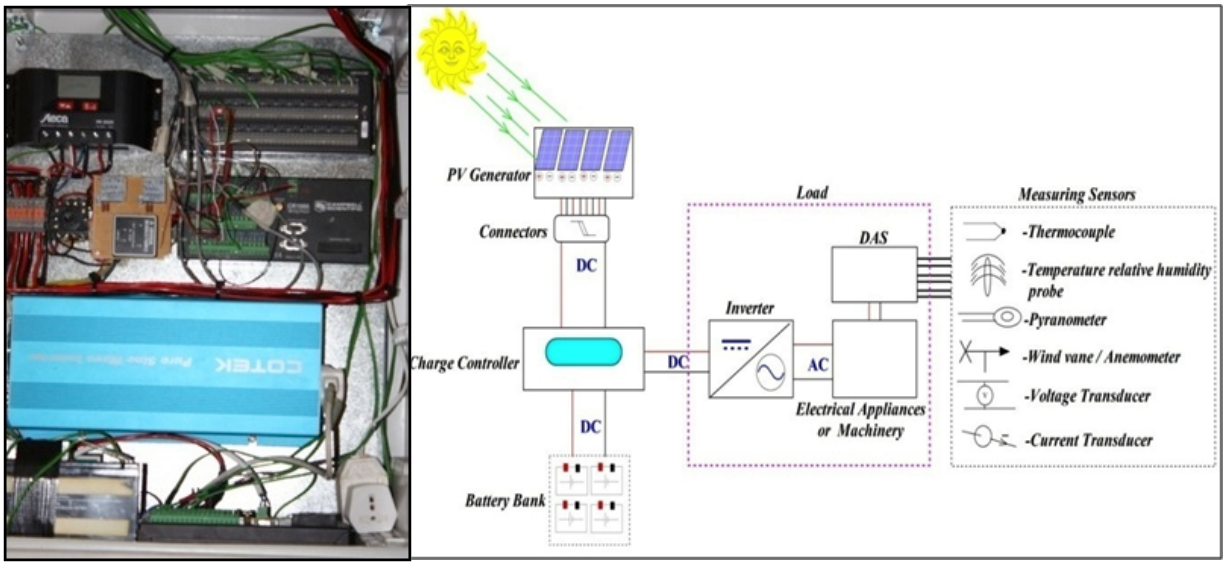

Figure 3.9: Photo and schematic of data acquisition system

The DAS are made up of a Campbell scientific CR1000 data logger supported by an AM16/32 relay multiplexer. The latter was used to increase the number of channels available for the eleven differentially connected thermocouples, and is equipped with cold temperature compensation. All other sensors were connected directly to the data logger. The data logger collects and stores data following a PC400 application which provides terminal between user and the CR1000 to generate programs, editing, data retrieval and real time monitoring. The data logger was programmed to sample the sensors every 30 seconds and then store the maximum and average values every 30 minutes. Multiplexing by the AM16/32 is accomplished with mechanical relays, which connect each of the sensor channels in turn to a common output destined for the data logger [Smith, 2004]. The multiplexer is programmed to scan through all eleven thermocouples every 5 minutes and send data to the data logger. The DAS is powered by a 12-volt battery charged by a 20-watt solar panel. The solar panel was oriented north at an angle of inclination of 32° to receive maximum insolation over the course of the year.

3.5 THE BUILDING THERMAL PERFORMANCE BASELINE

The thermal performance baseline of the house was analyzed for summer and winter seasons. Days with maximum solar irradiance $\geq$ 800 W/m^2 were considered as summer season while days with maximum solar irradiance $\leq$ 600 W/m^2 were considered as winter season. Before the inner surfaces of the external walls of the house were coated with TWAP, 23 February, 2012 received a maximum solar irradiance of 1364 W/m^2 and was used to represent a typical hot summer day. A typical cold winter day was represented by 13 July, 2012, with a maximum solar irradiance of 283.40 W/m^2.

More activities take place in the living room than any other room in a house; the thermal performance of the living room was used to represent the thermal performance of the entire building. Hence the roof, floor, middle-wall, and the three external walls of living room made up the building envelope in the context of this research. The three external walls refer to the North, West, and South walls. The heat transferred through the doors and windows were neglected, based on the aim of the study and the materials available for the research. To obtain the surface area of the building envelope involved in the heat transfer between the inner space of the building and its surrounding, the dimensions of the three external walls as well as the roof and floor were measured, from Figures 3.5 and 3.6. The thermal influence of weather factors on indoor temperature was also analyzed. The weather factors include: ambient temperature, indoor and outdoor relative humidity, solar irradiance, and wind speed.

3.6 APPLICATION OF TRANSLUCENT WATER-BASED ACRYLIC PAINT TO THE SURFACES OF THE BUILDING WALLS

After approximately 5 months of data collections, the inner surfaces of the external walls of the living room were coated with translucent water-based acrylic paint (TWAP) on 30 July, 2012. The paint was applied to the living room only due to limited amount available. The inner surface was coated and not the outer surface, in order to estimates the quantity of heat reduction by the paint's film. The paint was applied to the surface of the walls using a roller. Before the paint was applied, the surface of the walls were wiped to remove dirt, oil, grease or any contaminations that may lead to flaking or peeling of the paint. It was ensured that there were no flakes of the paint that was already on the walls surfaces. All thermocouple mounted on the surface of the walls were also removed. Three coats of TWAP were applied to the surface of the walls. Each coat was allowed to cure for 24 hours before the next coating, as a result 3 days were spent in coating the surface of the walls. After the third coat, the walls were left to cure completely for 2 weeks. Although, the recommended time for complete cure for 3 coats is 30 days, but thermal benefits of the paint starts after 2 weeks [Nansulate, 2011].

3.7 THERMAL INFLUENCE OF TRANSLUCENT WATER-BASED ACRYLIC PAINT

After coating, thermal monitoring of the building commenced on the 19 August, 2012. The thermal influence of translucent water-base acrylic paint on the thermal performance of the building was analyzed using cooling degree-hours (CDH) and heating degree hours (HDH). Heating and cooling degree-hours usually accompanies the design heat calculation and plays an important role in the selection of a heating or cooling system in a building (mostly at it design stage) [Bolatturk, 2007].

CDH are used to estimate the amount of cooling hours required to keep the indoor temperature of a building within the thermal comfort zone. Whereas, HDH are used to estimate the amount of heating required to keep the indoor temperature within the thermal comfort zone. The HDH and CDH of the house were analyzed for summer and winter season. Three months dataset for each season were filtered into hours. Monthly degree-hours were obtained from the average daily degree-hours. In the same way, the annual degree-hours were obtained from the average monthly degree-hours. The energy demand of the house is calculated using Equation [2.19] and the monthly degree-hours.

3.8 DEVELOPING OF INDOOR TEMPERATURE MODELS

Three months data for the summer and winter seasons were used to perform the reliefF algorithm and the development of the multiple linear regression models. The reliefF algorithm is a statistical test to rank predictors according to their weight of importance to an output. More generally the statistical test ranks the predictors by their weight of attribute to the response and also identifies both primary and secondary input parameters. The weight ranking ranges between -1 to 1 and if the value is positive for a particular predictor, it implies that input parameter is a primary factor to the output and if otherwise is a secondary factor, is excluded from the modeling parameter [Robnik-Sikonja and Kononenko, 1997]. In the context of the research, the predictors are the components of the building envelope and weather factors, while indoor temperature is the output. From the results and findings of the reliefF testing, multiple linear regression models that predict the indoor temperature were developed.

3.9 SUMMARY

The surface morphology of the paint was analyzed using SEM analysis. This was accompanied by EDX analysis which reveals the elemental compositions of the paint. FTIR was used to determine the functional as well as the organic molecular composition of the paint. Before coating, the paint underwent thermal resistance experiment using IR thermography. A low cost house located in Golf Course, Alice was used as a case study. The house was selected due to its orientation (N16°E), which is a typical orientation for passive solar design. The indoor and building envelope surface temperatures were measure by a set of 13 type-K thermocouples. Also, the indoor and outdoor relative humidity was measured by 2 set of HMP50 humidity sensor. The HP50 humidity sensor placed outside was also used to measure the ambient temperature. Wind speed & direction and solar radiation were measured by a 03001 wind sentry anemometer/vane and Li-Cor pyranometer respectively, placed at a height of 0.44 m above the roof of the house. All sensors were connected to a CR1000 data logger and AM16/32 relay multiplexer, from which data are stored and retrieved following a PC400 application in computer system.

The thermal performance baseline of the house was analyzed for winter and summer season. Days with maximum solar irradiance $\geq$ 800 W/m^2 were considered as summer while day with maximum solar irradiance $\leq$600 W/m^2 were used as winter season. The Thermal performance of the living room was used to represent the entire building. On 30 July, 2012, the inner surfaces of the external walls of the building were coated. The paint was applied to the living room only due to limited amount available. Three coats of TWAP were applied to the surfaces of the walls. Each coats were allowed to cure for 24 hours before the next coating, as a result 3 days were spent in coating the surface of the walls. After the third coat, the walls were left to cure complete 2 weeks. Although,

the recommended time for complete cure for 3 coats is 30day but thermal benefits of the paint starts after 2 weeks.

The thermal influence of translucent water-base acrylic paint on the thermal performance of the building was analyzed using cooling degree-hours (CDH) and heating degree hours (HDH). CDH are used to estimate the amount of cooling hours required to keep the indoor temperature of a building within the thermal comfort zone. Whereas, HDH are used to estimate the amount of heating required to keep the indoor temperature within the thermal comfort zone. The HDH and CDH of the house were analyzed for summer and winter season.

Three months data for the summer and winter season were used to perform the reliefF algorithm and the development of the multiple linear regression models. The reliefF algorithm is a statistical test to rank predictors according to their weight of importance to an output. In the context of the research, the predictors are the components of the building envelope and weather factors while indoor temperature is the output. From the results and findings of the reliefF testing, multiple linear regression models that predict the indoor temperature were developed.

CHAPTER 4

CHARACTERIZATION AND THERMAL RESISTANCE OF TRANSLUCENT WATER-BASED ACRYLIC PAINT

4.1 INTRODUCTION

The insulation properties of translucent water-based acrylic paint (TWAP) are as a result of special additive that are included in the paint's pigment, which is known as IR reflective pigment. Any material which is transparent to IR radiation in the required spectral range and which also has a refractive index substantially different from its binder's refractive index (e.g. about 1.5) may be used as an IR reflective pigment. Example of IR reflective pigments and their approximate refractive indices are: TiO_2 (2.5), Sb_2O_3 (2.2), Al_2O_3 (1.73), SiO_2 (1.54) and ZnO (2.2) [Ensminger, 1988; 127]. IR reflective pigment is based on the principle that internal reflections enhance the distribution of radiative energy within the film or coat, making the heat radiation variation more uniform. Figure 4.1 shows the effect of IR reflective film on a normal incident heat radiation.

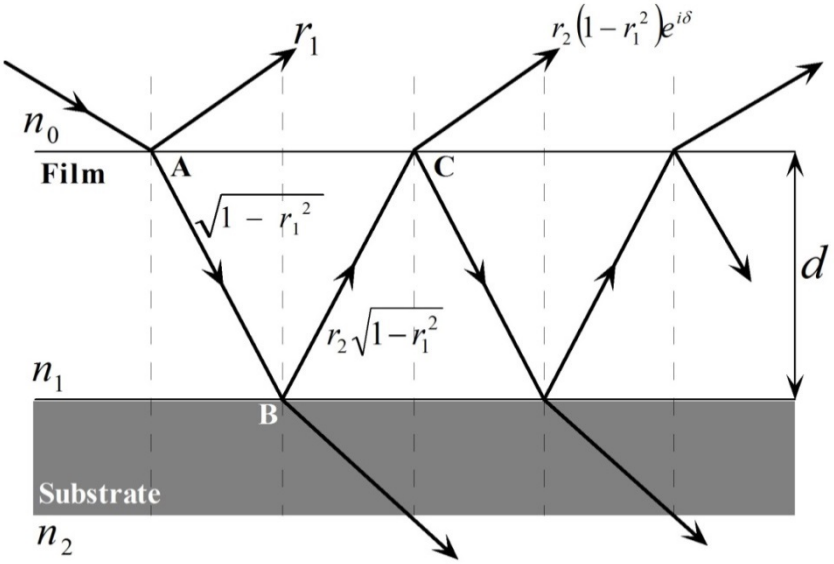

Figure 4.1: Effect of IR reflective film on a normal incident heat radiation [Adopted from Hass *el al*., 1997]

The reflectance (r) of the film depends on the thickness (d), radiation wavelength (λ) and the refractive index of the film (n_1) and substrate (n_2). From Figure 4.1, it shows that if a film is applied to a substrate with $n_1 > n_2$, then an increase in reflectance will occur; resulting in the reduction of the surface temperature of the substrate [Hass *et al*, 1997].

This chapter focuses on the analysis of the chemical composition of TWAP. The surface morphology of the paint (TWAP) in its dry state was examined with the aid of a Scanning Electron Microscope (SEM). The chemical characterization and orientation of the material was also tested using the techniques mentioned above. In conjunction with the SEM analysis, the Energy Dispersive X-ray spectroscopy (EDX) was used to find out the chemical elemental composition of the material. Fourier Transform Infra-red spectroscopy (FTIR) has gained significant importance for the investigation of polymer materials over the decades [Zhang, Berber and Smith, 2012]. The molecular composition of the paint was determined using FTIR techniques. Finally, the TWAP

was applied to a section of a wall surface; where it's thermal resistance was examined using IR thermography techniques. The paint has three basic components as follows; Binders, pigment and solvent or vehicle.

- **Binders**: Binders are responsible for holding the pigment particles into a uniform, continuous film adhering to the surface of the substrate. Water based paints use acrylic and/or vinyl emulsion as binders, while turpentine or other organic solvent are used in oil based paints.
- **Pigment**: Pigment plays a very important role in paints. It provides colouration and finishing appearance of paints. It also serves to protect the surface underneath from corrosion (in the case of metallic substrate) and weathering as well as helping to hold the paint together.
- **Solvent or vehicle**: This is the liquid portion of paints in which the pigment and binder dissolved. It is usually a volatile liquid that can evaporate after coating, leaving the paint dry on the substrate surface. Water-base (emulsion) paint uses water while oil-based paint used mineral turpentine.

Additive is an optional component used to give paints special properties or improve the properties of paints such as; corrosion control, UV-protection, thermal stability, control foaming, fire resistance and improve pigment stability [Weismantel, 1981: 175].

4.2 SEM/EDX ANALYSIS

Figure 4.2 presents the SEM images of TWAP at different magnifications. These were obtained after SEM/EDX analysis and are presented in order to quantify the inorganic components of the sample.

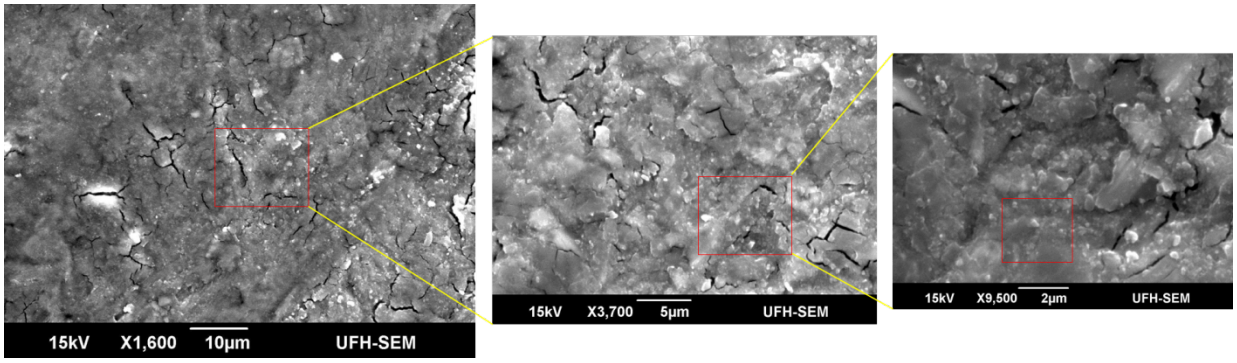

(A) (B) (C)

Figure 4.2: SEM images of TWAP at 1600X (A), 3700X (B) and 9500X (C)

Figure 4.2 reveals the surface of different part of the TWAP. The images clearly show cracks on different parts of the paint surface which are due to uneven coating. Areas with coats more than 127 microns in thickness result in cracking, peeling or flaking [Crolley, 2012]. These cracks may lead to reduction in the thermal performance of the paint, as the cracks will provide a direct penetration for the IR radiation. The images also show that in dry state the paint is transparent to visible light. This is clearly indicated by the white spots found in Figure 4.2 (A) and bright appearance of the SEM image in Figure 4.2 (B). The dark appearance of the paint mostly observed in Figure 4.2 (C) is as a result of the gold palladium (Au-Pd) used in coating the paint to increasing its conductivity. There were no morphological changes on the surface of different parts of the paint because no pretreatment processes were carried out on it prior to analysis.

The elemental composition of the paint was obtained from the EDX spectrum. The spectrum was generated from the highlighted area of the image in Figure 4.2(C). This section was chosen because it is one of the few sections without cracks on the coated surface. Therefore it will show the elemental composition of the paint with higher accuracy than any other section. Figure 4.3 shows the EDX spectrum of TWAP.

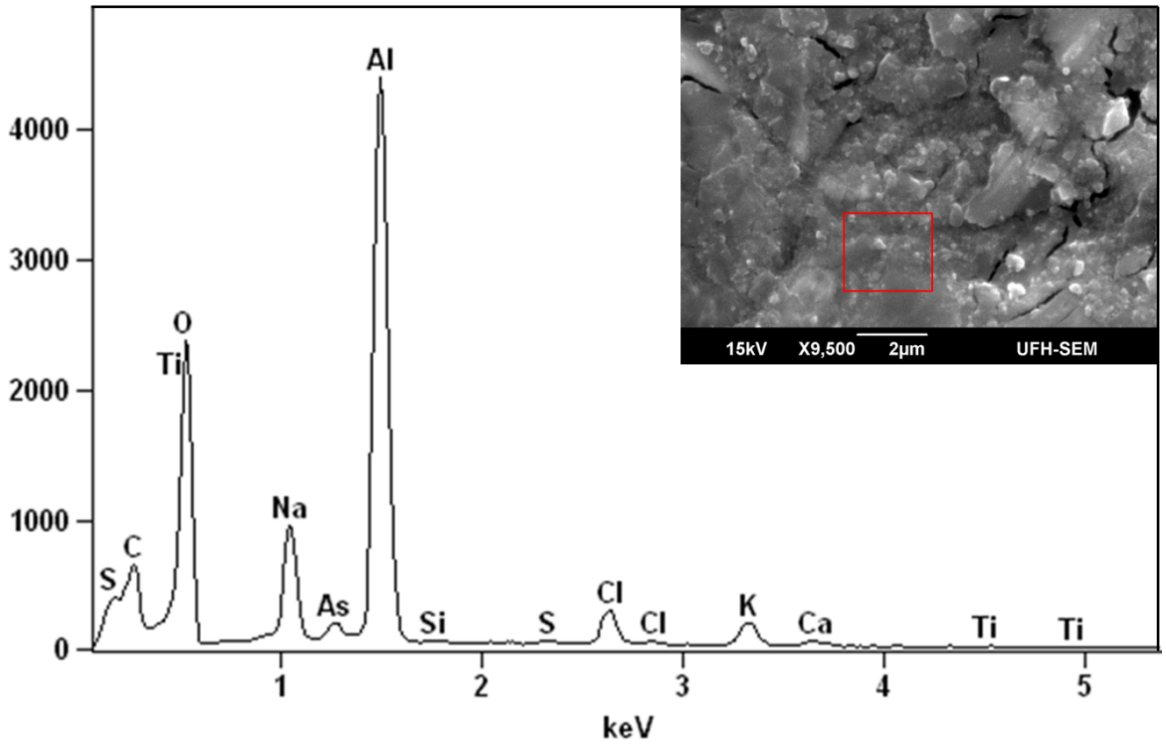

Figure 4.3: EDX spectrum of TWAP

The EDX spectrum was generated at 15 kV acceleration voltages and a take-off angle of 45.6°, the chi-squared value is 1.78. The EDX spectrum reveals the presence of oxygen, carbon and aluminum compounds in large quantities (above 10.00%). It also points out the presence of sodium, silicon, chlorine, potassium, arsenic and calcium in small quantity, ranging between 0.50 to 9.00%. All other compounds that are present but below 0.50%, such as Sulfur and Titanium are

considered as impurities. The presence of these elements is mainly due to some components used in the manufacturing of the paint, some of which are inorganic in nature. Table 4.1 presents the elemental composition of TWAP.

Table 4.1: Elemental composition of TWAP

Elements	**Symbols**	**wt (%)**
Carbon	C	16.45
Oxygen	O	31.47
Sodium	Na	6.72
Aluminum	Al	36.41
Silicon	Si	0.91
Sulfur	S	0.27
Chlorine	Cl	3.10
Potassium	K	3.00
Calcium	Ca	0.57
Titanium	Ti	0.04
Arsenic	As	1.04

It can be observed from Table 4.1 that TWAP contains primarily three inorganic elements; C, O and Al. The heat resistant nature of the paint is centred, not only around the organic constituents of the paint, but also around the inorganic components [Clark, 2002]. The element, Aluminum (Al) revealed by the EDX analysis in Table 4.1, is present in the paint as aluminum oxide (Al_2O_3) which is an effective IR reflective pigment. This compound gives the paint its characteristic heat resistant. Unlike other IR reflective element, Aluminum is not transparent to IR radiation. Aluminum is highly reflective in the IR due to the high concentration of mobile electrons. Its coatings contain

overlapping pigment flake which are parallel to and concentrated near the surface of the binder. Aluminum paint reflectance values of 0.75 to 0.8 for key spectral range of 1 – 8 μm [Berdahl, 1996].

4.3 FTIR ANALYSIS

Figure 4.4 presents the FTIR spectrum of TWAP. It shows the organic composition based on the functional group present in the main constituents of the sample.

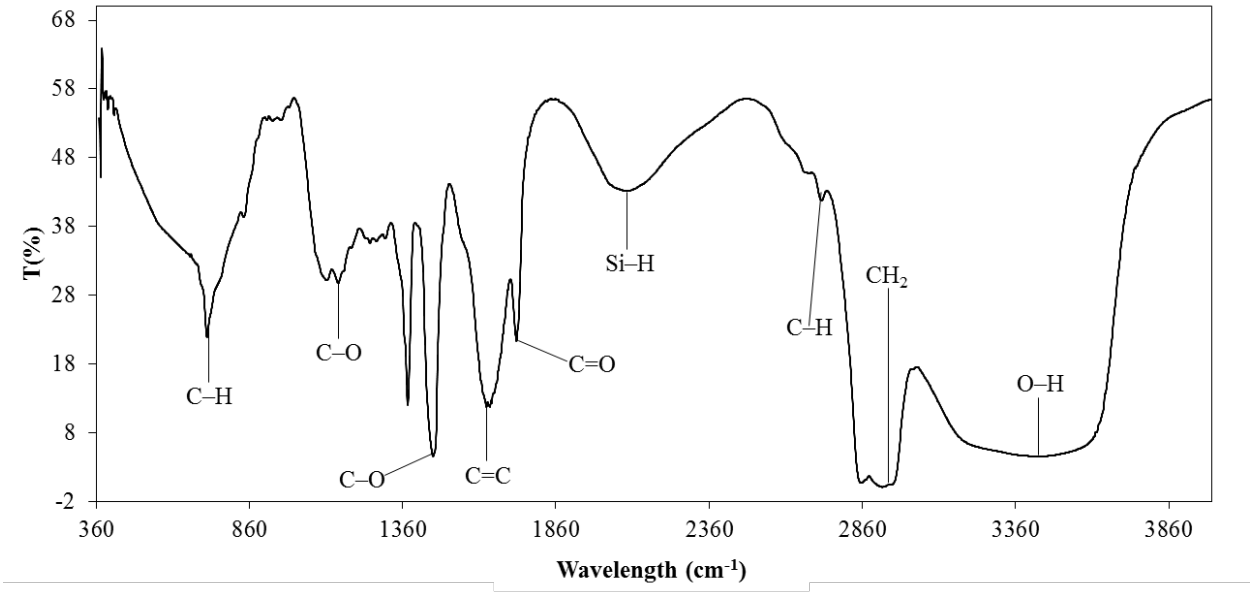

Figure 4.4: FTIR spectrum of TWAP

The Functional Group Region, 4000 to 1300 cm^{-1}; shows the appearance of strong absorption band in the region of 4000 – 2500 cm^{-1} which usually comes from stretching vibration between hydrogen and some other atom with a mass of 19 g or less. With reference to Figure 4.4, the broad absorption peak at 3438 cm^{-1} is attributed to O–H asymmetric stretching in the paint pigment. The CH_2 band at 2925 cm^{-1} is due to the oxidative chain cleavage reaction known to yield volatile

oxidation process [Meilunas, Bentsen and Steinberg, 1990]. The olefinic C–H stretching band at 2727 cm^{-1}, C=O stretching absorbance at 1850 – 1750 cm^{-1} and C═C stretching vibration (1680 – 1600 cm^{-1}) are features specific to the pigments, binders and solvents of the TWAP. The absorption bands at the 2700 – 1850 cm^{-1} region usually come only from triple bonds and other limited types of functional groups, such as C≡C at 2260 – 2100 cm^{-1}, C≡N at 2260 – 2220 cm^{-1}, allenes C=C=C at 2000 – 1900 cm^{-1} and Si–H at 2250 – 2100 cm^{-1}.

The Fingerprint Region, 1300 to 910 cm^{-1} absorptions in this region include the contributions from complex interacting vibrations, giving rise to the generally unique fingerprint for each compound. A good match between the IR spectra of two compounds in all frequency ranges, particularly in the fingerprint region, strongly indicates that they have the same molecular structures. From Figure 4.4, the absorption band in 1253 cm^{-1}, 1149 cm^{-1} and 1112 cm^{-1} are attributed to the C–O stretching pattern.

The Aromatic Region, 910 to 650 cm^{-1} the IR bands in this region do not necessarily come from the aromatic compounds, but the absence of strong absorption in the 910 to 650 cm^{-1} usually indicates the lack of aromatic characters. With reference to Figure 4.4, the C–H out-of-plane deformation gives rise to the strong band absorption at 722 cm^{-1}.

There were no spectra changes of the paint since it was not subjected to any chemical pretreatment process prior to analysis. However, Figure 4.4 reveals the presence of silicon (Si) in the functional group. Silicon which is present in the paint as SiO_2, also contributes to the heat resistance properties of the paint. According to Bardahl (1996), silicon has the ability to reflect IR radiation

due to its large refractive index (3.45). This made it a suitable binder for IR reflective coatings [Berdahl, 1996].

4.4 IR THERMOGRAPHY ANALYSIS

At temperatures above absolute 0°K all objects emit electromagnetic radiation in the form of heat [Maldague, 1993]. The higher the temperature of an object the more IR radiation it emits [Balaras and Argiriou, 2002]. Infrared thermography is required to detect the slightest temperature difference between two surfaces, in this case; a coated and uncoated wall surface. Infrared radiation received by an infrared sensor from a heated body surface is always composed by three fractions: the body radiation emitted, the surrounding infrared radiation reflected on the surface and infrared emission of the atmosphere layer between the infrared camera and the body. The atmospheric infrared radiation can be neglected at short distance (approximately 2 m) from the target surface. In addition, infrared temperature measurement is perturbed by the surrounding radiation, especially under conditions where the surrounding infrared radiation is approximately equal to the infrared radiation emitted by the target surface [Datcu *et al*, 2005]. Furthermore, ambient air temperature and relative humidity determine the rate at which a target surface emits IR radiation [Bagavathiappan *et al*, 2013]. Figure 4.5 shows the air temperature (indoor/outdoor) and relative humidity (indoor/outdoor) distribution during the period of the IR thermography measurement.

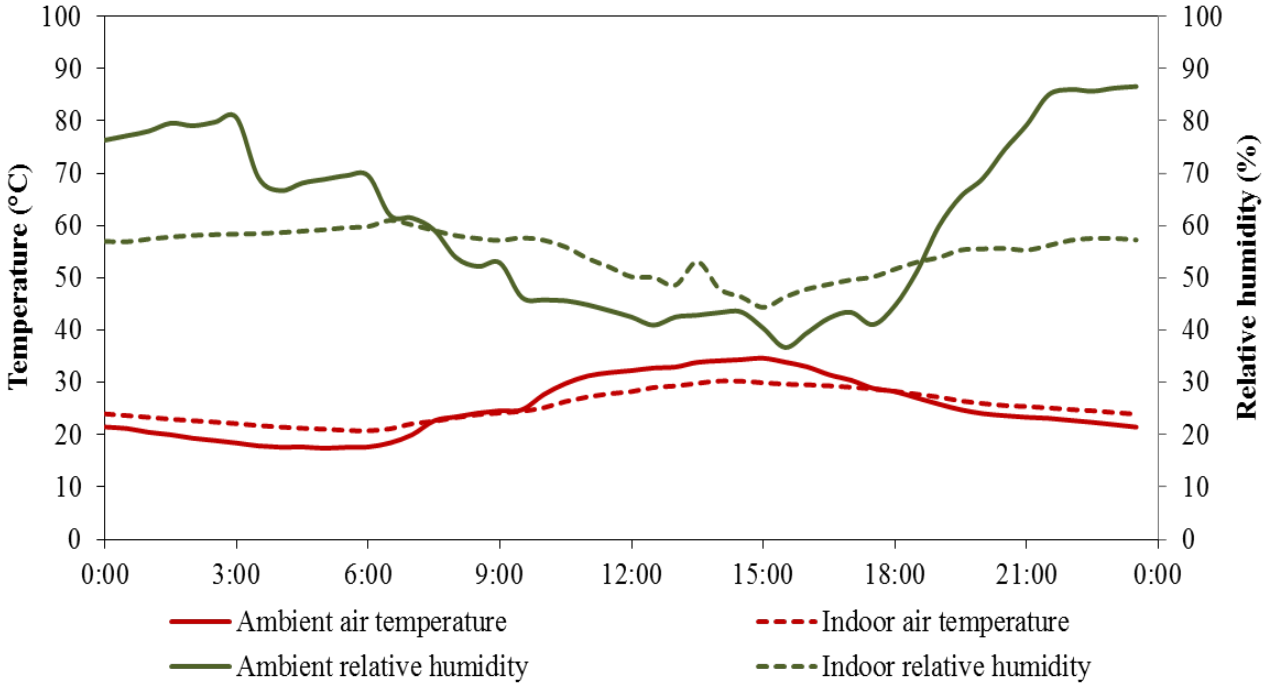

Figure 4.5: Indoor and outdoor air temperature and relative humidity

The ambient temperature of the building was greater than the indoor temperature from 0h00 to 7h00 (before sunrise) (Figure 4.5). Therefore, the inner space of the building tends to loss heat to its surrounding. On the other hand, a relatively high indoor and outdoor relative humidity was observed; ranging from 57% to 59% and 60% to 76%, respectively. Consequently, cold and moist air was experienced indoors, resulting in a low IR emissivity of the wall inner surface. At mid-day (9h30 to 17h30), the ambient air temperature was observed to be greater than the indoor air temperature; which will result in the flow of heat to the inner space of the building. It was also observed that in mid-day the indoor and outdoor relative humidity decreases, ranging from 44% to 57% indoors while the outdoor ranges from 36% to 52%. This resulted in warm and slight dry air indoors and hot and dry air outdoors. As such, the emissivity of the wall inner surface will therefore increase. As observed in Figure 4.5, the indoor and outdoor air temperature as well as the relative humidity distribution during the period after sunset (18h00 to 23h30) had a similar

distribution pattern to that of before sunrise (0h00 to 7h00). The indoor air temperature is greater than the ambient air temperature, with a sufficient higher relative humidity compared to mid-day. Table 4.2 shows the thermal parameters of the building obtained during the course of the measurements.

Table 4.2: Thermal parameters of the building (uncoated wall)

Period	**Phases (Ph)**	**Time**	**T_{out} (°C)**	**T_{in} (°C)**	**$R_{H\text{-}out}$ (%)**	**$R_{H\text{-}in}$ (%)**
Before sunrise	1	5:00	17.44	21.09	68.85	59.21
	2	5:30	17.61	20.85	69.56	59.62
	3	6:00	17.68	20.78	69.53	59.83
	4	6:30	18.46	21.16	61.92	61.02
Mid-day	1	12:30	32.78	29.05	50.07	40.98
	2	13:00	32.97	29.34	48.62	42.53
	3	13:30	33.87	29.85	53.09	42.87
	4	14:00	34.15	30.29	47.9	43.37
After sunset	1	18:30	27.06	27.76	51.24	53.02
	2	19:00	25.86	27.22	59.87	53.91
	3	19:30	24.8	26.48	65.57	55.32
	4	20:00	24.05	25.98	68.99	55.53

The periods; before sunrise, mid-day and after sunset are very significant in the heat transfer between the inner space of a building and its surrounding. The periods before sunrise and after sunset, the inner space of the building loses heat to its surrounding. At mid-day, the building

gained heat from the surrounding than other two periods. The IR thermography of the wall covers the above listed periods.

The following tools were used to analyze the IR thermography of the wall surface; spot meter (SP): it was used to measure the temperature at a particular spot on the image. Area tool (AR), this tool was used to measure the average temperature within the area of the wall surfaces. Lastly, the line tool (LI), this is the diagonal line drawn in the thermographs. It was used in place of a horizontal or vertical line to ensure the line covers more area on the wall surface. In the context of this study, the line tool was used to measure the maximum temperature along the line.

4.4.1 IR thermography of the wall surface before sunrise

The IR thermography of the wall surface before sunrise is shown in Figure 4.6. The thermography of the wall surface was captured between 5h00 to 6h30. With reference to Figure 4.5, the ambient air temperature was lower than the indoor temperature, during the period before sunrise. Therefore, an outward flow of heat from the inner space of the building occurs. The colours of the tape used to mark the sections on the wall do not reflect the actual temperature of the tapes. This is as a result of the masonry concrete block emissivity (0.94) selected in the thermal camera.

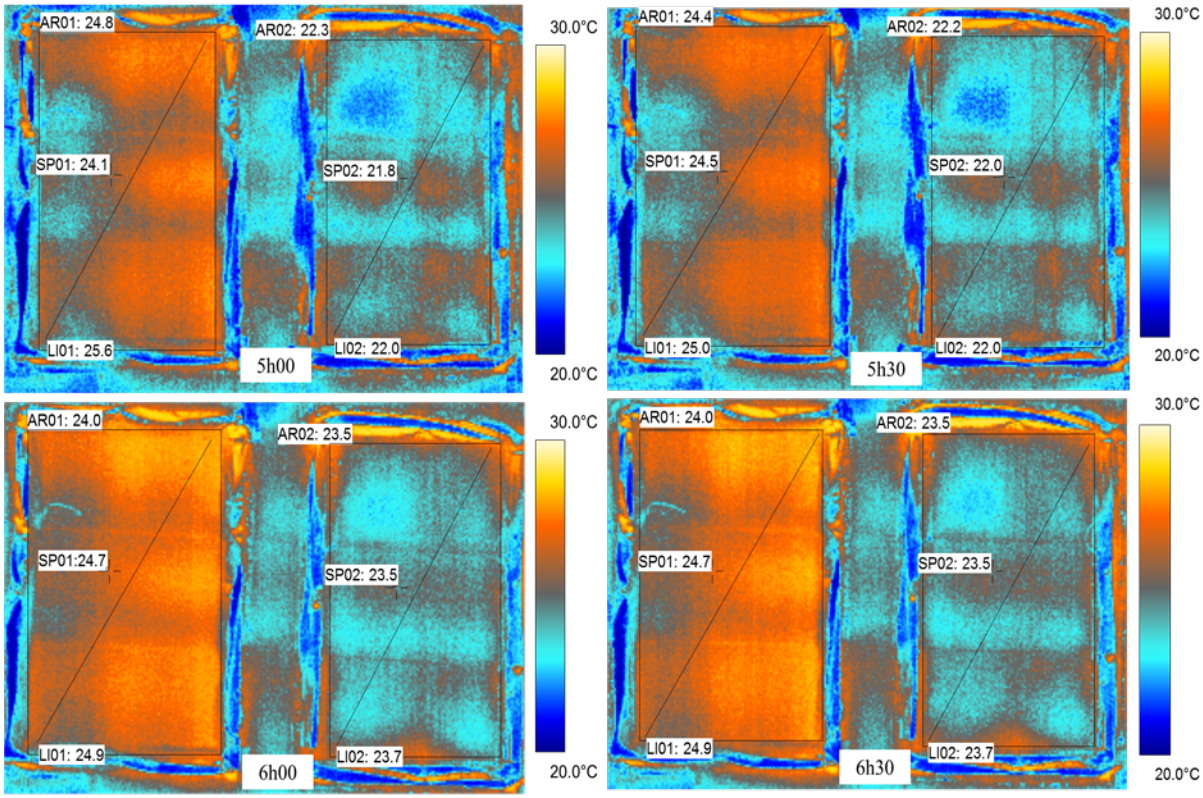

Figure 4.6: Thermograph of coated and uncoated wall surfaces before sunrise

From Figure 4.6, the coated surface appears as an orange colour, which lies between 24°C to 25°C according to the chart. Major area of the uncoated surface appears as sky blue, lying between 22°C to 24°C. Phases 3 and 4 of the uncoated surface temperature are 1.3°C higher than phase 1 and 2. In all phases, the surface area average temperature difference was 1.4°C between the coated and uncoated surface. The spot meter indicates an average temperature difference of 1.8°C between the two surfaces. Figure 4.7 shows the temperature distribution along the diagonal line across each sections of the wall surface.

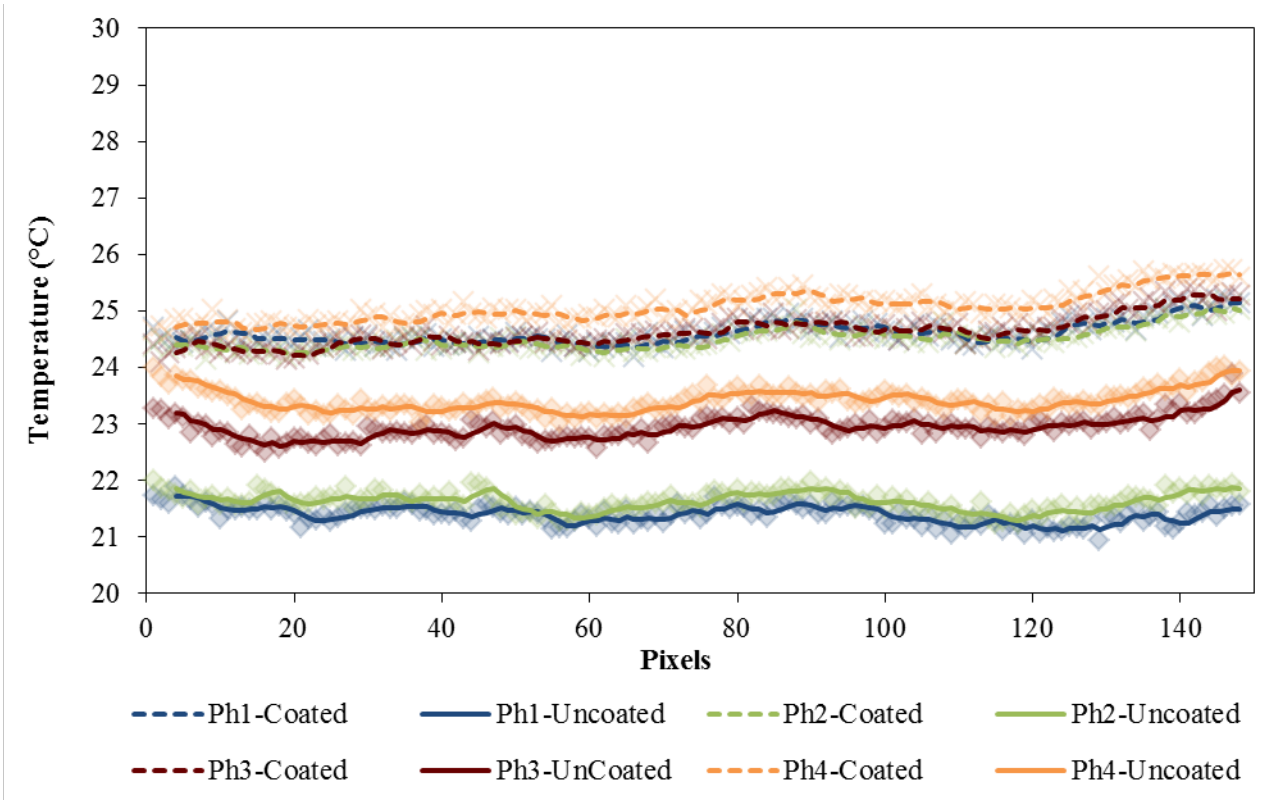

Figure 4.7: The wall inner surfaces temperature profile before sunrise

From Figure 4.7, the coated surface temperature was observed to be higher than that of the uncoated. Due to the temperature difference between the inner and outer space of the building, the indoor heat tend to flow outside. The TWAP film on the coated surface reflects some quantity of heat back into the building; as a result the coated surface appears warmer. Alternatively, the uncoated surface absorbed a large quantity of heat and transfer to the building surrounding, resulting in the relatively low surface temperature interpreted by the IR camera. It was also observed that the coated surface maintain a fairly constant temperature in all phases. However, a major change in temperature was observed on the uncoated surface in phases 3 and 4. Using Equation [2.16] i.e. $f = \frac{A_o}{A_e} = \frac{T_o^{max} - T_o^{min}}{T_e^{max} - T_e^{min}}$ and Figure 4.6, the decrement factor of the coated and uncoated surfaces was found to be 0.59 and 1.67, respectively. This implies that the coated surface

has more heat reduction compared to the uncoated surface. In other words, the uncoated surface allows more heat flow through its surface than the coated surface.

4.4.2 IR thermography of the wall surface at mid-day

The thermography of the wall surface at mid-day was captured between 12h30 to 14h00. The ambient air temperature was higher than the indoor temperature, at mid-day as shown in Figure 4.5. Thus, an inward flow of heat from outside of the building to the inner space occurs during this period. Figure 4.8 shows the IR thermography of the wall surface at mid-day. The coated surface was found covered in cold spots while the uncoated was covered in hot spots. This indicates that, at mid-day the uncoated surface emits more heat than the coated surface. In all phases, the lower regions of the coated surface appears as navy blue colour while the uncoated surface appears as dark orange colour mixed with little sky blue. The upper regions of the coated surface appear as sky blue colour while the uncoated surface appears bright orange colour. The vertical colour variation of the wall surfaces are attributed to the vertical temperature variation of the wall surface. Due to convectional current, temperature increased from the lower region of the wall surface to the upper region.

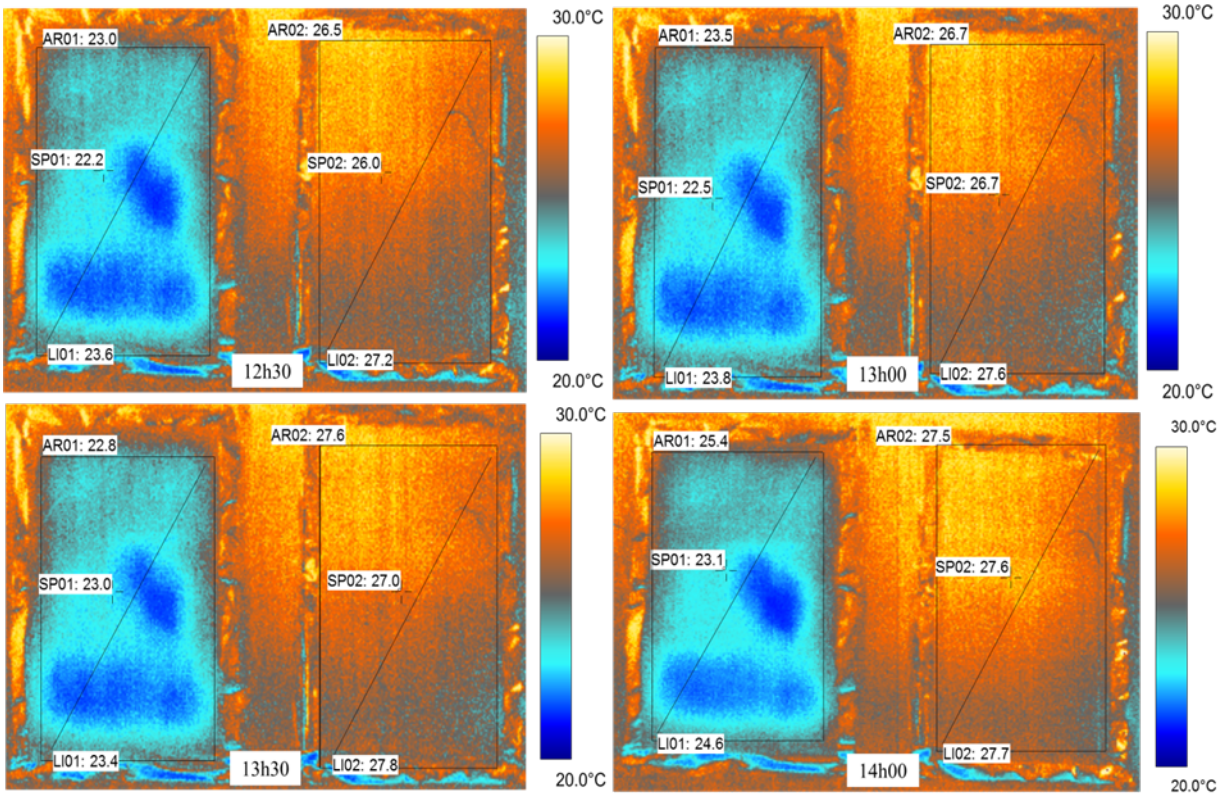

Figure 4.8: Thermograph of coated and uncoated wall surfaces at mid-day

Either way, the area tool in Figure 4.8, shows that the coated and uncoated surface area had an average temperature difference of 3.4°C. The spot meter indicates an average temperature difference of 4.1°C. Figure 4.9 shows the temperature distribution along the diagonal line across each section of the wall surfaces.

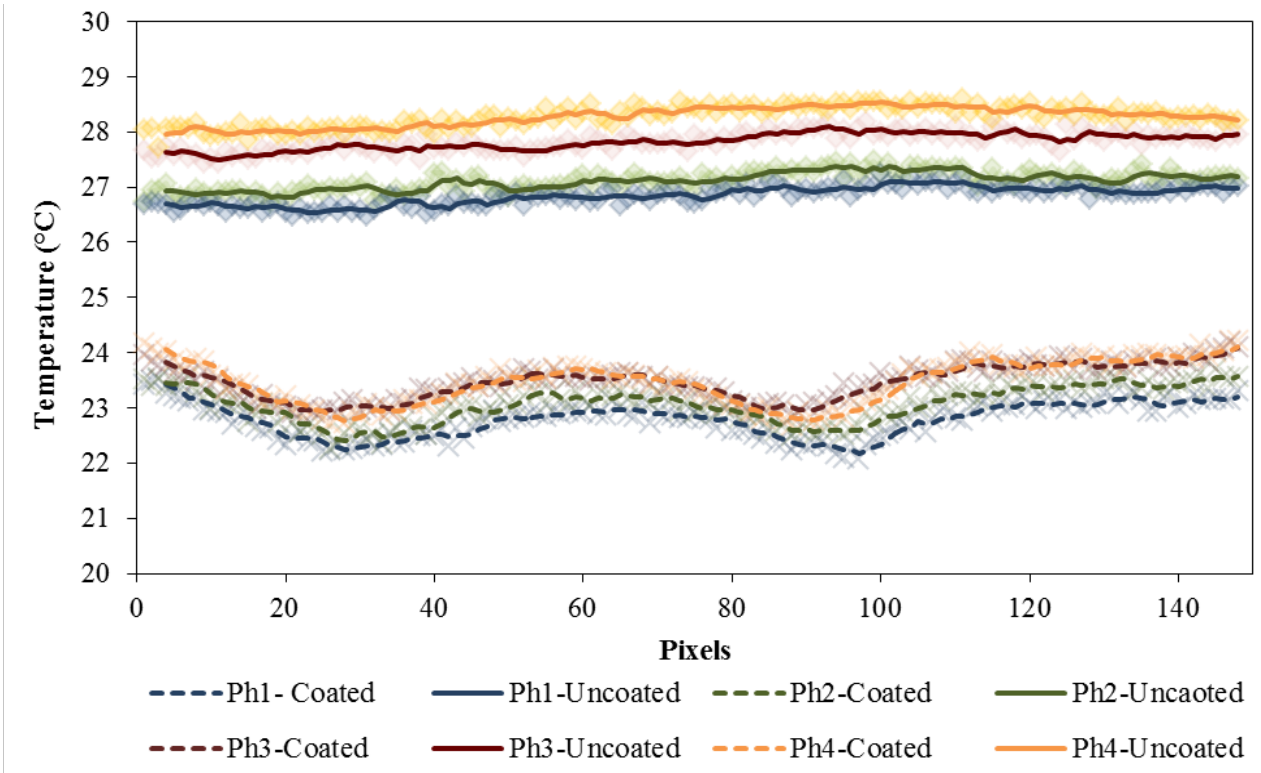

Figure 4.9: The wall inner surfaces temperature profile at mid-day

It was observed that the uncoated surface has higher temperature than the coated surface (Figure 4.9). This implies that the uncoated surface emits more heat than the coated surface. As a result of the outdoor and indoor temperature, heat flows from the outer surrounding to the inner space of the building. The ambient heat flows into the building easily through the uncoated surface compared to the coated surface. This is as a result of the IR reflectivity of the TWAP film on the coated surface. The film tends to reflect the heat from the outer wall surface, thereby reduce the amount of heat transmitted to the inner surface. Figure 4.10 illustrates the heat flow pattern of the coated and uncoated wall at mid-day.

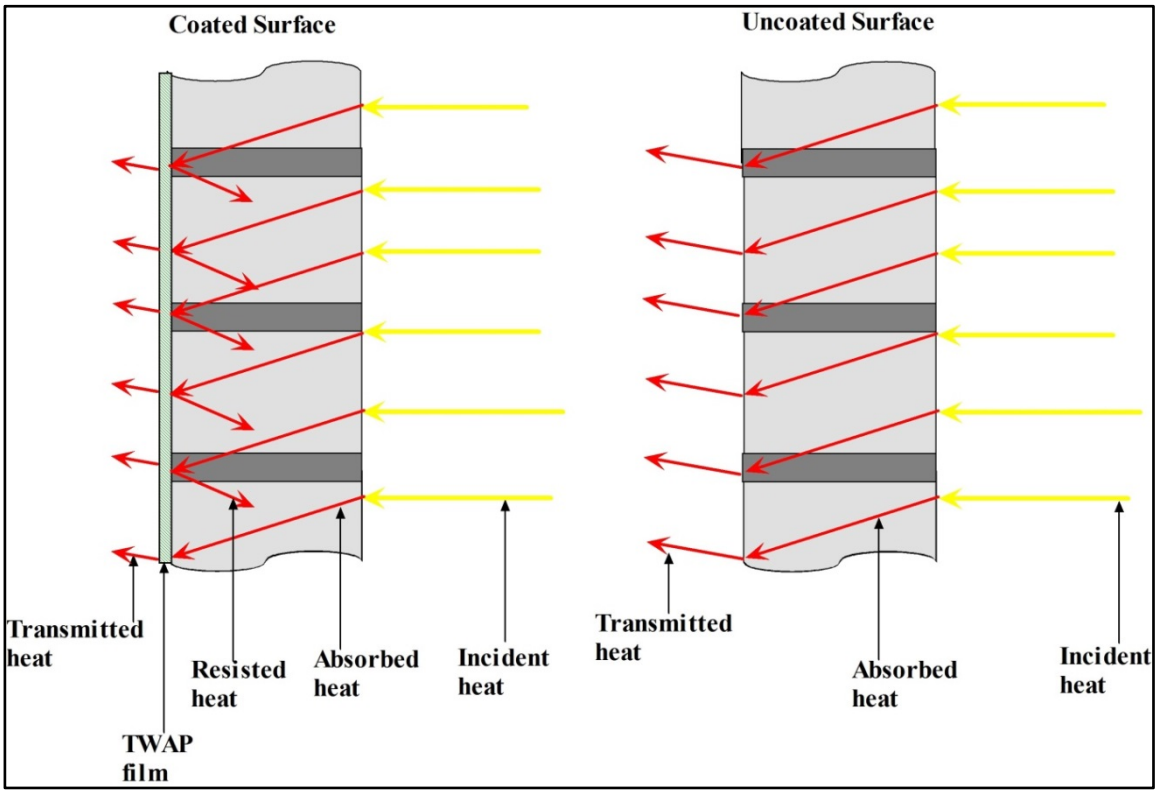

Figure 4.10: Pattern of heat flow in coated and uncoated wall surface at mid-day

From Figure 4.10, heat from the outer surface of the wall was reflected at the surface of the TWAP film. Although, some of the heat was transmitted through the surface of the film, but transmitted heat was also reflected by means of internal reflection. As a result of the transparent nature of TWAP (in dry state) and it's relatively high refractive index. Nevertheless, the heat from the outer surface increase with time, as a result heat escapes through the film to the inner surface of the wall. This results in the temperature increase with time of the coated surface as shown in Figure 4.9. Heat from the outer surface was transmitted with little resistance. Using Equation [2.16] and Figure 4.8, the decrement factor of the coated and uncoated surface was found to be 0.66 and 1.17. Again, it indicates that the uncoated surface has little heat reduction between the outer surface compared to the coated surface.

4.4.3 IR thermography of the wall surface after sunset

The process of heat transfer during the period after sunset is similar to the process before sunrise. The inner space of the building loses heat to the outer space. The thermography of the wall surface after sunset was captured between 18h00 to 20h00. Figure 4.11 shows the IR thermography of the wall surface after sunset.

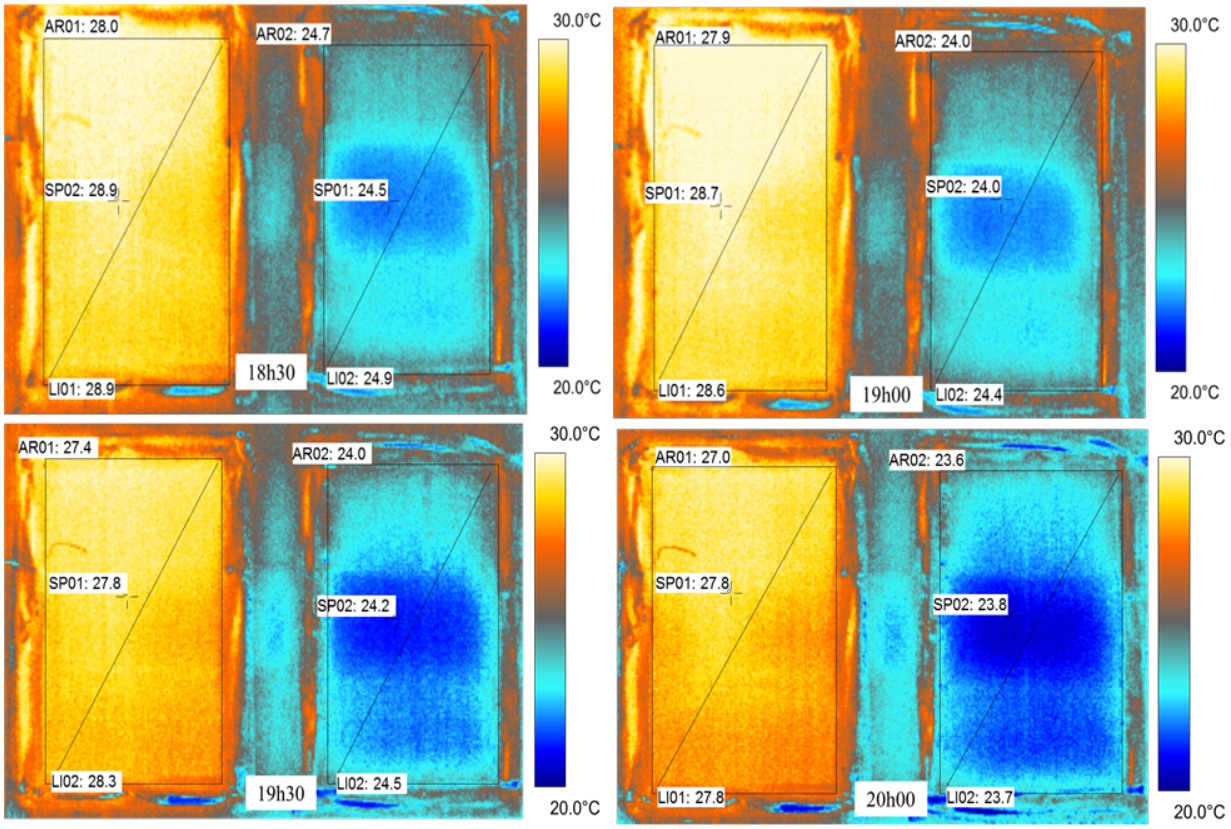

Figure 4.11: Thermograph of coated and uncoated wall surfaces after sunset

The coated surface appears gold-yellow whereas the uncoated surface was blue, indicating that the coated surface has a higher temperature than the uncoated surface (Figure 4.11). However, the orange colour of the coated surface and the navy blue colour of the uncoated surface in phases 3

and 4 were due to the decrease in the surface temperature with time. The vertical temperature variation of the wall was also noticed in phases 3 and 4, with orange colour on the lower region of the coated surface and navy blue on the uncoated surface. In all phases, the surface area average temperature difference was 3.5°C between the coated and uncoated surface. The spot meter indicates an average temperature difference of 4.2°C between the two surfaces. Figure 4.11 shows the temperature distribution along the diagonal line across each section of the wall surfaces.

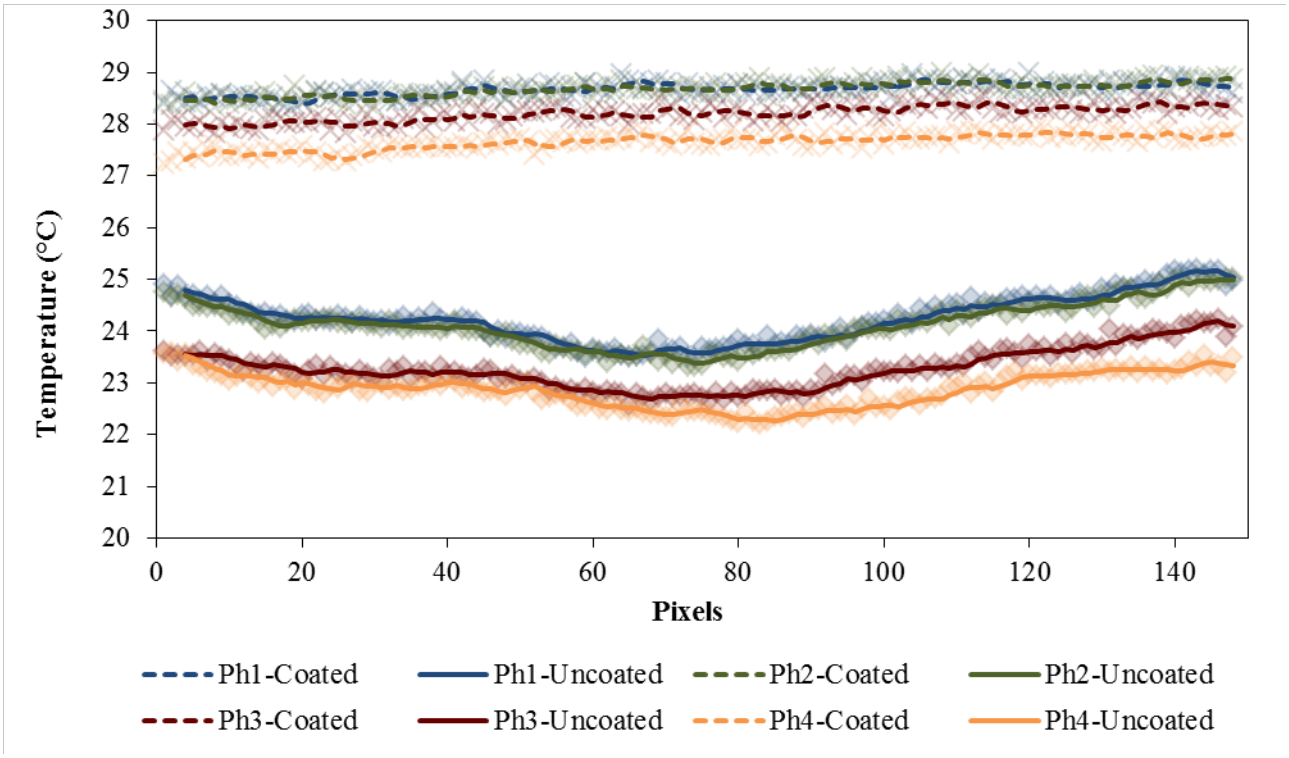

Figure 4.12: The wall inner surfaces temperature profile after sunset

The indoor temperature was greater than the ambient air temperature between 18h30 to 20h00 after sunset (Figure 4.5). Therefore, during this period (after sunset), the inner space of the building loses heat together with the building, resulting in the low temperature of the uncoated surface as shown in Figure 4.11. Nevertheless, a higher temperature was observed on the coated surface. As a

result of the IR reflection of the TWAP film. Figure 4.12 illustrates the heat flow pattern of the coated and uncoated wall after sunset.

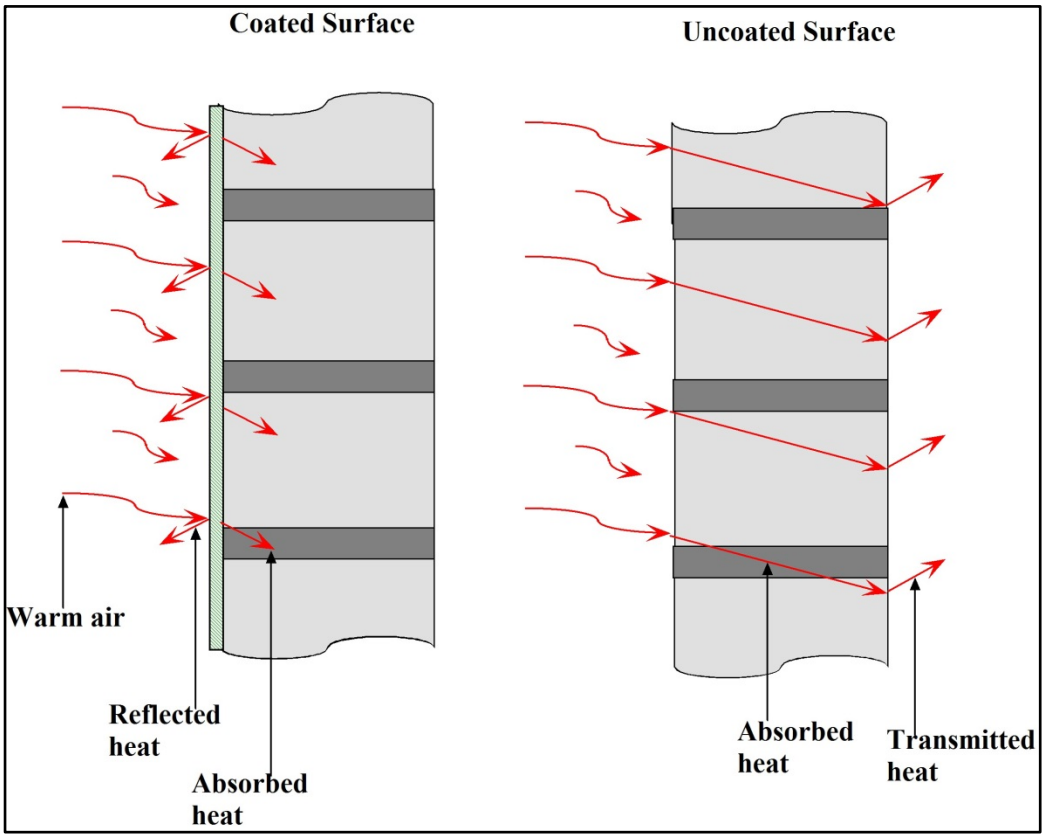

Figure 4.13: Pattern of heat flow in coated and uncoated wall surface after sunset

Since the wall was not coated on both surfaces (inner and outer), the coated suraface also loses heat to the building surrounding (Figure 4.12). The intention of the TWAP film was not to reduce heat lost in the wall but to minimise the indoor and outdoor heat transfer through the wall. As in Figure 4.12, the TWAP film managed to reduce the heat transfer by reflecting heat backing to the inner space of the building. The reflected heat was sensed as emitted heat by the IR camera, which is interpreted as the surface temperature of the coated surface. The uncoated surface on the other hand, allows the flow of heat through the wall with little or no resistance. Thereby resulting in low

temperature of the uncoated surface revealed by the IR thermography. With reference to Equation [2.16] and Figure 4.12, the decrement factor of the coated and uncoated surface was found to be 0.37 and 0.27.

4.5 SUMMARY

The surface texture of TWAP in its dry state was shown by the SEM analysis. It was observed that TWAP coatings thicker than 127 microns (approximately 3 strokes of paint brush) results in crack and flake of the film. Consequently, reduces the thermal performance of the material, as IR radiation will flow freely through these cracks.). EDX spectrum of the paint reveals Aluminum (Al) which is present as Al_2O_3. Al_2O_3 with a refractive index 1.73 serves as one of the IR reflective pigments used in reflective paints. Other compounds like SiO_2 that contribute to the thermal properties of the paint, were also identified. The functional groups that made up the different molecular bonding of the paint were clearly shown by the FTIR spectral, namely O–H, CH_2, Si–H, C═C and others. The IR thermography showed the temperature difference between the coated and uncoated surface. It was found that before sunrise and after sunset, the coated surface temperature was higher than the uncoated. At mid-day, the temperature of the coated surface was lower than the uncoated surface. This implies that the TWAP film was able to reduced the outward flow of heat during the period before sunrise and sunset; this also reduces the inward flow of heat at mid-day.

CHAPTER 5

THERMAL PERFORMANCE PROFILE OF THE BUILDING

5.1 INTRODUCTION

Thermal performance of a building describes the thermal influence of the building envelope on the indoor thermal comfort level. Building envelope on the other hand, are those components such as; walls, roof, floor, windows and doors, that protect the inner space of a building from the weather factors. Indoor thermal comfort is influenced by air temperature, thermal radiation, air speed, relative humidity, metabolic rate (sitting versus physical activity) and clothing [Markov, 2006]. However, indoor air temperature and relative humidity have significant impact on an occupant's perception to indoor thermal comfort. The South African Building Code (SABC) recommends the indoor temperature range of 16°C to 28°C and relative humidity of 30% to 60% [Agrement, South Africa, 2002]. A poor thermal performance building implies that the building envelope shows minimal thermal resistance to the weather factors, hence shifting the indoor temperature and relative humidity out of the comfort zone.

This chapter presents the thermal performance baseline of the building before the inner surfaces of the walls were coated with translucent water-based acrylic paint. The results and findings in this chapter show the thermal performance of the living room. Therefore, the building envelope in this context includes; the roof, floor and walls. The three external walls refer to the North, West and South walls enclosing the inner space of the living room from the building surrounding.

5.2 THERMAL PERFORMANCE IN SUMMER

5.2.1 Thermal influence of building envelope on indoor temperature

Figure 5.1 shows a simulation of the solar altitude of a typical summer hot day

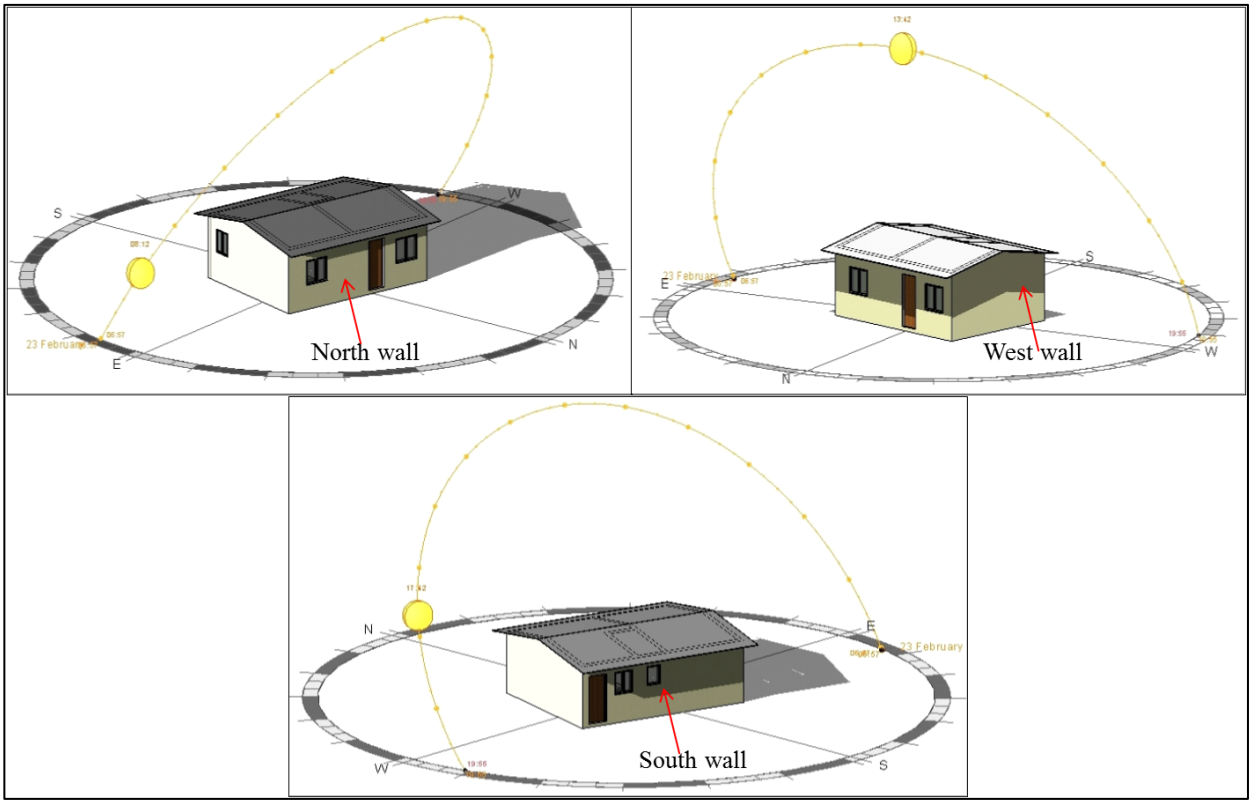

Figure 5.1: Simulation of solar altitude of a typical hot summer day

From Figure 5.1 it was observed that the East wall of the house received direct solar radiation at the early hours of the morning while the other walls are covered in shade. The house was designed such that in summer the house sits on its own shade, thus keeping the indoor temperature within the comfort zone. Consequently, more than half of the outer surface area of the North wall was in shade. The West wall was exposed to direct solar radiation at about 13h00 and received maximum

intensity from 15h00 to 17h00. The south wall was observed to only receive direct solar radiation from 17h00 to 18h30, with more than half of its outer surface in shade. As a result, the geographical orientation of the external wall creates a temperature variation among the walls, which cause the thermal influence of the external walls on the indoor temperature to vary.

However, the indoor temperature results from the thermal influence of each component of the building envelope subjected to the weather condition. Figure 5.2 shows the temperature profile of the building envelope and indoor temperature in summer season. It was seen that the roof dominates the surface temperature of the building envelope, with an average temperature of 33.00°C The roof attains a maximum temperature of 81.00°C on 26 February at 13h00 and a minimum temperature of 10.40°C at 06h30 on 12 April. The temperature of the middle-wall was found to closely follow the temperature of the variation of the roof. The average temperature of the middle-wall was found to be 31.72°C. The West wall was found to have the highest temperature of 43.59°C with respect to the external walls.

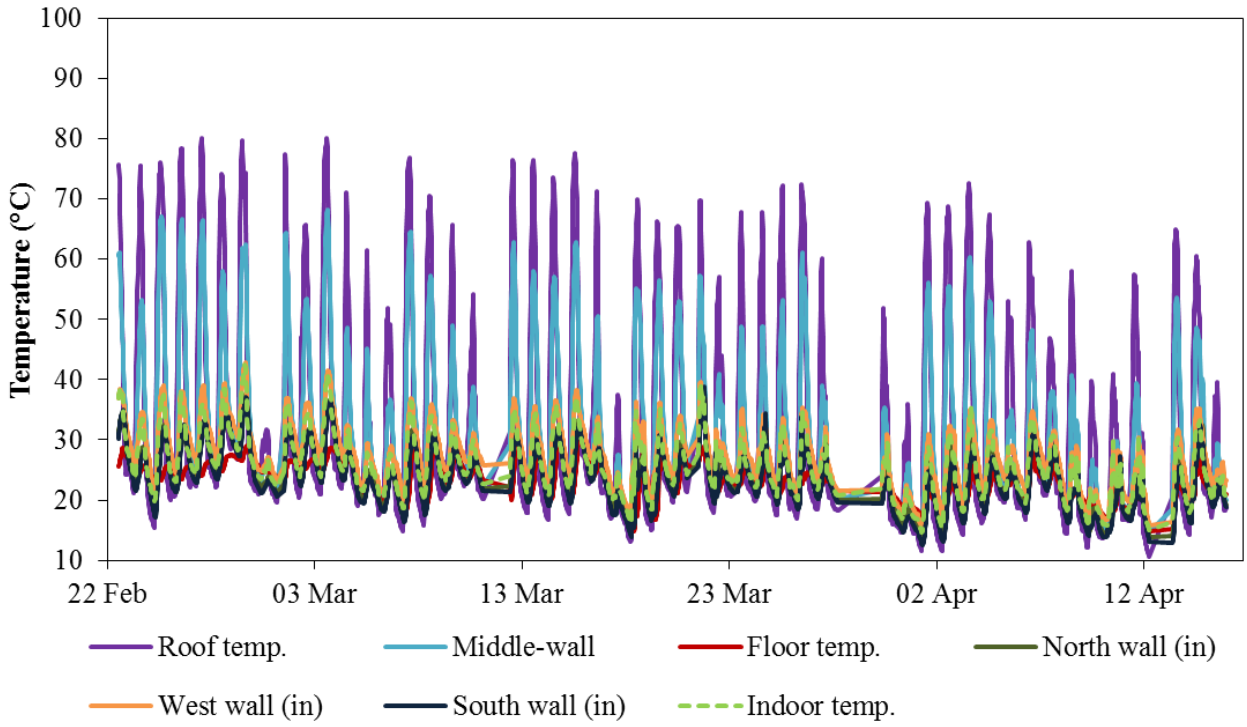

Figure 5.2: Building envelope and indoor temperature profiles in summer season

Despite the relatively high temperature of the roof and middle-wall, the indoor temperature fluctuation was seen to follow the temperature variations of the three external walls. A typical hot summer day was used to analyze the thermal influence of the building envelope on the indoor temperature. 23 February, 2012 received a maximum solar irradiance of 1364 W/m^2 and was used as the typical hot summer day. Figure 5.3 shows the thermal influence of the building envelope on the indoor temperature on a typical hot summer day.

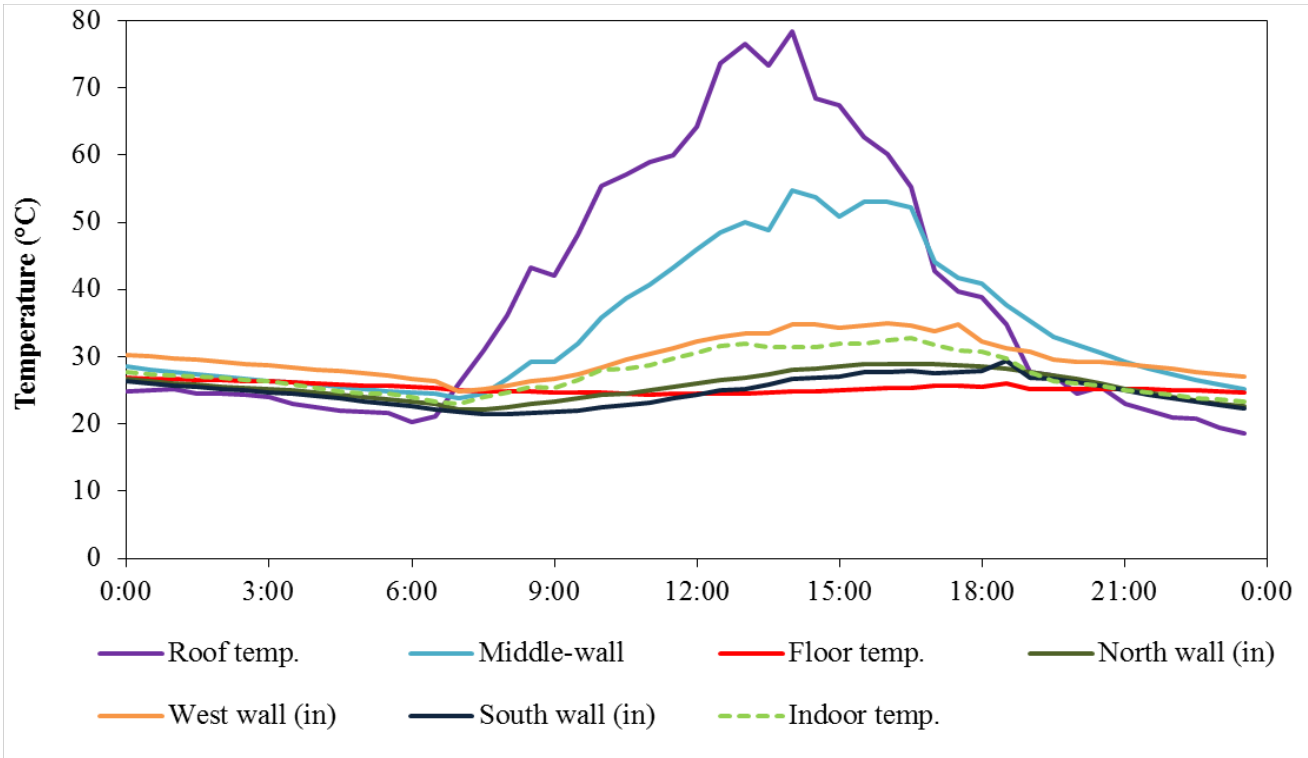

Figure 5.3: Thermal influence of the building envelope on indoor temperature on a typical hot summer day

It is evident from Figure 5.3, that the indoor temperature follows the external walls temperature fluctuation despite the temperatures of the roof and middle-wall. The roof of the house is made of galvanized iron sheet of 0.3 mm thick. Galvanized iron sheet is a good thermal conductor but has a very low thermal storage capacity. During the day, the roof temperature is higher than the indoor temperature, as a result warm air indoor rises to the roof. As the roof temperature increases, the temperature of air closer to the roof also increases. This therefore creates almost a stagnant vertical temperature gradient, trapping the heat to the roof. At night the roof temperature will be lower than the indoor temperature, and the tendency that warm air raises resulting in the warm air being cooled by the roof, making it descend again. This will result in indoor temperature swing. The relatively high surface temperature of the middle-wall is as a result of its position. As the name implies, the wall is located at the middle of the house, shielded from the weather conditions. This

tends to increase its thermal conductivity due to its high moisture content. Since the house has no mechanic cooling system, slight indoor temperature change will increase the middle-wall temperature. During the day, the middle-wall absorbs and stores heat from the living and bedroom. At night when the indoor temperature (bedroom and living room) drops, it releases heat back into the rooms.

Among the three external walls, the West wall was found to have the highest surface temperature with an average of 29.89°C (Figure 5.3). The lowest temperature was recorded in the South wall with an average value of 24.77°C. The indoor temperature was observed to closely follow the temperature variation of the West wall. This is as a result of the large surface area of the West wall (14.99 m^2) compared to the middle-wall (7.780 m^2). The middle-wall is approximately half the surface area of the West wall and less than a third of the total surface area of the external walls. Due to the significant temperature difference between the middle-wall and the external walls, the indoor temperature was dominated by the West wall. The floor attained a maximum and minimum temperature of 26.82°C and 24.43°C, respectively, with a daily temperature swing of 0.12°C. During the day, the indoor temperature increases above the floor temperature, due to convectional current cool air drop to the floor. This forms a dense cold air on the floor due to its fairly constant low temperature, thereby having no significant influence on the indoor temperature. However, it was seen that the thermal influence of the external walls on indoor temperature depends on the walls orientation and surface area. Figure 5.4 shows the indoor temperature, inner and outer surface temperature of the three external walls in summer season.

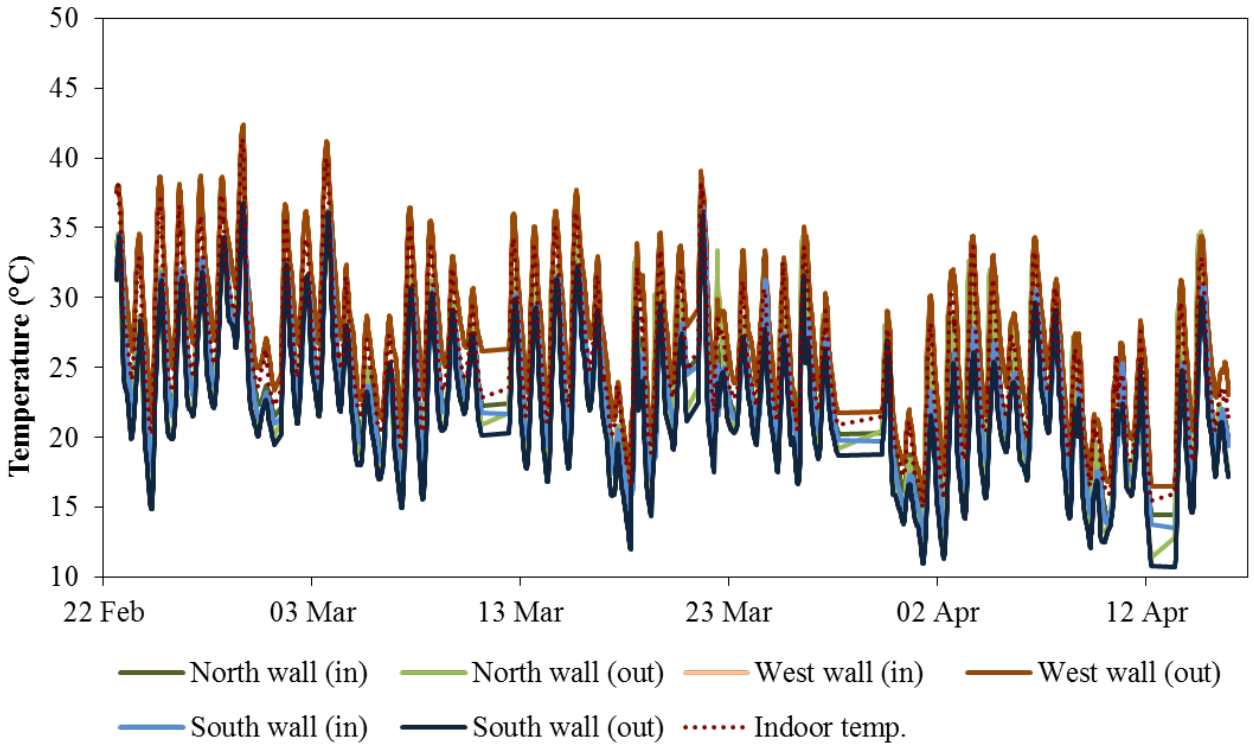

Figure 5.4: Indoor temperature response to wall inner and outer surface temperature variation in summer season

In Figure 5.4, it was observed that the west wall has the highest outer and inner surface temperature while the South wall has the lowest. The outer and inner surface temperatures of the North wall were relatively moderate, lying between the West and South walls temperature. It was also observed that the indoor temperature closely follows the temperature variation of the west wall throughout the season. Figure 5.5 shows the temperature distribution of the indoor, inner and outer surface of the three external walls on a typical hot summer day.

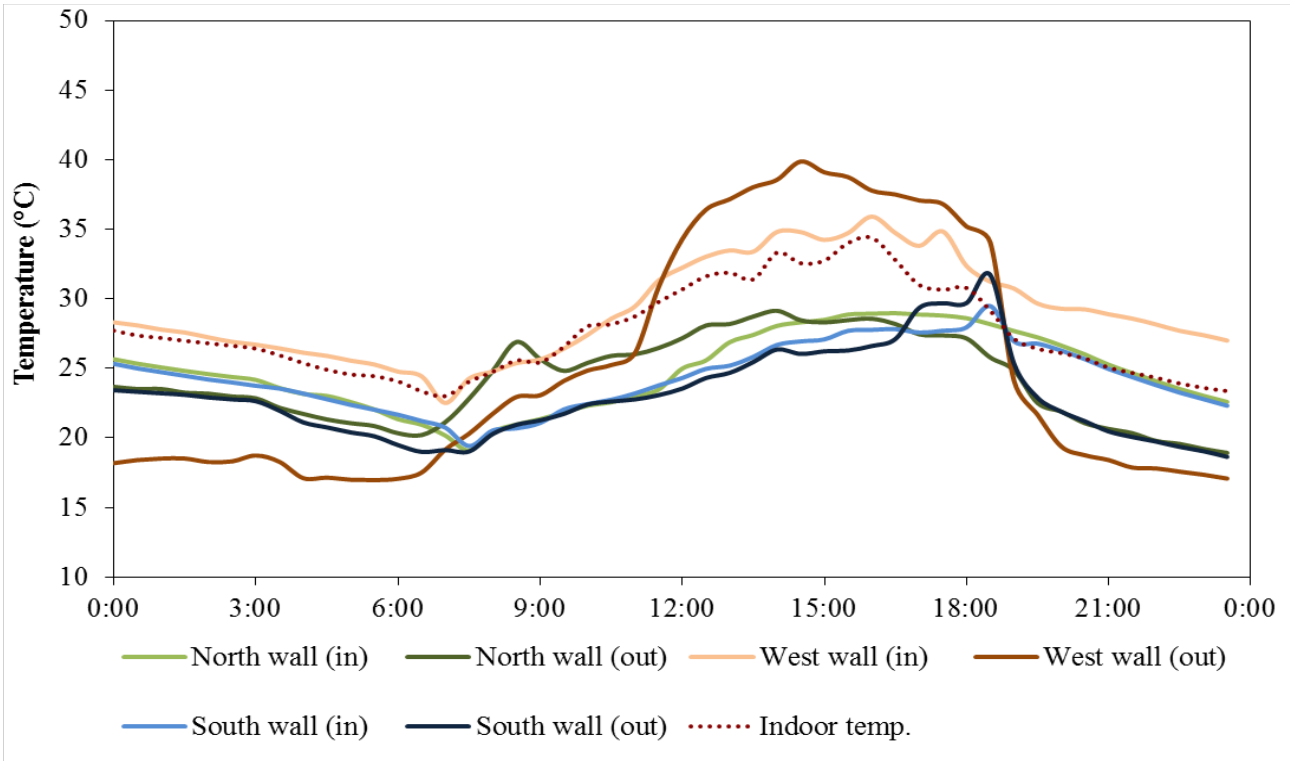

Figure 5.5: Indoor temperature response to wall inner and outer surface temperature variation on a typical hot summer day

In Figure 5.5 it was observed that the average temperature of the West wall is approximately 24.82°C. During the day (6h00 to 19h00), the West wall has the highest (inner and outer) surface temperature and the lowest outer surface temperature at the early hours of the morning (0h00 to 5h30) and at night (19h00 to 23h00). However, Figure 5.1, the West wall which is facing geographical Northwest was found to receive direct solar radiation from 13h00 to 17h00 and attains a peak outer surface temperature of 39.87°C at 14h00. Whereas, the corresponding inner surface attained its peak temperature of 35.91°C at 16h00; thus giving a time lag of 2 hours. The relatively high outer and inner surface temperature of the west wall is attributed to the high thermal mass of the wall. Furthermore, the thermal mass was also responsible for the low outer surface temperature of the wall at night. From Figure 5.5, the North wall outer surface temperature was found to have a sharp peak at around 08h30, then gradually increases and attain a maximum

temperature of 29.14 °C at 14h00. Due to the passive solar design, at mid-day more than half of the surface area of the North wall was in shade (Figure 5.1). Hence the wall experiences a low rate of temperature increase. However, the inner surface temperature of the North wall peaks at 16h00 with a temperature of 28.97°C, therefore have a time lag of 2 hours. The South wall was found to attain maximum temperature at a much later hour of the day, that is., between 17h00 to 18h30. It was also seen that the inner surface temperature of the South wall was greater than that of the outer surface, although both surfaces attain maximum temperature at the same time (18h00). The South wall; which is facing geographical Southwest, was found to receive direct solar radiation for only 2 hours of the day (Figure 5.1). As such, the inner surface temperature of the South wall is influenced more by heat gained indoors, either from human activities or heat from other components of the building.

The indoor temperature was found to be higher than the North and South walls surface temperatures but lower than the surface temperature of the west wall, during the day (Figure 5.5). It was also seen that, during the early hours of the morning and at night, the indoor temperature was closer to the surface temperatures of the North and South walls than the West wall. During the day the surface temperature of the West wall dominates the indoor temperature while at night and in the early hours of the morning, the indoor temperature is dominated by the North and South walls. Although the inner surface temperature of the West wall was relatively high at night and the early hours of the morning, but due to the low outer surface temperature, the West wall loses more heat to outside than inside of the building. Thus, the North and South walls serve as heat source to the inner space of the building at night and the early hours of the morning.

The temperature variations on the inner and outer surface of the three walls imply fluctuations in the rate of transfer among the walls. Figure 5.6 shows the temperature difference between the outer and inner surface of the external walls on a typical hot summer day.

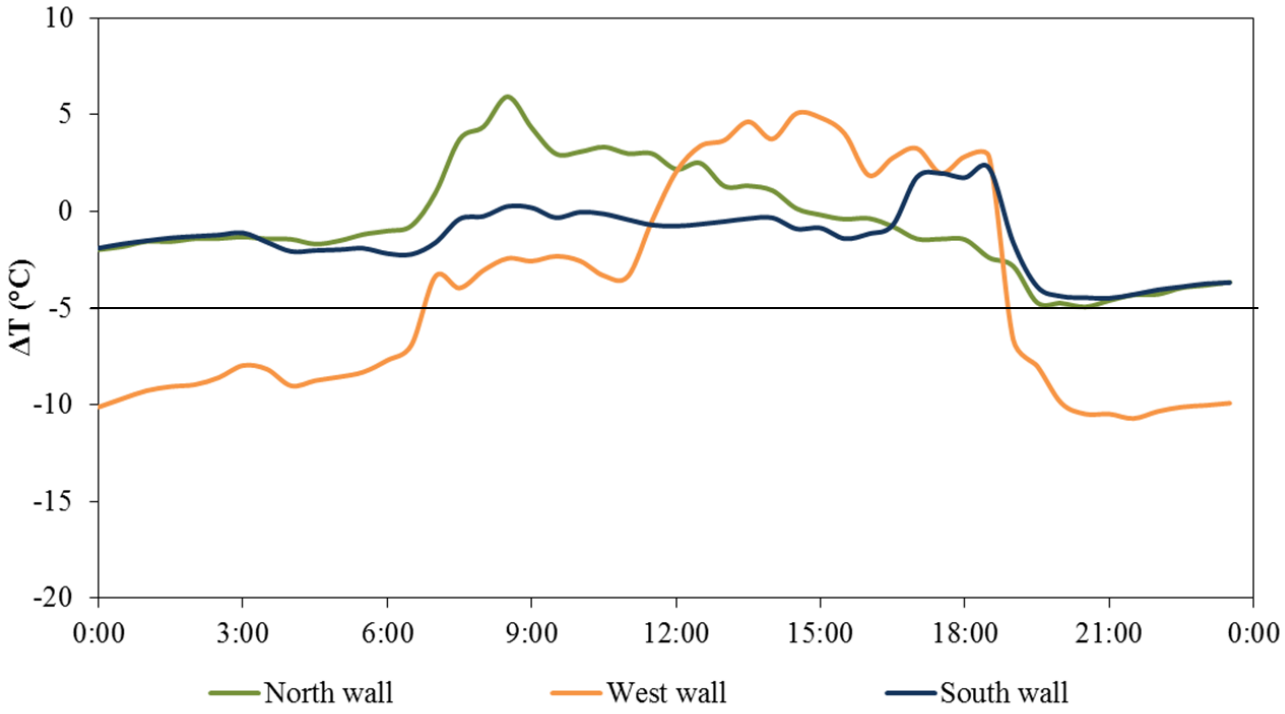

Figure 5.6: Outer and inner temperature difference of the external walls on a typical hot summer day

With reference to equation [2.3] i.e., $q = -kA\frac{\Delta T}{\Delta l}$ and Figure 5.6, and taking the thermal conductivity of concrete block to be 0.51 W/m°C [Al-Jabri, 2004], the average maximum heating rate of the North wall was found to be 5.93 W, which occurs at 8h30. Also, the average maximum heating rate of the West and South walls were found to be 5.07 W and 2.24 W, respectively, occurring at 14h30 on the West wall and 18h30 on the South wall. The times at which the walls (North, West and South) attain maximum heating rate correspond to the period at which the walls were exposed to direct solar radiation (Figure 5.1). Furthermore, the average maximum cooling

rate of the walls were also calculated; it was found that the North, West and South walls had an average maximum cooling rate of 4.94 W, 10.71 W, and 4.49 W, respectively. Furthermore, all three walls attained maximum cooling rate at approximately 21h00. This is just after the period when the family activities such as cooking, eating and other domestic activities have taken place, thus resulting in the increase of indoor temperature. It is evident from the results obtained from the rate of heat transfer through the walls that the thermal effect of the walls depends on the orientation and surface area. Figure 5.7 shows the rate of heat transfer through the external wall on a typical hot summer's day.

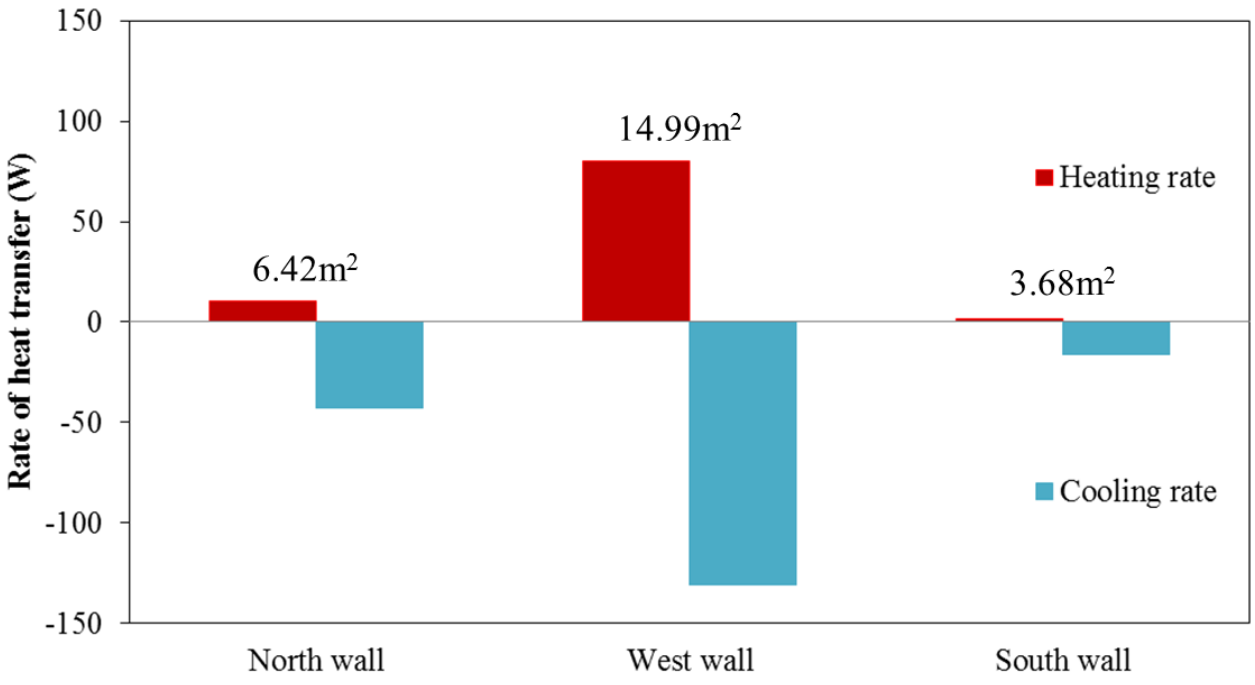

Figure 5.7: Heat transfer rate through external walls on a typical hot summer day

From Figure 5.7, it was observed that the West wall has the highest heating and cooling rate while the South wall has the least heating and cooling rate. This can be attributed to the orientation and the surface areas. It can be said that the West wall with a surface area of 14.99 m^2 is the most

thermally active wall while the South wall is the least thermally influential wall to the indoor temperature distribution.

5.2.2 Indoor air temperature and humidity

The indoor temperature is as a result of mechanical or domestic heating and heat transfer between the inner space of the building and its surrounding. The indoor temperature at a given outdoor temperature was found to be a distribution rather than a single value. Figure 5.8 shows the indoor, outdoor temperature distribution and relative humidity for summer season.

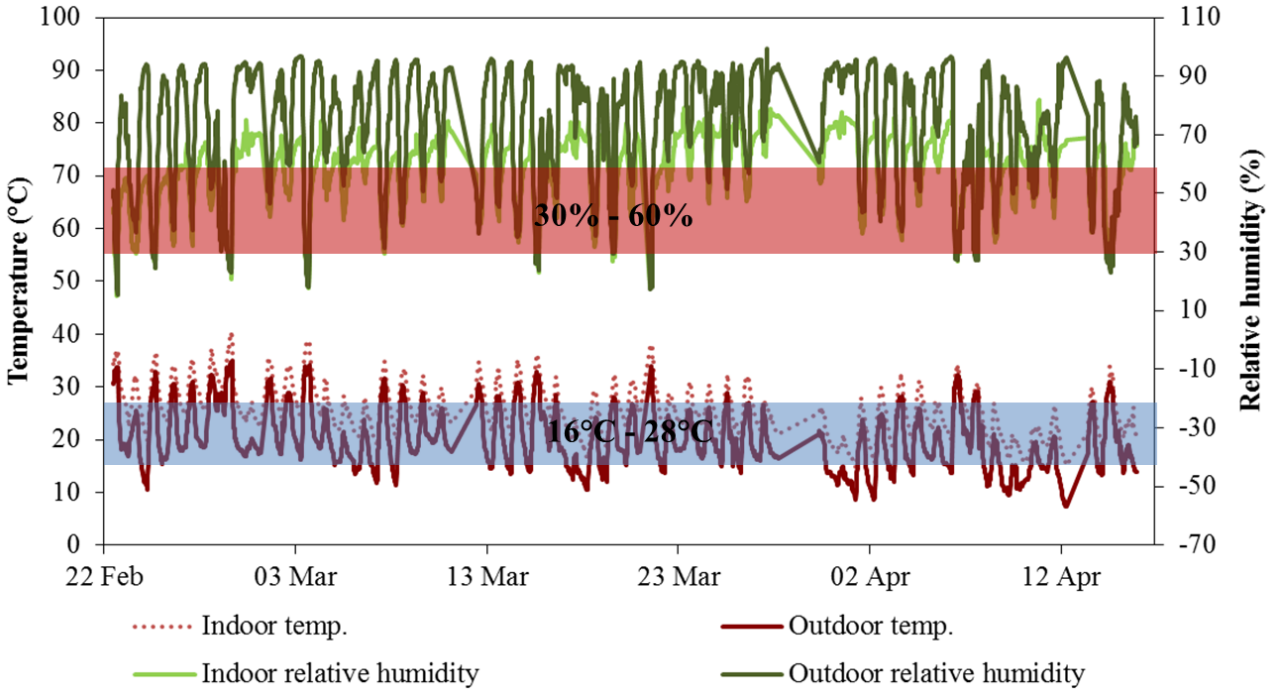

Figure 5.8: Temperature and humidity response in summer season

In Figure 5.8 the indoor temperature was generally higher than the outdoor temperature with an average temperature difference of 5.59°C. The maximum indoor temperature attained was 40.79°C

while the outdoor temperature was 33.38°C. During the day, the occupants are usually out, leaving the doors and windows closed. Hence, heat generated, from electrical appliances and the building envelope are trapped indoors, increasing the indoor temperature.

Figure 5.9, shows the indoor & outdoor temperature distribution and relative humidity on a typical hot summer day. It was found that the indoor temperature was within the comfort zone for 46% of the time, while the outdoor temperature was within the comfort zone throughout the day. The indoor relative humidity followed the outdoor relative humidity distribution but with a time lag of 1 hour.

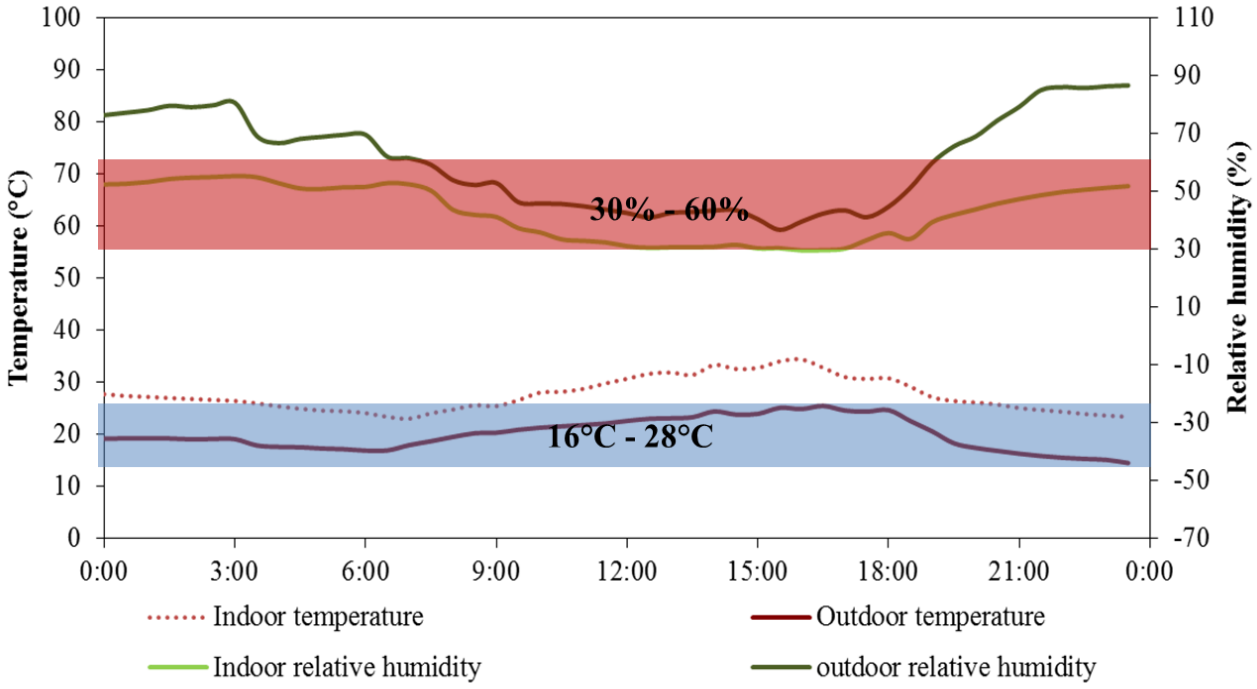

Figure 5.9: Temperature and humidity response on a typical hot summer day

With reference to Figure 5.9 the outdoor relative humidity was found to have higher amplitudes than the relative humidity, and that the indoor relative humidity was completely within the comfort

zone throughout the day. The maximum indoor and outdoor relative humidity recorded were 55% and 85%, respectively. The mean outdoor and indoor relative humidity difference was 17%. From all observations the outside of the house is more thermally comfortable than the inside. This is attributed to the design and the size (approximately 19.8 m^2) of the living room. The used appliances and cooking tend to increase the indoor temperature above the comfort zone.

5.2.3 Wind speed and direction

Wind can be channelled to different zone in a building to maintain a thermal comfortable indoor environment through proper operation of the ventilation components. Correct management of the design of ventilation components will regulate the indoor temperature and relative humidity, keeping the indoor environment within the comfort zone. Figure 5.10 shows the wind speed distribution of Golf course settlement, Alice, while Figure 5.11 shows the wind direction distribution.

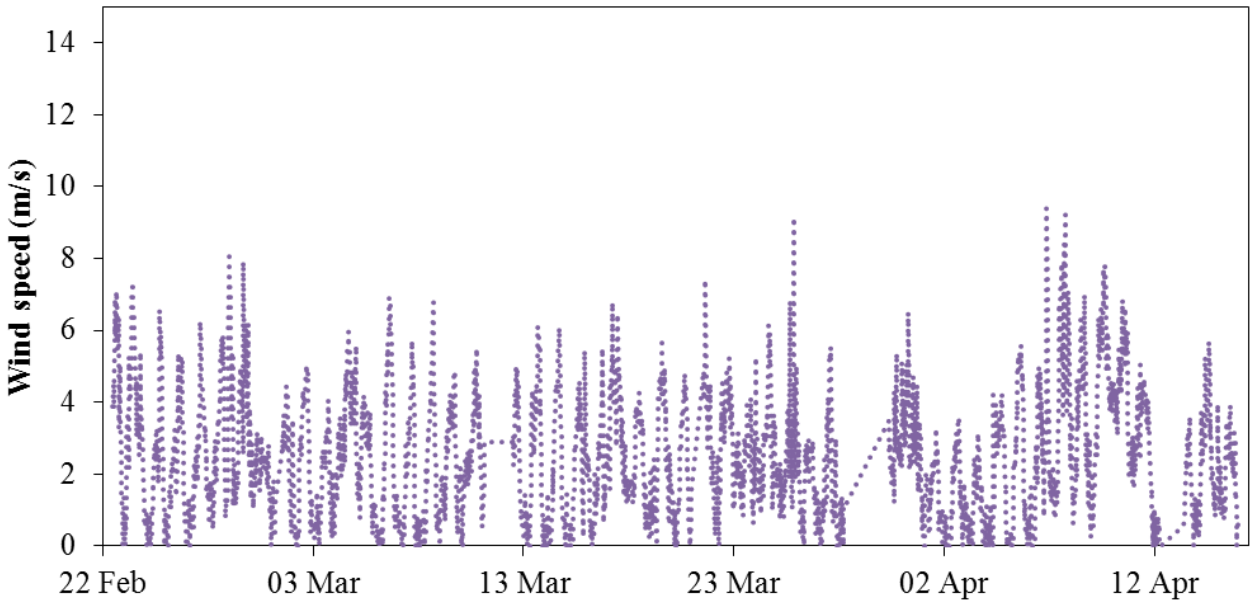

Figure 5.10: Wind speed distribution in summer season

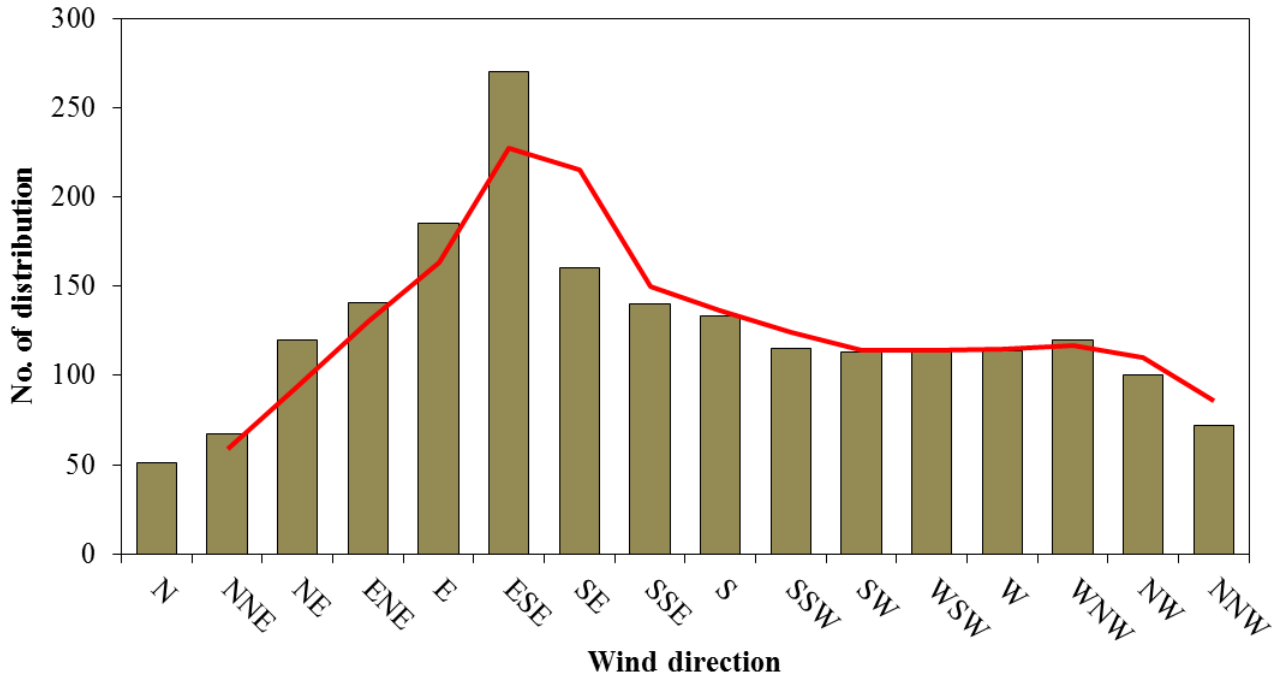

Figure 5.11: Wind direction in summer season

Figures 5.10 and 5.11 show that Golf Course, Alice experiences S (110°) E prevailing wind with an average wind speed of 2.4 m/s in summer. The highest wind speed of 9.13 m/s was recorded on 25 March at 20h00. In addition, the time range at which the wind speed was mostly at its maximum was between 8h00 to 20h00. Due to the direction of the wind, the east elevation of the building experiences much of the cooling effect of the wind.

5.2.4 Solar radiation

The daily and seasonal sun path, cloud cover and wind speed, etc., attribute to the indoor temperature swing. Figure 5.12 shows the outdoor and indoor temperature response to solar radiation.

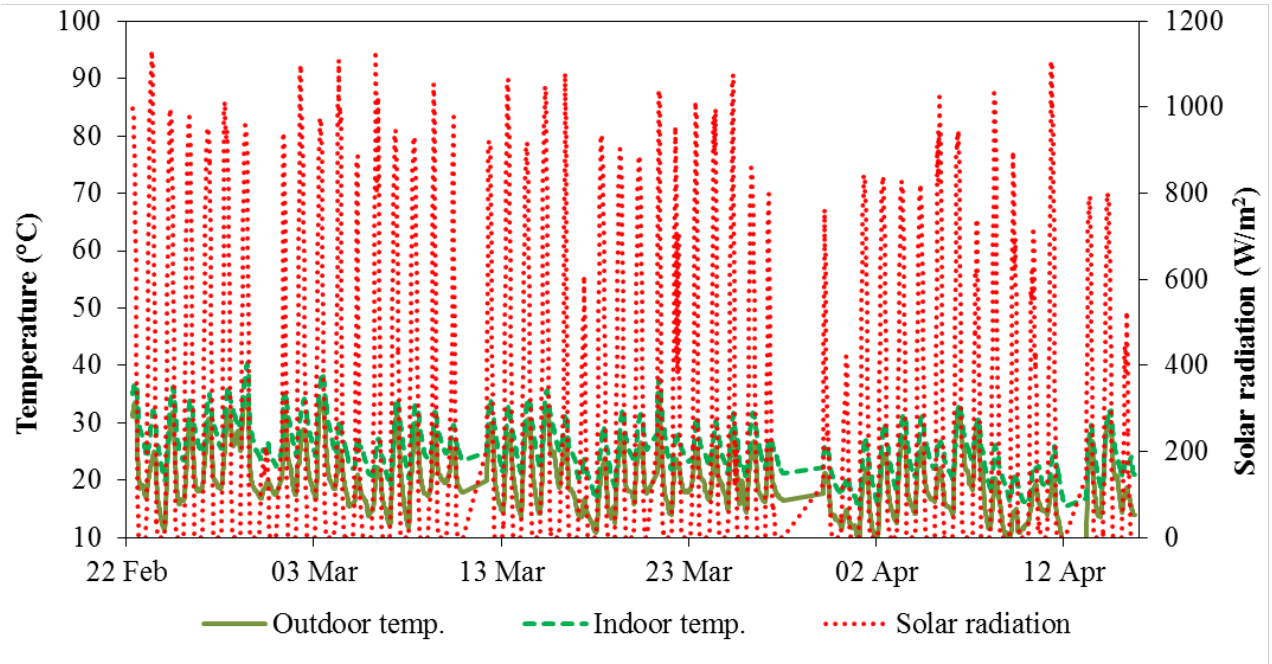

Figure 5.12: Outdoor and indoor temperature response to solar radiation in summer season

In Figure 5.12, it was observed that the indoor and outdoor temperature followed the fluctuations of the solar radiation, with the outdoor temperature responding faster than the indoor temperature. When the solar radiation was at its maximum, the indoor maximum temperature lagged behind by approximately 2.5 hours while the outdoor temperature lagged by 0.5 hours. A typical hot summer day was used to show the indoor temperature response to the solar radiation. Figure 5.13 shows the outdoor and indoor temperature variation to solar radiation on a typical hot summer day.

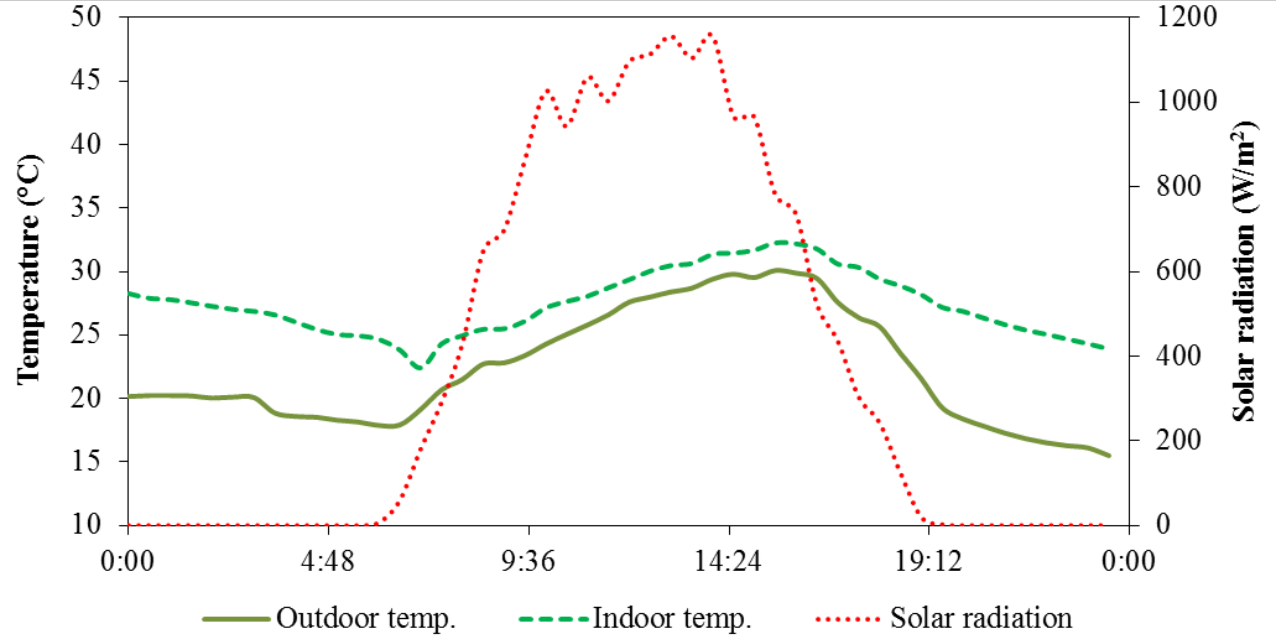

Figure 5.13: Outdoor and indoor temperature response to solar radiation on a typical hot summer day

From Figure 5.13 it was observed that the indoor and outdoor temperature rate of increase and decrease were different indicating different response to the solar radiation. The indoor temperature response to solar radiation relies on thermal performance of the building envelope. The outdoor temperature increase at an average rate of 3.5 °C/h while the indoor increased at 2.7 °C/h. The average rate of temperature decrease for the outdoor was found to be 5.3 °C/h while the indoor was

3.4 °C/h. The outdoor temperature start increasing 30 minute after the sun rises (6h00) while the indoor temperature took approximately 1 hour to respond to the sun radiation. The indoor temperature increase is as a result of the solar energy transfer through the building envelope. The penetrated solar radiation influences the indoor temperature and relative humidity, interfering with the indoor thermal comfort level. The penetrated solar radiation increases the indoor temperature, as a result indoor relative humidity decreases. At mid-day, the house seat on its own shade, thereby reducing the rate of indoor temperature increase.

5.3 THERMAL PERFORMANCE IN WINTER

5.3.1 Thermal influence of building envelope on indoor temperature

Figure 5.14 show a simulation of the building solar altitude of a typical winter cold day. It was observed that a relatively low solar altitude was experienced in winter season. The sun was seen to rise at approximately N72°E of the house, thus the East and West walls were exposed to direct solar radiation at the early hours of the morning. At mid-day, the North wall receives the solar radiation at high intensity, with no shade of the eaves on the wall. This was as a result of the low solar altitude. On other hand, the West wall was exposed to solar radiation around 13h00 and receives the solar radiation at high intensity from 16h00 to 18h00.

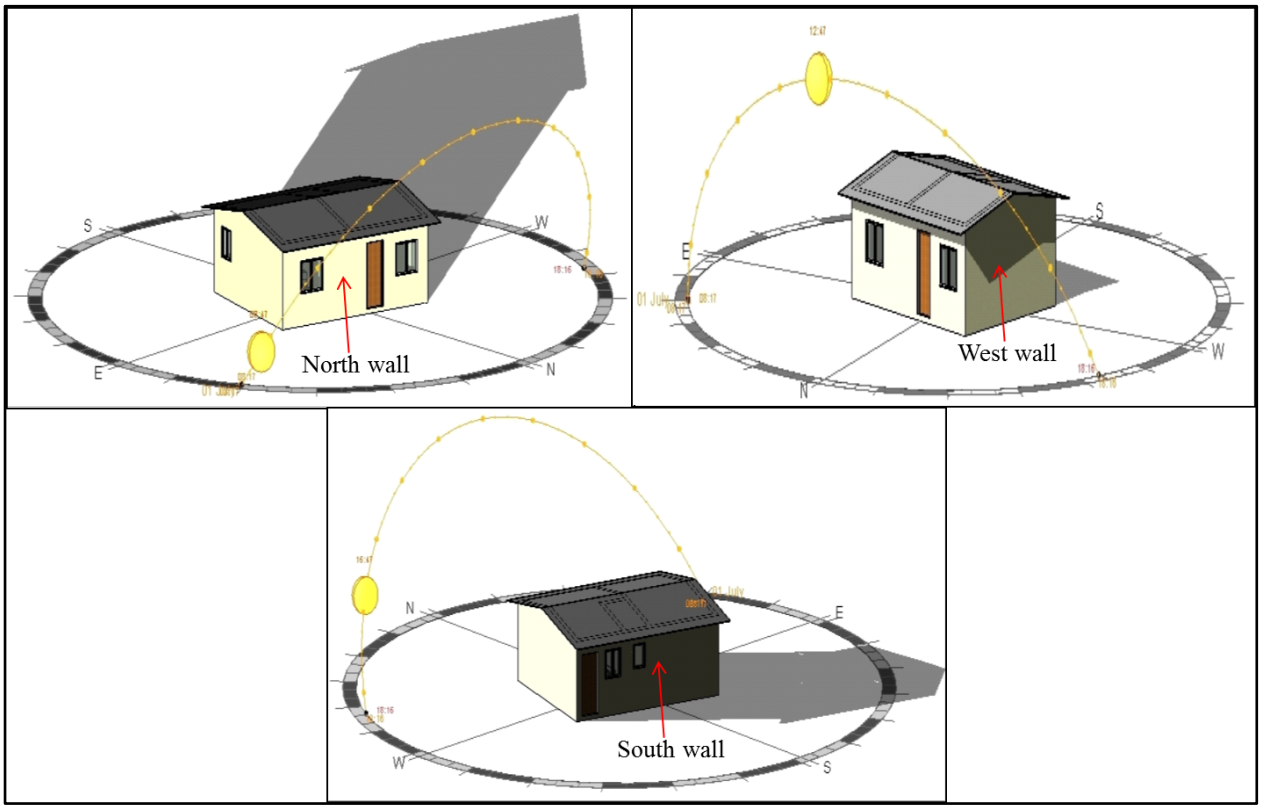

Figure 5.14: Simulation of solar altitude of a typical cold winter day

According to 5.14, the sun sets completely at approximately N81°W of the house, as a result the South walls receives no direct solar radiation. The low solar altitude created a different temperature profile of the external walls from what was observed in the summer. This will also affect the thermal influence of the walls as well as other components of the building envelope on the indoor temperature.

Figure 5.15 shows the temperature profile of the building envelope and indoor temperature in winter season. The roof temperature was found to dominate the temperature of the building envelope, with an average temperature of 21.02°C. The maximum temperature attained by the roof was 54.98°C on 31 May at 12h00. A minimum temperature of 0.81°C was observed for the roof on

11 June at 16h30, which was similar; to the building envelope temperature profile observed in the summer, as the middle-wall temperature closely follow the roof temperature, with an average temperature of 20.70°C. The middle-wall has a maximum and minimum temperature of 54.39°C on 17 May at 17h30 and 6.03°C on 24 July at 07h30, respectively.

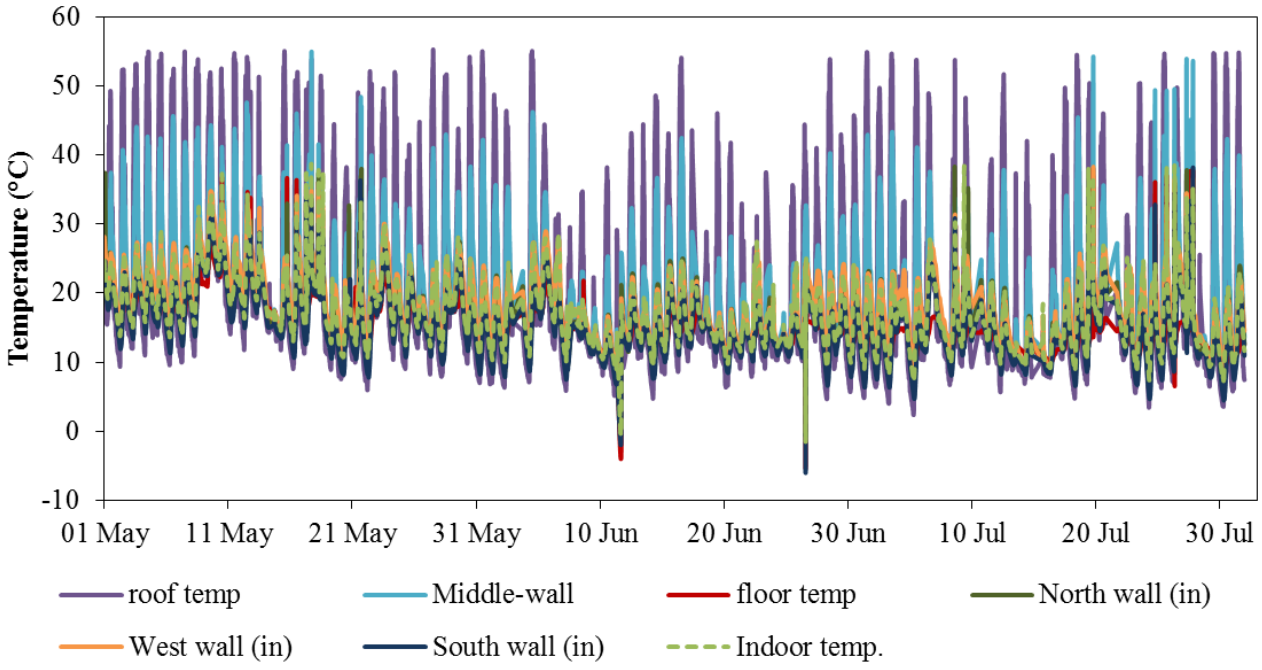

Figure 5.15: Building envelope and indoor temperature profiles in winter season

The South wall had the lowest temperature of -6.02°C on 26 June at 14h00. However, the indoor temperature variation was found to follow the West wall. A typical cold winter day was used to show the thermal influence of the building envelope on the indoor temperature. 13 July, 2012 received a maximum solar irradiance of 283 W/m^2 and was used as a typical cold winter day. Figure 5.16 shows the thermal influence of the building envelope on the indoor temperature on a typical cold winter day.

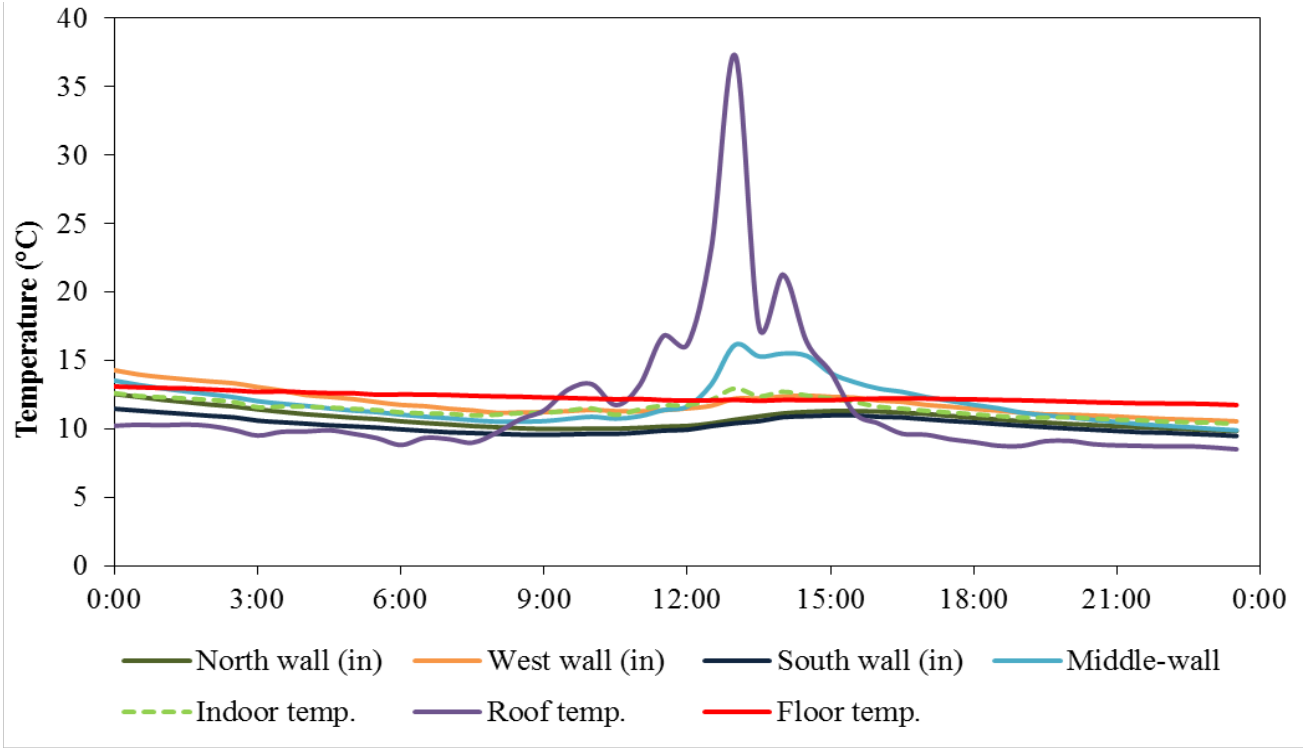

Figure 5.16: Thermal influence of the building envelope on indoor temperature on a typical cold winter day

In Figure 5.16, the roof was seen to have the highest temperature but the indoor temperature closely follows the temperature of the middle-wall and external walls. It was noted that the occupant of the house, occasionally uses paraffin heater in warming the inner space. Heat from the heater and other human activities is absorbed and stored by the middle-wall, which is later released to the inner space of the building. Heat absorbed by the external walls is transferred to the outside of the building. Hence, the middle-wall contributes to the increase of the indoor temperature while the external walls reduce the indoor temperature, which is similar to the floor temperature profile in the summer season, where the floor maintains a fair constant temperature throughout. Due to convectional current, cold dense air is formed on the floor surface, showing that the floor has no significant influence on the indoor temperature.

Figure 5.17 shows the temperature distribution of the indoor, inner and outer surface of the three external walls.

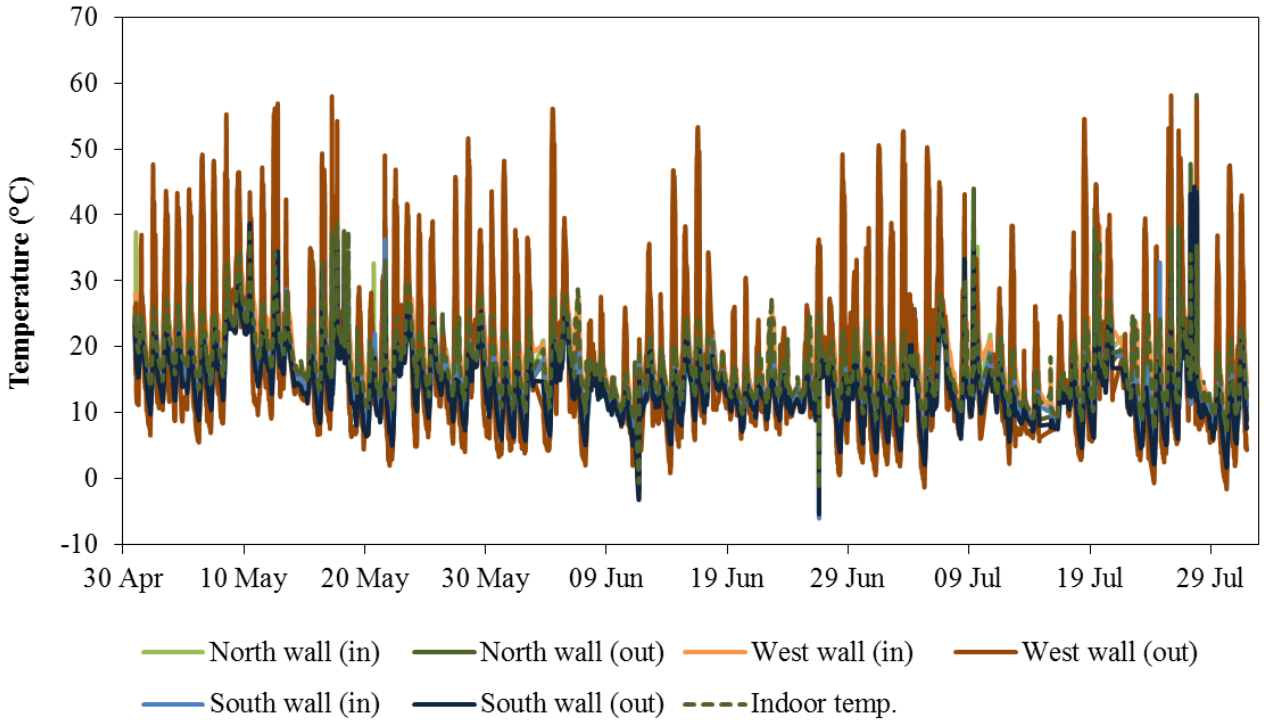

Figure 5.17: Indoor temperature response to walls inner and outer surface temperature variation in winter season

In Figure 5.17, it was observed that the outer surface of the West wall attained a maximum and minimum temperature of 56.01°C at 13h00 on 4 May and -1.59°C at 07h00 on 30 July, respectively. The South wall shows relatively low outer surface temperature distributions throughout the season, recording an average temperature of 13.72°C. The maximum temperature observed for the South wall was 38.30°C at 12h00, 10 May with a minimum temperature of –5.38°C at 14h00 on 26 June. A relatively moderate average temperature was observed on the outer surface of the North wall, with an average temperature of 17.10°C. The North wall attained a

maximum temperature of 57.40°C at 19h30 on 27 July and a minimum temperature of 0.79°C at 16h30 on 16 May.

The indoor average temperature was found to be 17.20°C and the variation of the indoor temperature followed the variation of the external walls temperature. A maximum temperature of 38.7°C was experienced indoors at 17h00 on17 May while the minimum temperature recorded was -1.57°C at 14h00 on 26 June. A typical cold winter day was used to show the indoor temperature response to the external walls. Figure 5.18 shows the temperature distribution of the indoor, inner and outer surface of the three external walls on a typical cold winter day (13 July, 2012).

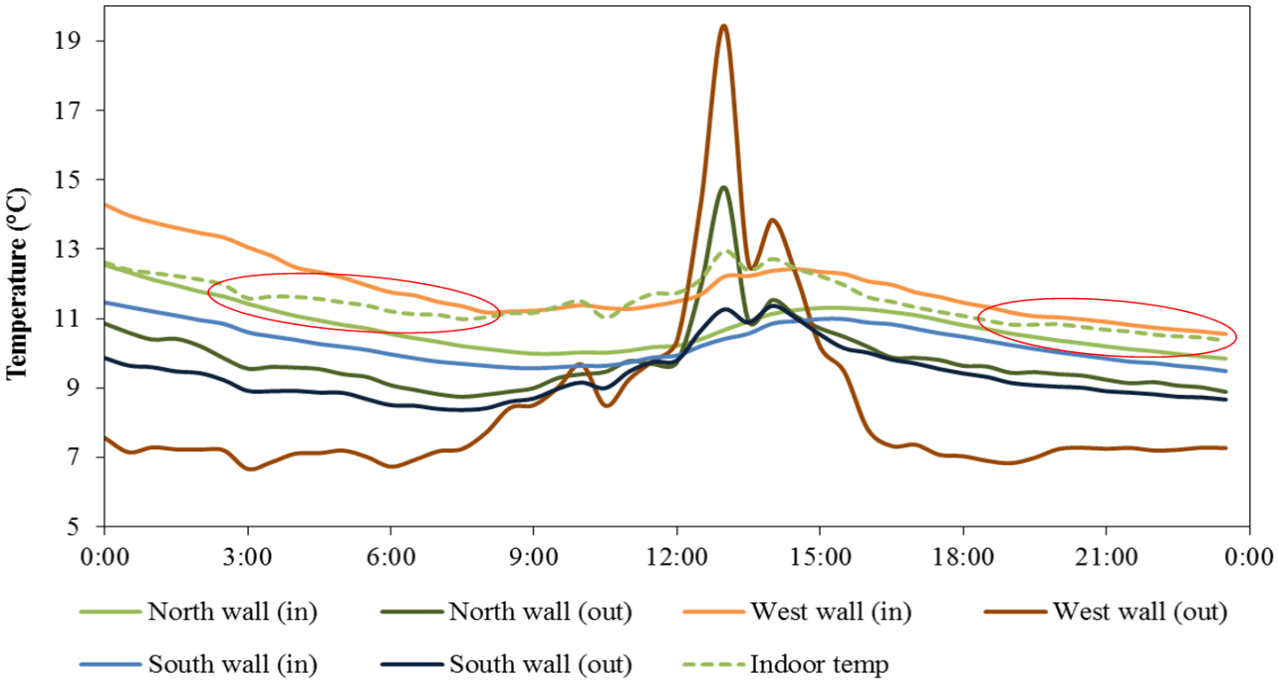

Figure 5.18: Indoor temperature response to walls inner and outer surface temperature variation on a typical cold winter day

It is evident in Figure 5.18 that the outer surface of the West wall has the highest temperature during the day and lowest temperature at night as well as in the early hours of the morning. The

outer surfaces of the North and West walls attained maximum temperature of 14.78°C and 19.43°C, respectively at 13h00. The South wall outer surface temperature reached its maximum value of 11.37°C, at 14h00. During the day, the inner surface of the North, West and South walls attained a maximum temperature of 11.31° at 15h00, 12.43°C at 15h00°C and 10.99°C at 15h30, respectively. Thus a time lag of 2 hours was observed on the North wall while the West and South wall has a time lag of 1.5 hours. The periods at which the outer surface temperatures of the walls start increasing corresponded to the period of sun rise and sun set.

However, in Figure 5.18 it was observed that between 10h00 to 15h00 the indoor temperature was higher than the surface temperatures of the external walls. This is as a result of heat gained from penetrated solar radiation. The building was designed such that solar radiation penetrates through the North elevation window at mid-day (Figure 5.14); thus avoiding the use of conventional heating to achieve indoor thermal comfort. As a result the indoor temperature increases above the temperatures of the external walls. According to the 2nd law of thermodynamics, the inner space of the building will lose heat to the external walls. Around 16h00 to 18h00 and 00h00 to 03h00, the indoor temperature was observed to closely follow the North Wall. As seen in the red highlighted circles in Figure 5.18, the temperature of the West wall drops drastically between 3:00 – 7:30 and 19:00 – 23:00. Due to the large surface area of the West, it absorbs significant quantity of heat from the inner space of the building; causing the indoor temperature to shift from the North wall to the West wall. The inner and outer surface temperature fluctuations of the three walls create an indoor temperature variation. Figure 5.19 shows the temperature difference between the outer and inner surface of the external walls on a typical cold winter day (13 July, 2012).

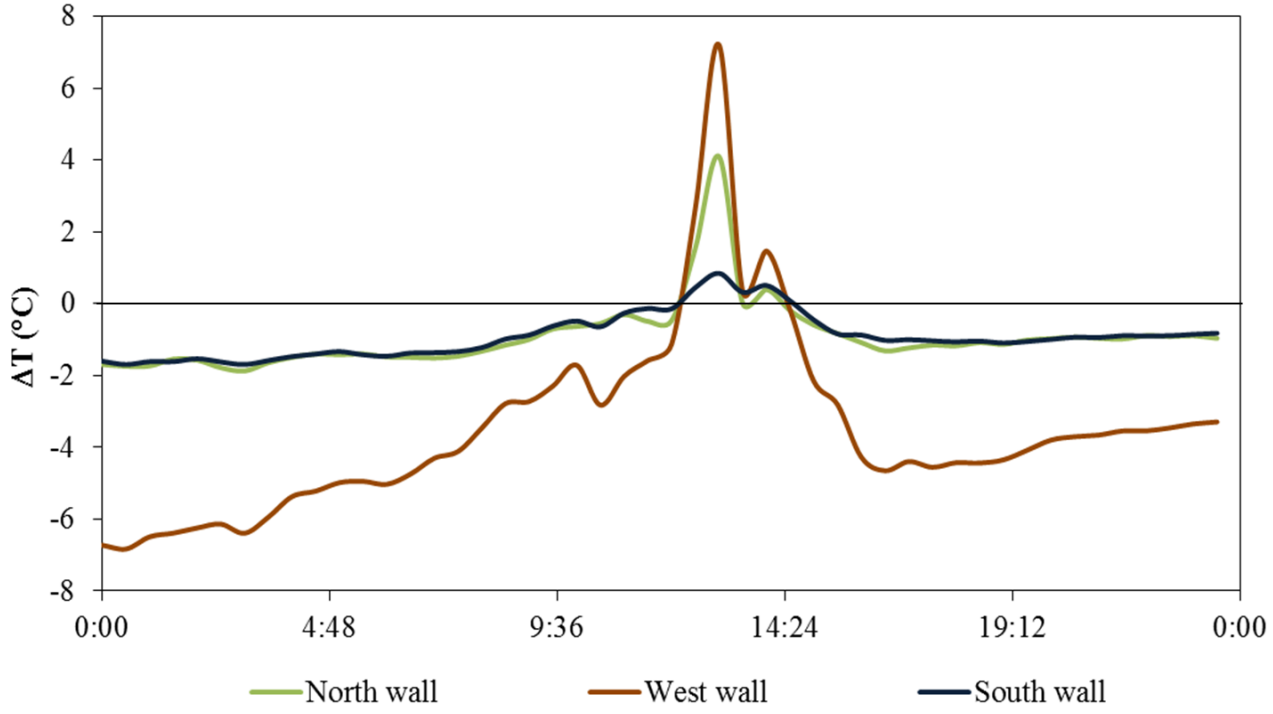

Figure 5.19: Outer and inner temperature difference of the external walls on a typical cold winter day

With reference to Equation [2.3] i.e., $q = -kA\frac{\Delta T}{\Delta l}$ and Figure 5.19; taking the thermal conductivity of concrete block to be 0.51 W/m°C. The average maximum heating rate of the North, West and South walls were found to be 1.95 W, 8.73 W and 0.15 W, respectively. All three walls attained maximum heating rate at 13h00. The cooling rate of the walls was also calculated; the average maximum cooling rate for the North was found to be 0.89 W at 03h00, while the average maximum cooling rate for the West and South walls were 8.27 W and 0.30 W, which occurs at around 01h00. Figure 5.20 shows the rate of heat transfer through the external wall on a typical cold winter day.

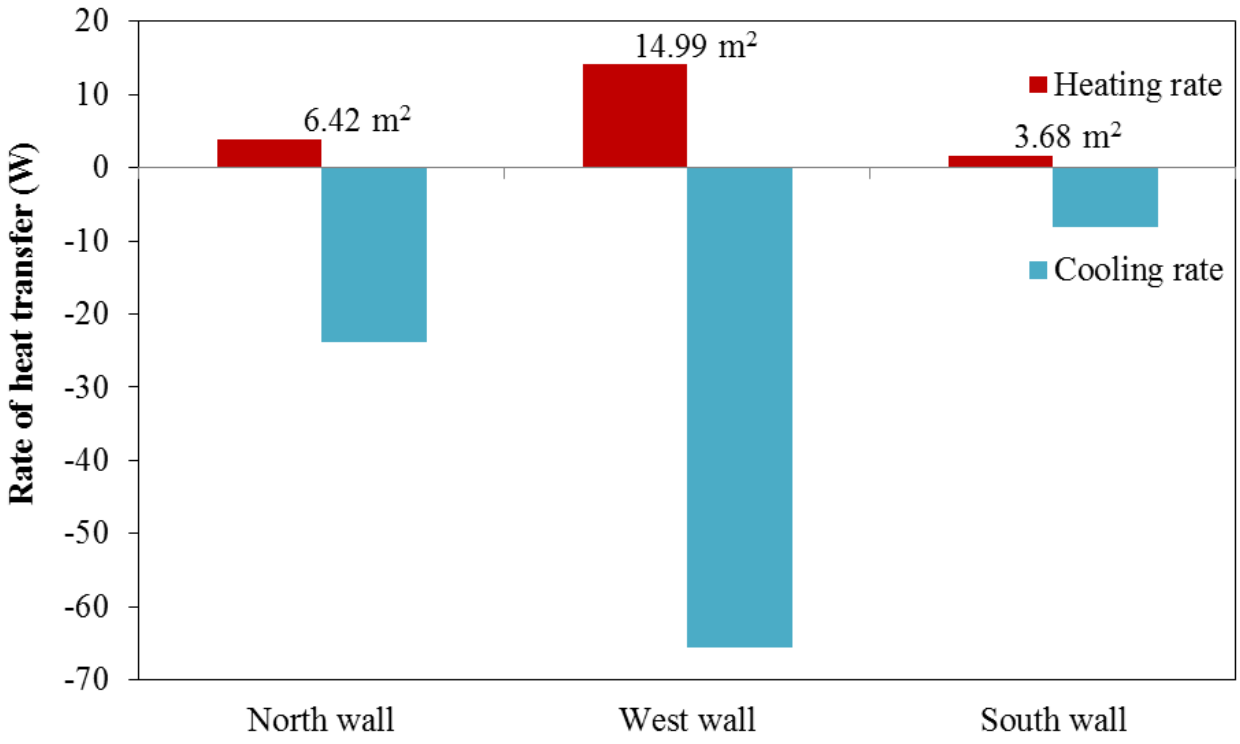

Figure 5.20: Heat transfer rate through external walls on a typical cold winter day

Figure 5.20, shows that in winter, the rate of cooling of the walls was approximately twice the rate of heating. The West wall with a surface area of 14.99 m^2 has the highest heating rate of 14.1 W and cooling rate of 65.7 W. The thermal behavior of the west wall is a typical behavior of uninsulated thermal mass walls; such wall increases the rate of heat loss in buildings. It was observed that the South wall with a surface area of 3.68 m^2 has the lowest heating rate of 1.6 W and cooling rate of 8.15 W. The rate of heat transfer through the walls was found to vary with their geographical orientation and surface area of the walls.

5.3.2 Indoor air temperature and humidity

Figure 5.21 shows the indoor and outdoor temperature distribution and relative humidity for winter season.

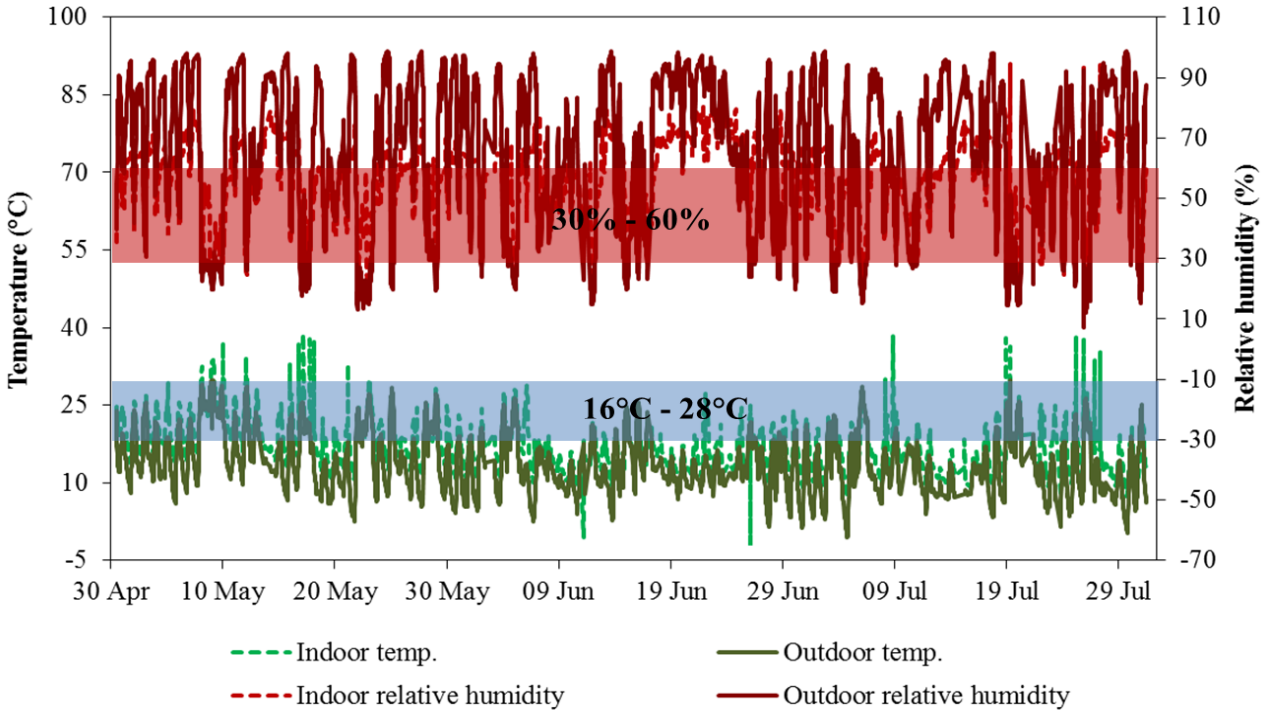

Figure 5.21: Temperature and humidity response in winter season

With reference to Figure 5.21 the winter season is characterized by low outdoor temperature with average of 12.72°C. The outdoor temperature attained a minimum temperature of -0.55°C at 06h00 on 12 July while the corresponding indoor temperature was 6.56°C. A maximum temperature of 29.86°C was recorded for the outdoor temperature at 14h00 on 09 May with a corresponding indoor temperature of 33.76°C. An average outdoor relative humidity of 64% and indoor relative humidity of 56% was observed. At 07h00 on 03 July, the outdoor relative humidity attained its maximum value of 99% while the indoor relative humidity was 67%. The outdoor relative

humidity drop as low as 7% on 26 July, 8h00, with a corresponding indoor relative humidity of 18%. The indoor relative humidity was observed to be influenced by various human indoor activities. Throughout the winter season, the indoor temperature and relative humidity as well as the outdoor temperature and relative humidity were observed to be out of the comfort zones. A typical cold winter day (13 July, 2012) was used to show the indoor thermal comfort level of the house, with respect to indoor temperature and relative humidity. Figure 5.22, shows the indoor and outdoor temperature distribution and relative humidity on a typical cold winter day.

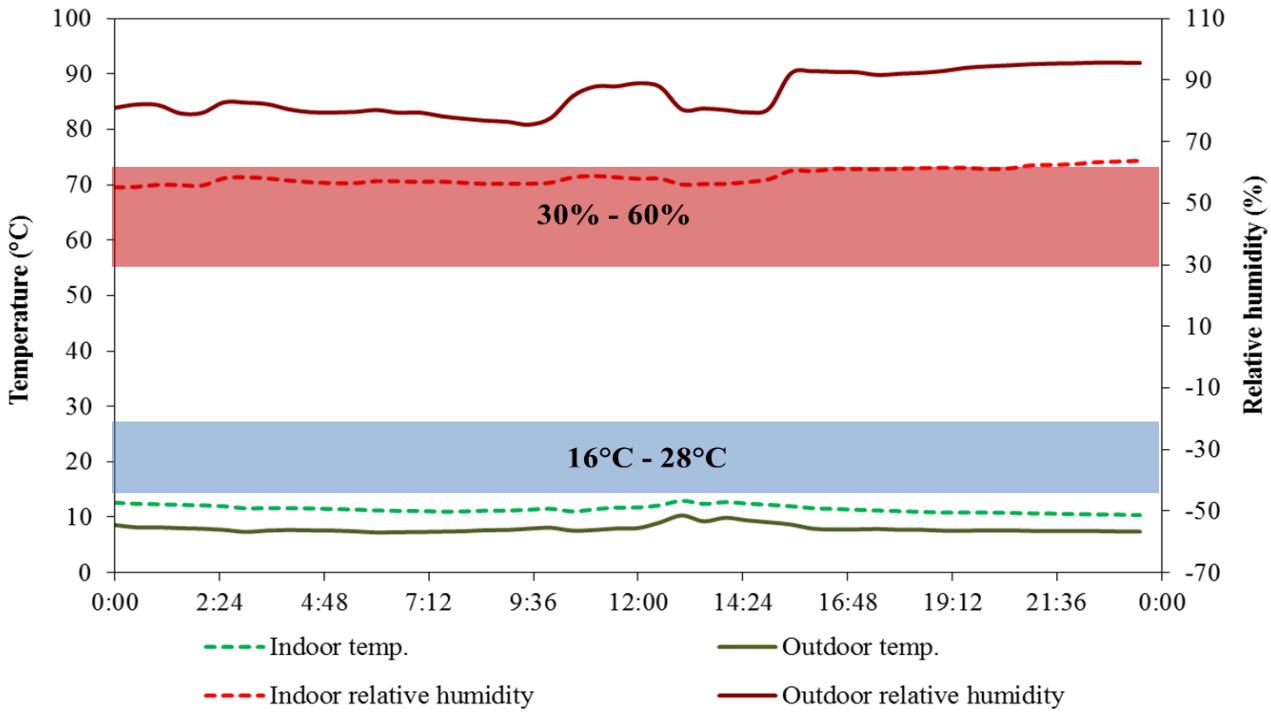

Figure 5.22: Temperature and humidity response on a typical cold winter day

Figure 5.22, shows that the indoor and outdoor temperatures were completely out and below the comfort zone. The outdoor relative humidity was also observed to be out and above the comfort zone, while the indoor relative humidity was found to be at the upper region of the comfort zone,

ranging from 55% to 65%. Consequently, with an average indoor temperature of 10.34°C and high indoor relative humidity, a cold and moist air will be felt indoors. This will leave the walls, floor and furniture damp. Such environment facilitates the growth of fungi (mould) and bacteria that can cause respiratory problems and allergic reaction [Level, 2013].

5.3.3 Wind speed and direction

In winter, wind speed and direction poses a negative influence to indoor thermal comfort as a result of its chilling factor. Thus proper operation of ventilation system to regulate air inflow is required to maintain indoor environment with the thermal comfort level. Figure 5.23 and Figure 5.24 show winter wind speed and direction distribution, respectively, of Golf Course Settlement, Alice.

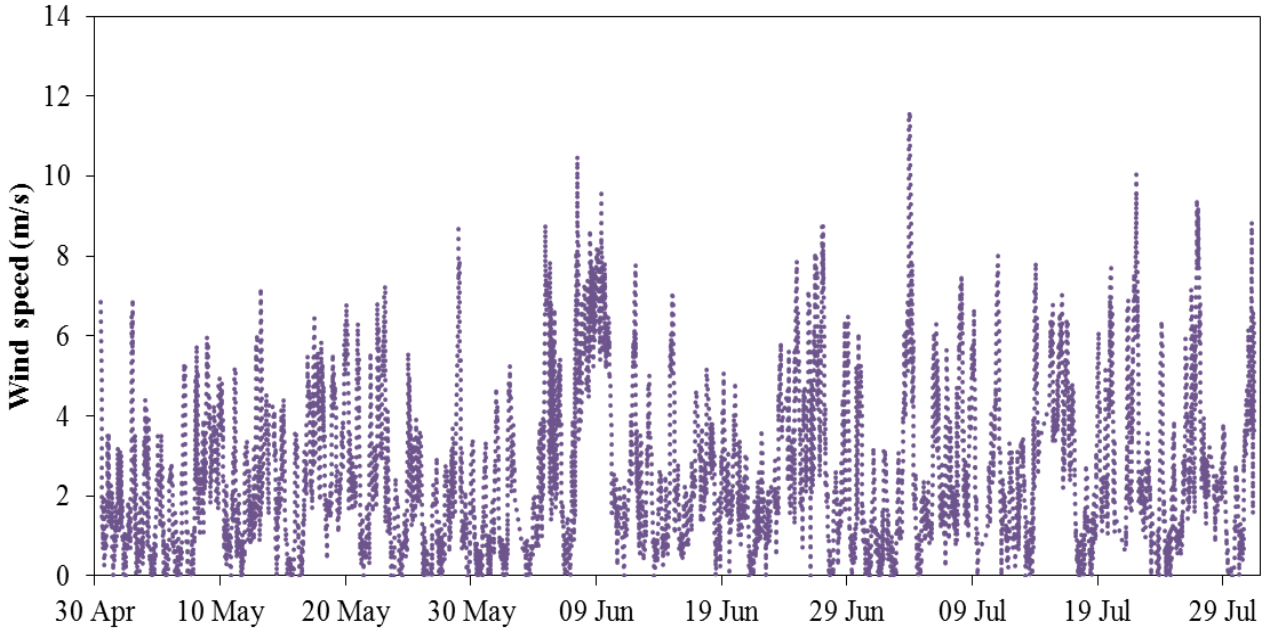

Figure 5.23: Wind speed distribution in winter season

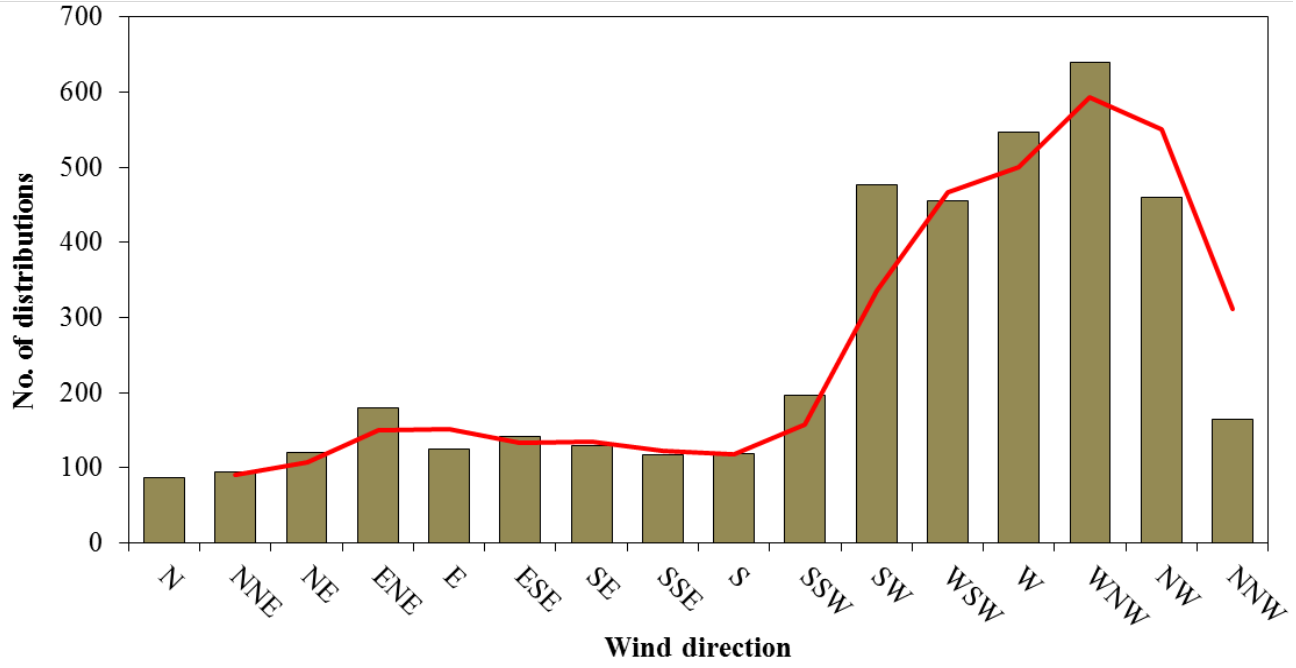

Figure 5.24: Wind direction in winter season

Figures 5.23 and 5.24 show that Golf Course experiences N (65°) W prevailing wind with an average wind speed of 2.4 m/s in winter. The highest wind speed of 11.61 m/s was recorded on 04 July at 20h00, approximately 12% higher than the highest wind speed experienced in summer.

5.3.4 Solar radiation

Figure 5.25 shows the outdoor and indoor temperature response to solar radiation in winter season. The season is characterized with low solar irradiance compared to the summer.

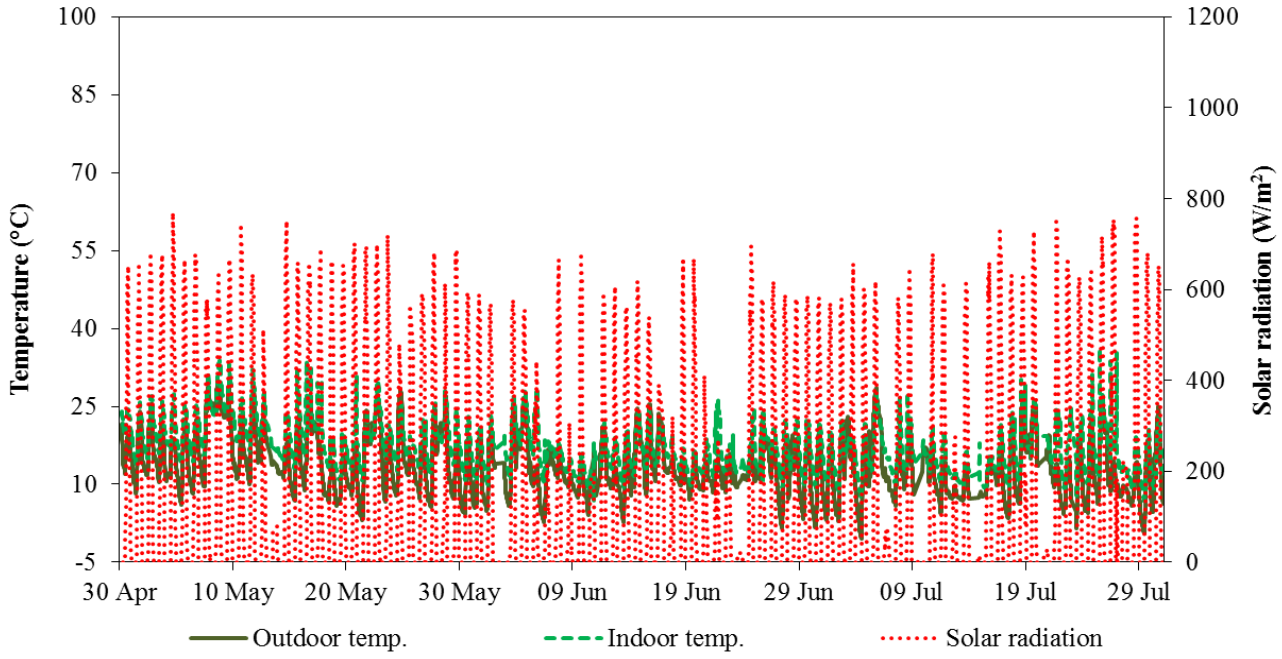

Figure 5.25: Outdoor and indoor temperature response to solar radiation in winter season

In Figure 5.25, an average solar radiation of 150.40 W/m^2 was observed in the winter season. The maximum solar radiation of 789.00 W/m^2 was recorded on 27 July at 12h00, approximately 20% lower than the maximum solar radiation experienced in summer. The indoor temperature and outdoor temperature followed the fluctuations of the solar radiation, with the outdoor temperature responding faster than the indoor temperature.

A typical cold winter day with a maximum solar irradiance of 283.40 W/m^2 was selected to give further analysis of the outdoor and indoor temperature response to solar radiation. This day was chosen due to its relatively clear skies. Figure 5.26 shows the outdoor and indoor temperature variation to solar radiation on a typical cold winter day.

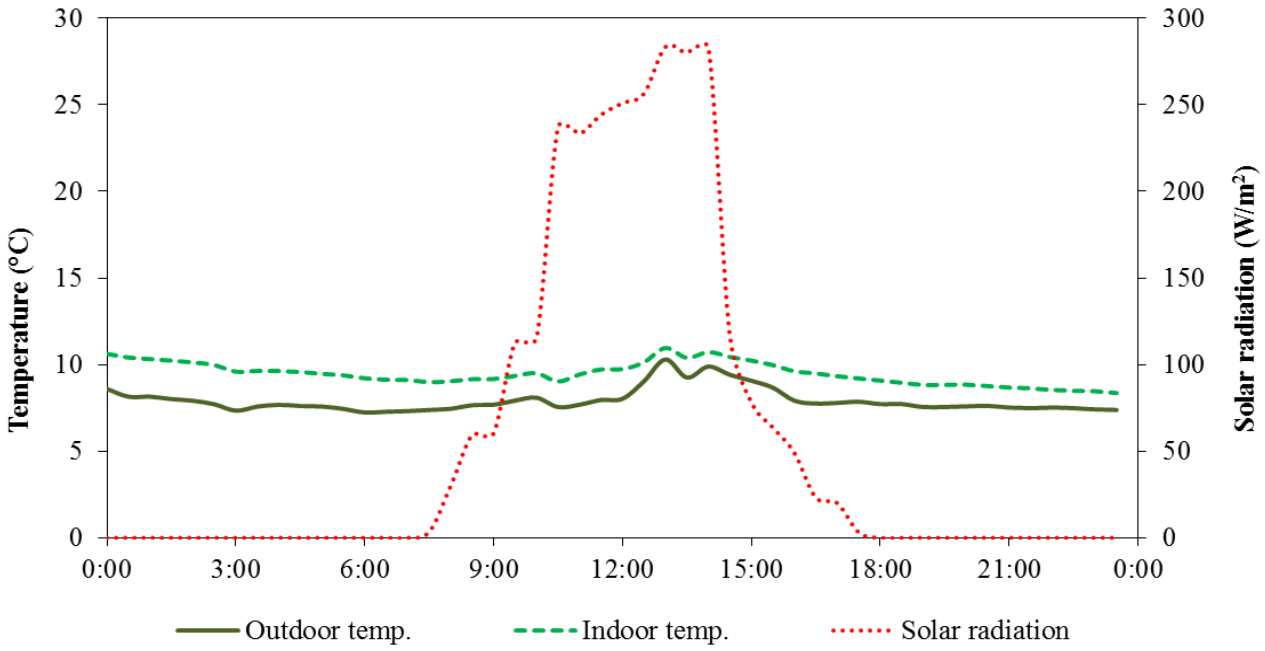

Figure 5.26: Outdoor and indoor temperature response to solar radiation on a typical cold winter day

From Figure 5.26 it was observed that the solar radiation as well as the indoor and outdoor temperature reached their maximum values at 13h00. The indoor temperature was higher than the outdoor temperature throughout the day. The inner space loses heat to the outside surrounding of the building, throughout the day. The average rate of temperature increase of the indoor and outdoor temperature was found to be 0.40 °C/h, while the average rate of outdoor temperature decrease was 0.50 °C/h and 0.30°C/h for indoors. The indoor and outdoor rate of temperature change observed in winter was smaller than the summer value. This is due to the short winter days (approximately 11 hour) and the low solar radiation.

5.4 SUMMARY

The indoor temperature was found to be influenced by the temperature of the building envelope in both summer and winter seasons. In summer, it was observed that the indoor temperature variation closely followed the external wall temperature. Due to the large surface area (14.99 m^2) of the West wall, it was seen to influence the indoor temperature more than the North and South walls. On a typical summer hot day, the average maximum heating rate of the North, West and South walls were 5.93 W, 5,07 W and 2.24 W, respectively. The times at which the walls attain maximum heating rate correspond to the period at which the walls were exposed to direct solar radiation. It was found that the indoor temperature was mostly higher than the outdoor temperature, also that the indoor temperature was within the comfort zone for only 46% of the time. The indoor relative humidity was within the comfort zone throughout the day. A time lag of 2.5 hours was observed between the time the solar radiation and indoor temperature were at their maximum value.

In the winter season, it was found that the indoor temperature is influenced more by the middle and external walls temperature. Due to the locations of the walls, the middle-wall tends to stabilize the indoor temperature, while the external walls reduce the indoor temperature. On a typical cold winter day, the average cooling rate for the North, West and South walls were found to be 0.89 W, 8.27 W and 0.30 W, respectively. The indoor and outdoor temperatures were completely below the comfort zone. Also, the indoor relative humidity was found at the upper region of the comfort zone, which ranges from 55% to 65%. It was also found that the wind speed experienced in winter was 12% higher than the maximum wind spend in the summer season.

CHAPTER 6

THERMAL INFLUENCE OF TRANSLUCENT WATER-BASED ACRYLIC PAINT ON THE BUILDING THERMAL PERFORMANCE

6.1 INTRODUCTION

Space cooling and heating of the building is greatly influenced by the thermal properties of the building envelope. These properties include heat conductivity (U-value) and resistivity (R-value). The use of effective thermal insulation reduce conductive heat gain or loss through building envelope, which could lead to significant reduction in thermal energy demand and consequently reduce the overall electric energy consumption [Budaiwi and Abdou, 2013]. In addition, it helps in extending the periods of thermal comfort without reliance on mechanical cooling or heating systems, especially during the winter season [Kumar and Suman, 2012].

The thermal profile of the building shows that the external walls of the building influences the indoor thermal comfort more than any other components of the building envelope; since the indoor temperature follows the external wall temperature than the roof. In order to enhance the thermal performance of the building, the inner surface of the North, West and South (external walls) walls were coated with Translucent Water-based Acrylic Paint (TWAP). This chapter presents results and findings of the thermal influence of the TWAP on the thermal performance of the external walls and indoor temperature. The period before or after coating was used as a reference to the period before or after the inner surfaces of the external walls was coated with TWAP. It also presents mathematical model predicting the indoor temperature of the house after coating.

6.2 THERMAL INFLUENCE ON EXTERNAL WALLS OF THE BUILDING

6.2.1 Thermal performance of external walls in summer season

Figure 6.1 shows the outer and coated inner surface temperature distribution of the building external walls in summer season.

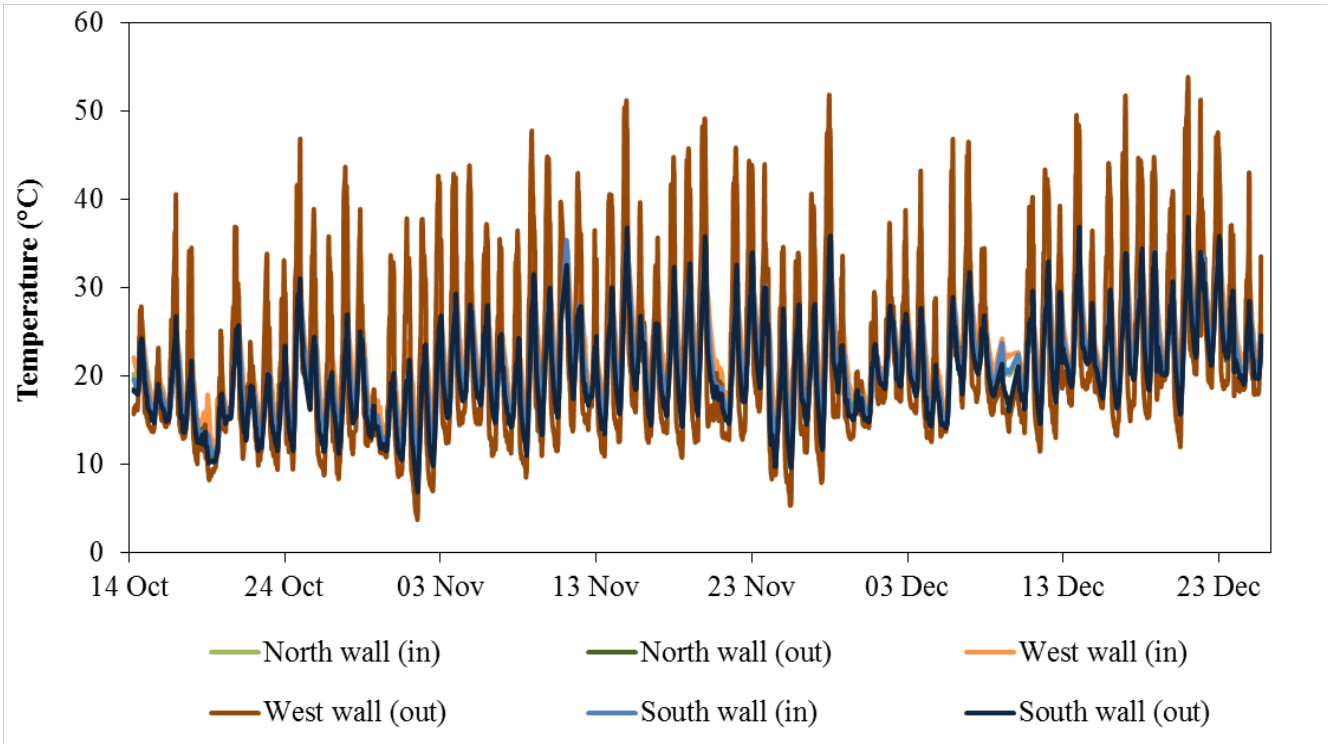

Figure 6.1: External walls inner and outer surface temperature distributions in summer season

In Figure 6.1, the North wall appears thermally inactive throughout the season; recording an average outer surface temperature of 20.44°C. A maximum temperature of 36.40°C was observed on the outer surface of the North wall on 22 December at 12h00 while its corresponding inner surface temperature was 32.59°C. This implies a temperature difference of 3.81°C between the inner and outer surface. The outer surface temperature of the West wall was observed to be the

dominant temperature of the walls throughout the season, with an average value of 21.87°C. The outer surface of the West wall attained its maximum temperature of 53.88°C on 21 December at 17h00 and the least surface temperature of 3.76°C on 02 November at 05h00. While the outer surface of the West wall temperature was at its maximum, the corresponding inner surface records a temperature of 36.38°C. As a result, a temperature difference of 17.5°C was found between the outer and inner surfaces. The South wall had an average temperature of 20.17°C, attaining a maximum temperature of 38.01°C on 21 December at 17h00. On the other hand, the corresponding inner surface records a temperature of 33.74°C. This implies a temperature difference of 4.27°C between the two surfaces. Therefore an average temperature difference of 8.53°C was observed between the outer and inner surfaces of the external walls in summer season.

To analyze the thermal influence of translucent water-based acrylic paint (TWAP) on the thermal performance of the external walls, 20 November with a maximum solar irradiance of 1043.00 W/m^2 was used as a typical hot summer day. Figure 6.2 shows the outer and coated inner surface temperature distribution of the building external walls on a typical hot summer day. The results show that the outer surface temperature of the North and West walls both attained maximum temperature of 32.95°C and 47.74°C, respectively, at 14h00. Their corresponding inner surfaces were found to reach a maximum temperature of 30.01°C for North wall and 32.75°C for West wall at 17h00.

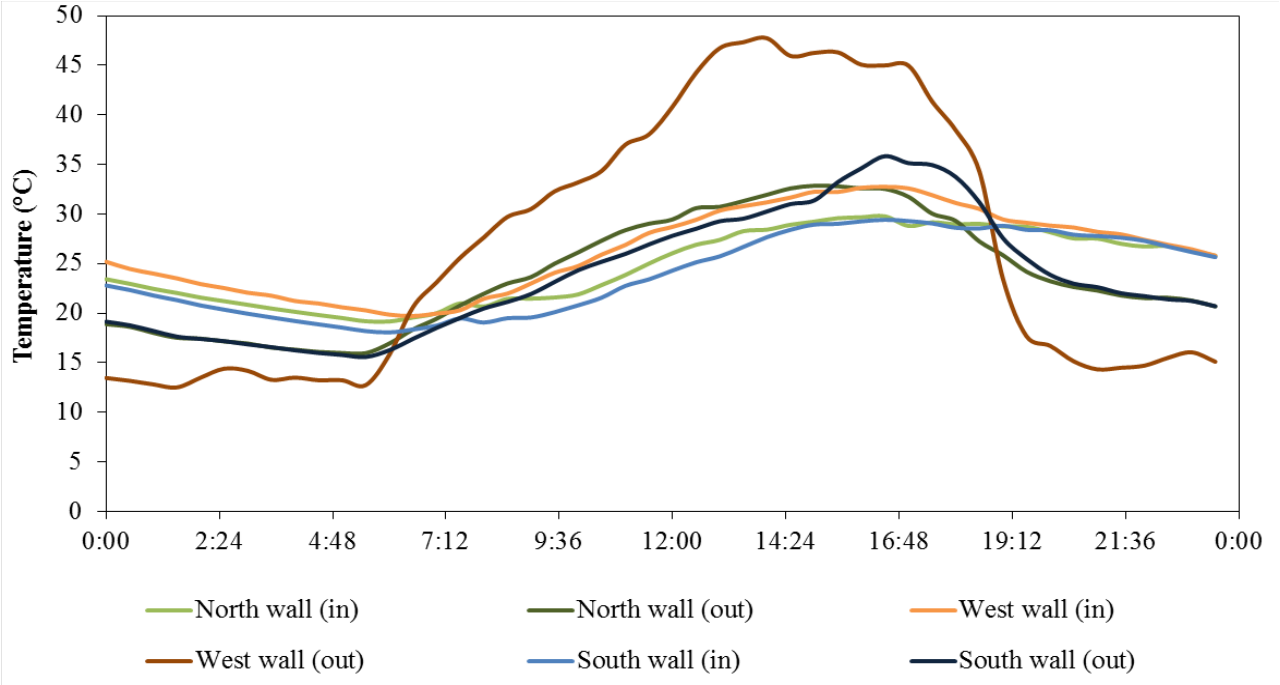

Figure 6.2: External walls surface temperature distributions on a typical hot summer day

The South wall outer surface reached a maximum temperature of 35.62°C at 16h00, while the inner surface attains a maximum temperature of 29.89°C at 17h00. With reference to Figure 6.2 and Equation [2.16] i.e. $f = \frac{A_o}{A_e} = \frac{T_o^{max} - T_o^{min}}{T_e^{max} - T_e^{min}}$; where T_o^{max} and T_o^{min} are maximum and minimum inner surface temperature of the wall. T_e^{max} and T_e^{min} represents the maximum and minimum outer surface temperature of the wall. The decrement factor of the North, West and South walls were found to be 0.64, 0.37 and 0.59, respectively. A corresponding time lag of 3 hours was obtained for the North and West walls and 1 hour for the South wall. The North wall was found to have the lowest heat reduction capacity. As shown in Figure 5.1, from mid-day to sunset, more than half of the total surface area of the North was in shade. This tends to increase moisture content of the North wall, thereby increases its thermal conductivity. On the contrary, the West wall was found to have the highest heat reduction capacity among the three external walls. It was noted that the West

wall was exposed to direct solar radiation for a longer period, causing the thermal energy from the sun to reduce the moisture content of the wall, in return reduces its thermal conductivity. However, the decrement factors of the external walls, before coating were higher compared to the period after coating. With reference to Figure 5.5 and Figure 6.2; Table 6.1 summarized the decrement factor and time of the external wall before and after coating on a typical summer hot day.

Table 6.1: Decrement factor and time lag of the external walls during the period before and after coating on a typical hot summer day

Periods	Before coating			After coating		
External walls	North	West	South	North	West	South
Decrement factors	0.97	0.58	0.77	0.64	0.37	0.59
Time lag (h)	2	2	0	3	3	1

Table 6.1 shows that after coating the external walls had higher heat reduction capacity than the period before coating. Due to the high reflectivity of (TWAP), heat from the walls outer surfaces are reflected back, consequently, reducing the quantity of heat transferred through the walls. Also the time taken for the inner surface to attain maximum temperature with respect to the outer surface was increased due to the heat transfer delay caused by the TWAP film. After coating, the decrement factor of the North, West and South walls were found to reduce by 21%, 22% and 13%, respectively. The time lags of the external walls increased by 1 hour.

6.2.2 Thermal performance of external walls in winter season

Figure 6.3 shows the outer and coated inner surface temperature distribution of the building external walls in winter season. Average temperatures of 17.58°C, 18.18°C and 16.04°C were observed in the outer surfaces of the North, West and South walls, respectively. The West wall attained the highest outer surface temperature of 42.97°C on 01 October at 12h30 while the corresponding inner surface was 14.67°C. The lowest temperature of -13.17°C was also attained on the outer surface of the West wall. At the same time, the inner surface temperature of the West wall was -0.98°C. However, the outer surface temperature of the South wall was relatively low, ranging from 30.31°C to -7.57°C. On 26 September, 15h30 the South wall outer surface attained its maximum temperature; at the same time, the inner surface temperature reached 27.03°C. The wall (South wall) records its minimum outer surface temperature while the inner surface temperature was -3.15°C. On the other hand, a maximum temperature of 35.05°C was observed for the outer surface of the North wall on 17 September, 10h30 with a corresponding inner surface temperature of 27.33°C. The lowest outer surface temperature of the North wall was observed to be -6.96°C with an inner surface temperature of -2.60°C.

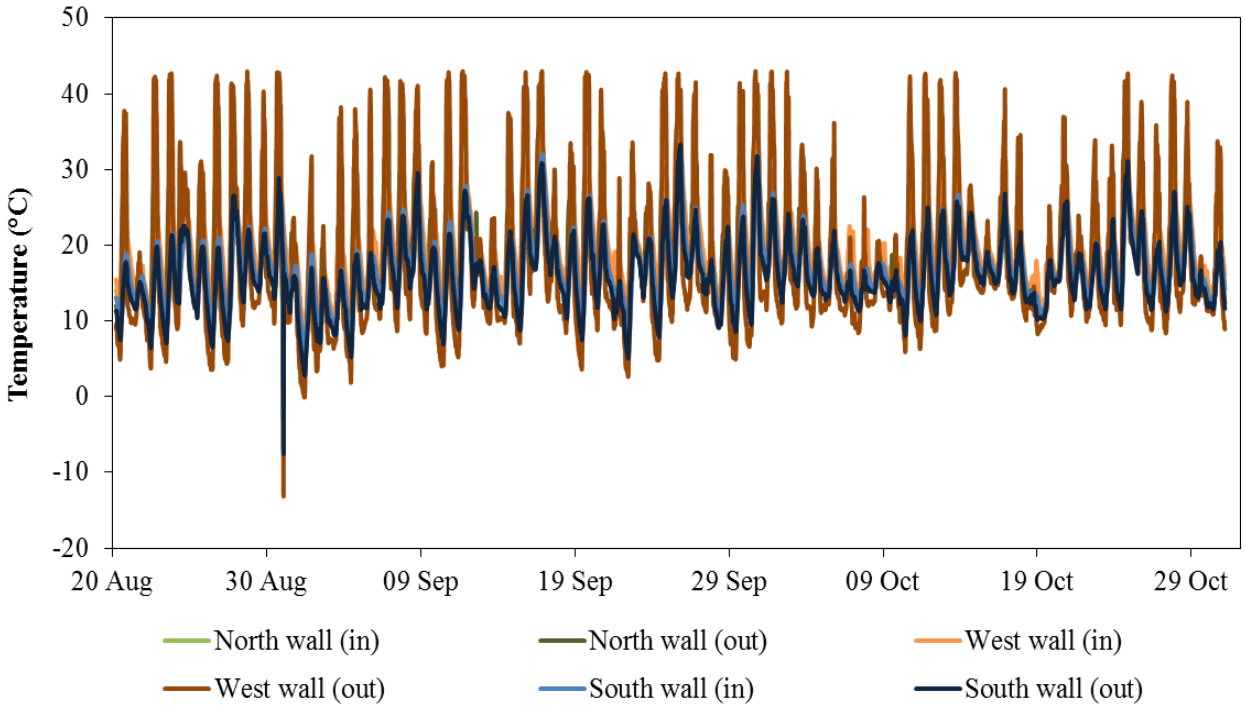

Figure 6.3: External walls inner and outer surface temperature distributions in winter season

The outer surfaces of all three walls were found to attain minimum temperature on 31 August at 21h30. An average maximum and minimum temperature difference of 7.99°C and 6.99°C, respectively was experienced by the external walls.

Figure 6.4 shows the outer and coated inner surface temperature distribution of the building external walls on a typical cold winter day. Typical cold winter day was represented by 22 August with a maximum solar irradiance of 260.40 W/m^2. The outer surfaces of the North, West and South walls were seen to attain maximum temperatures of 2.42°C, 3.48°C and 0.67°C, respectively at 13h00. Whereas, the inner surfaces of the North, West and South walls attained maximum temperature of 18.32°C, 18.49°C and 18.23°C, respectively at 16h00.

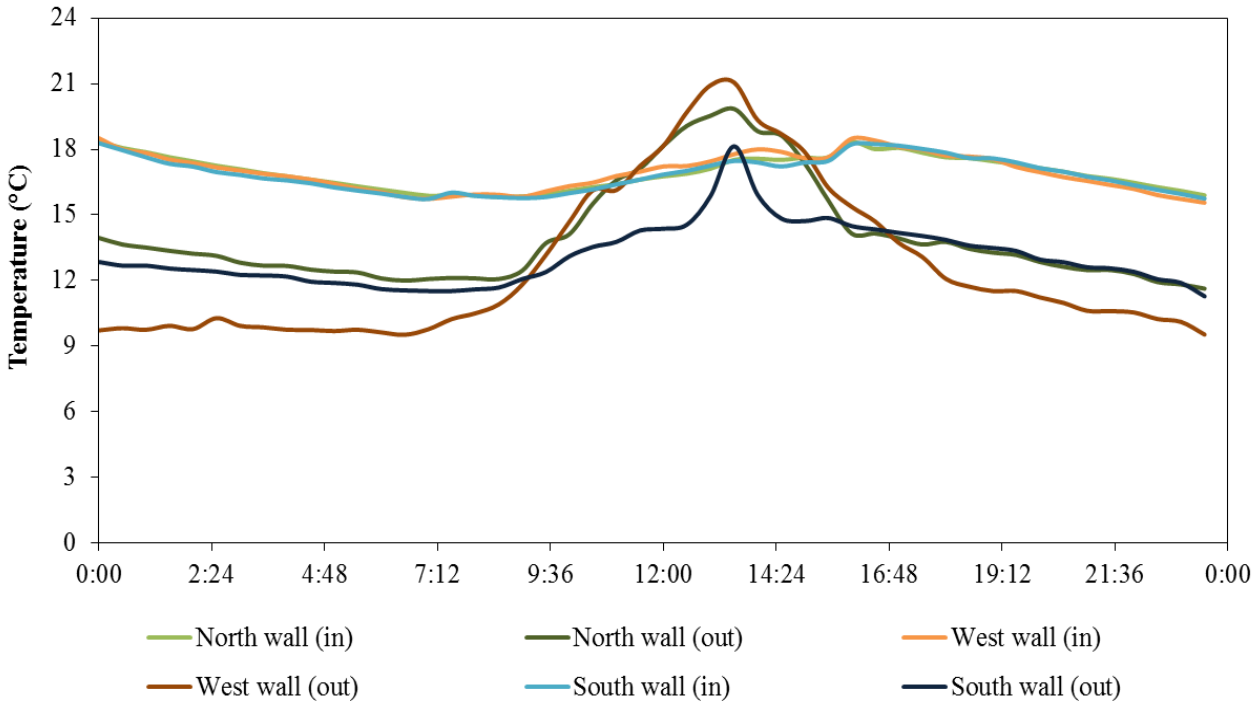

Figure 6.4: External walls surface temperature distributions on a typical cold winter day

With reference to Figure 6.4 and using Equation [2.16] i.e. $f = \frac{A_o}{A_e} = \frac{T_o^{max} - T_o^{min}}{T_e^{max} - T_e^{min}}$, the decrement factor for the North wall was found to be 0.10, 0.09 for the West wall and the South wall was 0.17. A time lag of 3 hours each was observed between the outer and inner surfaces of the external walls. The South wall was seen to have the lowest heat reduction capacity among the three external walls. From Figure 5.14 it was noticed that the South wall of the house was completely in shade throughout the day. This created a damp air around the outer surface of the South wall, as a result the moisture content of the wall increases, which further increased its thermal conductivity. After coating, it was found that the decrement factor of the external wall was improved significantly. Table 6.2 summarizes the decrement factor and time of the external wall before and after coating on a typical cold winter day.

Table 6.2: Decrement factor and time lag of the external walls during the period before and after coating on a typical hot winter day

Periods	Before coating			After coating		
External walls	North	West	South	North	West	South
Decrement factors	0.45	0.29	0.66	0.10	0.09	0.17
Time lag (h)	2	1.5	1.5	3	3	3

Table 6.2, the TWAP film reduced the heat transfer through to the building walls to the outer surrounding. On a typical cold winter day, due to temperature difference between the outer and inner space of the building, heat tends to flow out of the outer space. The TWAP film reduces the heat transfer through the walls, by reflecting the back to inner space. As a result, the heat reduction capacity of the wall increases. Hence, the decrement factor of the North, West and South walls was found to reduce by 64%, 53% and 59%, respectively.

6.3 THERMAL INFLUENCE ON INDOOR TEMPERATURE

Thermal influence of the TWAP on the indoor temperature was analyzed using heating degree hours (CDH) and cooling degree hours (CDH). A Base temperature of 16°C and 28°C were used in calculating the CDH and HDH.

6.3.1 Cooling and heating degree-hours

Three conditions were considered to determine the amount of CDH or HDH the inner space of the building required to maintain thermal comfort.

- $T_i < 16°C$ indoor heating required (HDH),
- $T_i > 28°C$ indoor cooling required (CDH), and
- $16°C < T_i < 28°C$ no heating or cooling required.

With reference to Equations [2.18] and [2.19] i.e. $CDH = \sum_{i=1}^{N} (T_i - T_b)^+$ and $HDH = \sum_{i=1}^{N} (T_b - T_i)^+$, Figure 6.7, shows the monthly cooling and heating degree hours of the inner space of the building. It was observed that as the outer temperature decreases from February to July the CDH decreases while the HDH increased. This was due to the climate condition of Golf Course, Alice. Referring to the seasons grouping criteria in chapter 3, Alice experienced summer season from mid-October to mid-April, with an average temperature of 18°C to 26°C. A mild winter season with an average temperature of 7°C to 20°C is experienced from May to October. Using the three conditions outlined above and Figure 6.7, it was found that from February to April (summer period before coating) the inner space of the house requires an average HDH of 0.59 and CDH of 4.36. During the period (May to July) of winter before coating, an average CDH of 1.02 and HDH of 2.74 were required indoor. The relatively high CDH required indoors from February to April, is attributed to the poor ventilation system operated by the occupants of the house (highlighted in chapter 5).

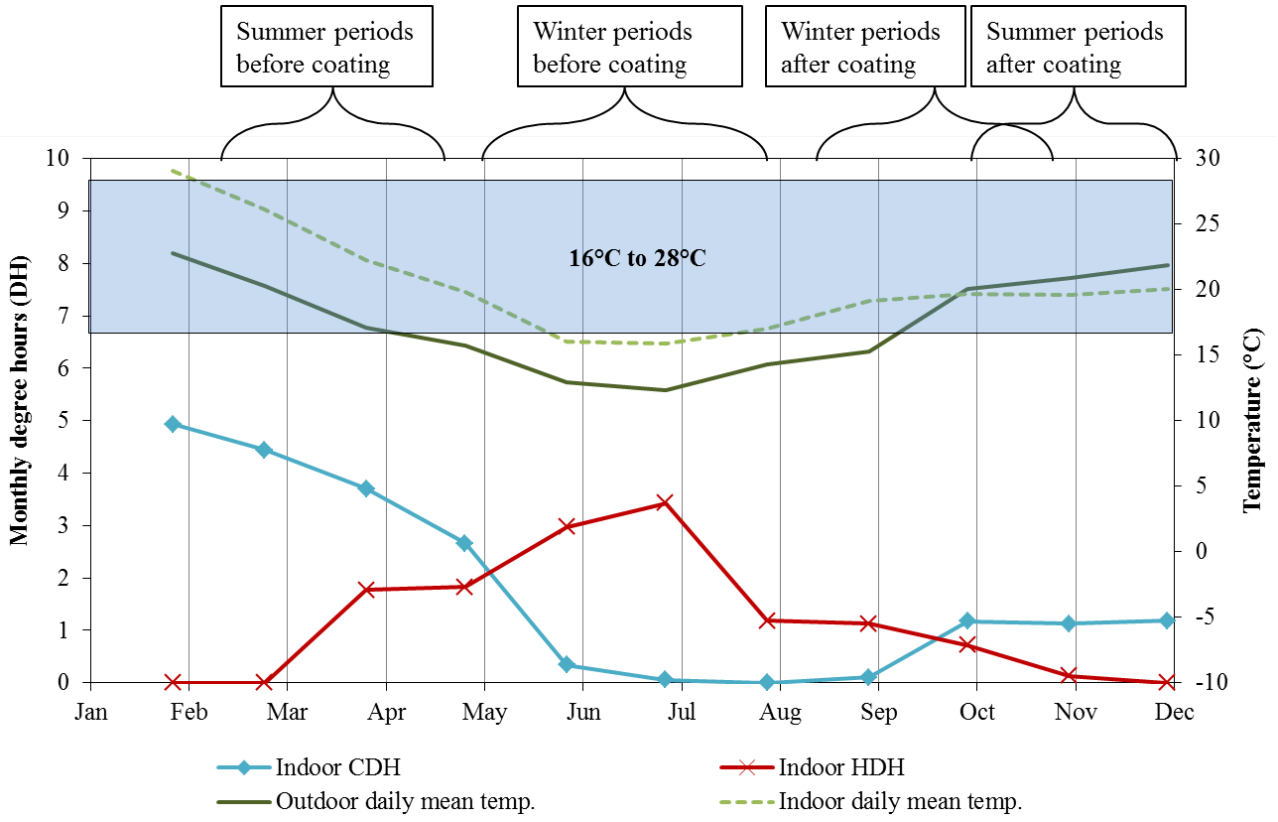

Figure 6.7: Monthly cooling and heating degree hours

In Figure 6.7, it was found that during winter period (August to October) after coating, the inner space requires an average HDH of 1.01 as well as CDH of 0.42. At the end of September, the summer season begins; hence, the outdoor and indoor temperature increases as well as the CDH while HDH decreased (Figure 6.7). Either ways, during the summer period (October to December) after coating, it was found that the building inner space requires an average CDH of 1.16 and HDH of 0.28. From all observations, after coating, the inner space requires approximately 46% HDH and 42% CDH less compared to what was required in the winter period before coating; in order to maintain thermal comfort. It was also found that in the summer period after coating, the inner space requires approximately 58% CDH and 36% HDH less compared to the amount required in summer period before coating. After coating, the rate of heat transfer out or into the inner space of

the building was minimized. As a result the amount of CDH and HDH required to maintain indoor thermal comfort were reduced.

The average annual heating and cooling degree hours were deduced. Figure 6.8 shows the average annual heating and cooling hours of the inner space of the building.

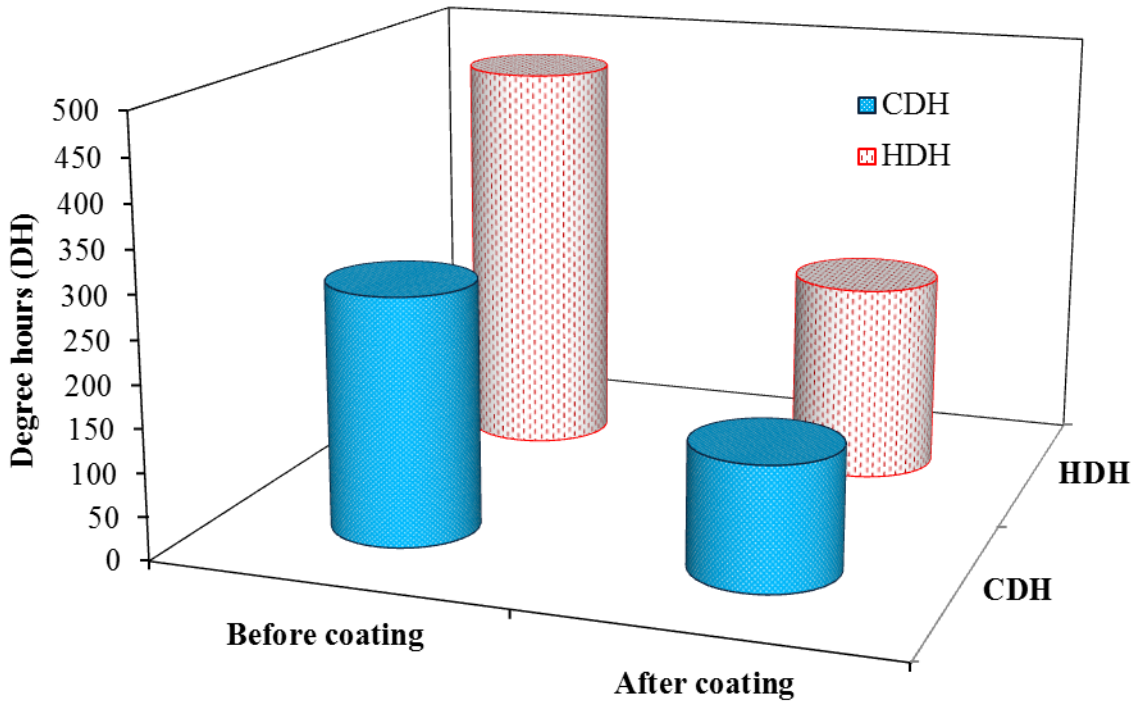

Figure 6.8: Annual cooling and heating degree hours

From Figure 6.8, it was seen that most energy in the house was consumed in heating rather than cooling in order to maintain thermal comfort. It was found that during the period before coating, the inner space of the house requires an average of 287.75 CDH and 464.91 HDH. After coating, the inner space was found to require an average CDH and HDH of 143.64 and 230.75, respectively. In both cases (before and after coating), the average annual HDH was approximately

double the CDH. However, the amount of CDH and HDH required by the inner space during the period before coating is approximately 34% higher than the amount CDH and HDH required during the period after coating.

The annual heating energy demand of the house was also computed using equation [2.20] i.e., $\eta = UA \times DD \times 24$, recall that;

η Heating or cooling energy demand (kWh)

UA Overall heating coefficient (kWK^{-1})

DD Degree days (°C day)

24 Convert day in hours

Table 6.3 gives the summary of the indoor cooling and heating demand

Table 6.3: Annual cooling and heating demand

					Energy demand (KWh/m^2)	
Periods	Months	Seasons	$CDH_{(indoor)}$	$HDH_{(indoor)}$	Cooling	Heating
Before coating	February – April	Summer	543.44	31.91	5.66	0.33
	May – July	Winter	32.07	897.90	0.33	9.35
After coating	August – October	Winter	21.32	453.45	0.22	4.72
	October – December	Summer	221.10	25.50	2.30	0.27

In deducing the cooling and heating energy demand of the house, it was assumed that:

- The building has an overall heat loss coefficient *UA* equal to 10.42 WK^{-1} (Ecotect, 2012; Giancoli, 1998; Al-Jabri, 2004 chapter 2).
- The "24" which convert days to hours in the heating/cooling energy demand equation was excluded since the cooling and heating degrees are in hours.

Based on the above assumptions, the total degree hours for the year correspond to a heating demand of about 14.68 kWh/m^2 and a cooling demand of 8.52 kWh/m^2. It was found that the house demanded the highest quantity of energy for heating (9.35 kWh/m^2) in winter season before coating. After coating, the house was found to save 41% of cooling energy demand and 32% in heating energy demand per annual.

6.4 INDOOR TEMPERATURE MODELLING

Predicting the indoor temperature of an occupied house is a very difficult and complex process, as the occupants have complete freedom to change the condition according to their need or desires. The activities of the occupants have significant influence on the indoor temperature distribution [Makaka and Meyer, 2006]. In developing the indoor temperature prediction models, the influence of the building envelope and weather factor were considered. Hence, the building envelope and the weather factors were the predictors, while the indoor temperature was the output. Before developing the model, ReliefF algorithm was used to determine if the predictors were primary contributor or secondary contributor to the output. Figure 6.9 shows the reliefF ranking of the predictors by their weight of important to the indoor temperature for summer and winter periods.

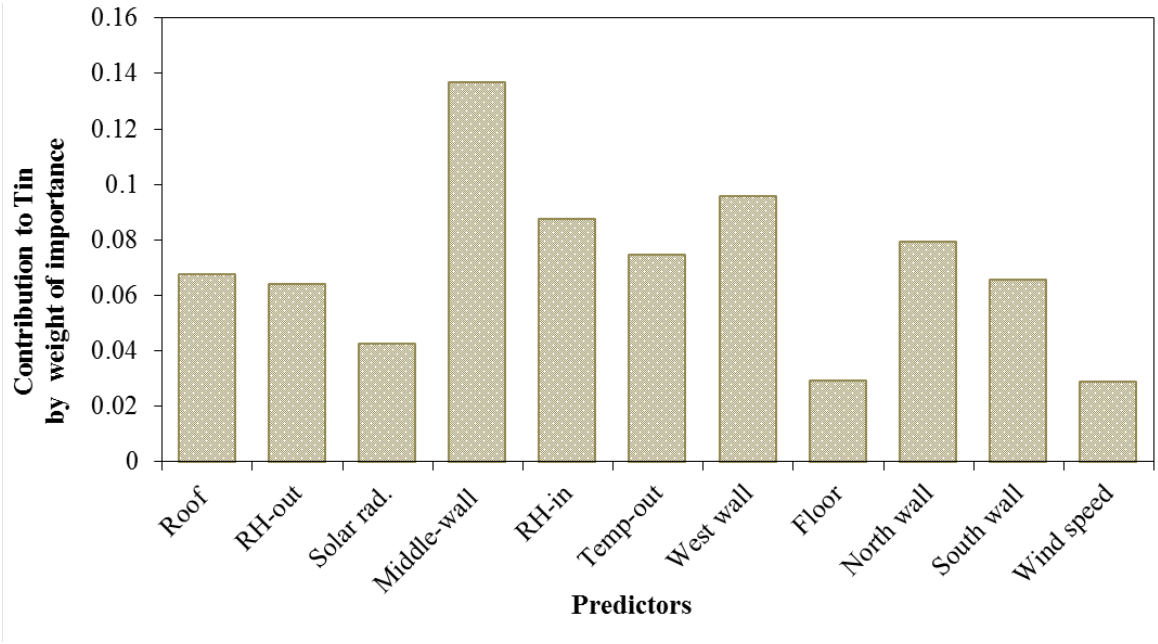

Figure 6.9: ReliefF ranking of building envelope and weather factors by weight of importance to indoor temperature for summer period

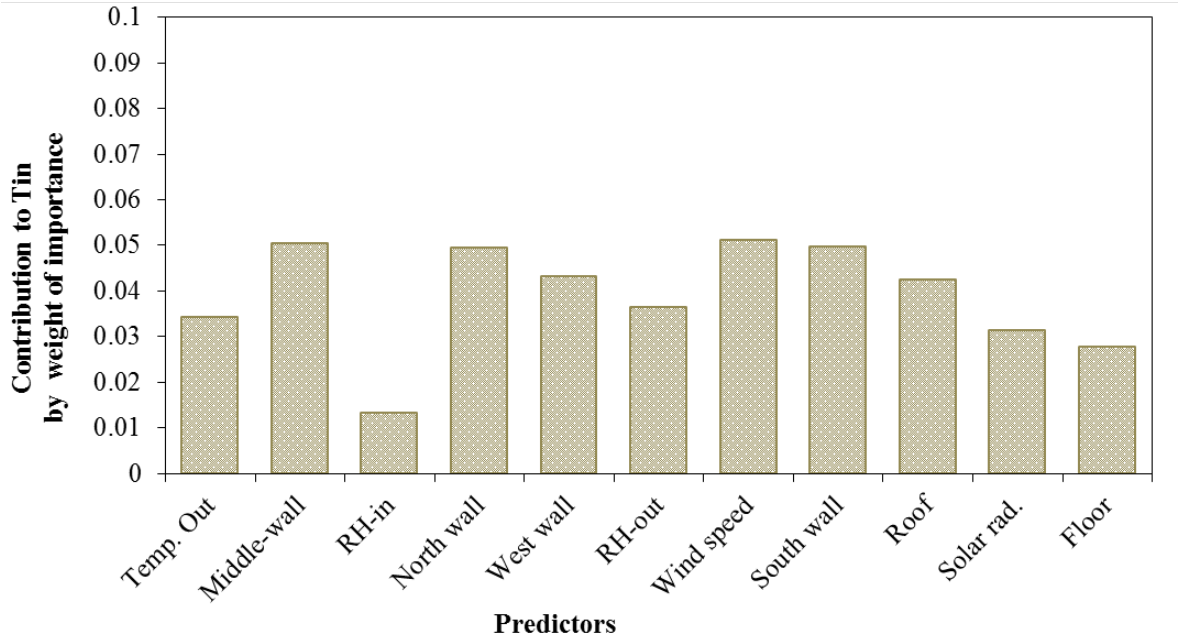

Figure 6.10: ReliefF ranking of building envelope and weather factors by weight of importance to indoor temperature for winter period

In figures 6.9 and 6.10, it was depicted that all the predictors were primary contribute to the outdoor temperature in both seasons and can be used in developing the model. In summer, the contributions from the middle and West walls were significant when compared to the contribution from the other components of the building envelope. The middle and West walls contribute 18% and 12%, respectively. The floor was found to be the lowest contributor of 4%. Considering the weather factors, indoor relative humidity contributed the most to the indoor temperature, with 11%. Wind speed was found to contribute the lowest, with 4%. It is very important to point out that the contribution to the indoor temperature by the predictors' turns to be lower in the winter than in the summer period. In winter period, the middle and external walls were found to contribute significantly to the indoor temperature. With respect to the weather factors, wind speed turns out to be the most contributor with 12% while indoor relative humidity contribute the lowest, with 3%.

Based on the findings and results of the reliefF algorithm, multiple linear regression models for indoor temperature were developed. For summer, the following indoor temperature model was obtained:

$$T_{in} = 0.250918T_r + 0.191115T_{mw} + 0.23130T_f + 0.456418T_{nw} + 0.33412T_{ww} + 0.323593T_{sw} + 0.174091T_{out} - 0.032943RH_{in} - 0.001504RH_{out} + 0.00676I - 0.01731W_s - 6.12741 \quad [6.1]$$

For winter, the following indoor temperature model was obtained:

$$T_{in} = 0.089269T_r + 0.12732T_{mw} - 0.32414T_f + 0.639732T_{nw} + 0.569245T_{ww} - 0.51118T_{sw} + 0.193597T_{out} - 0.098170RH_{in} + 0.008156RH_{out} + 0.00303I - 0.11053W_s + 11.53374 \quad [6.2]$$

Table 6.4 shows the list of predictors and symbols

Table 6.4: Predictor and symbols

Predictors	**Symbols**	**Predators**	**Symbols**
Roof temp.	T_r	South wall	T_{sw}
Middle wall temp.	T_{mw}	Outdoor temp.	T_{out}
Floor temp.	T_f	Outdoor relative humidity	RH_{out}
North wall	T_{nw}	Wind speed	W_v
West wall	T_{ww}	Solar radiation	I

From Equation (6.1), it can be deduced that all component of the building envelope have a positive contribution to the indoor temperature. This implies that increase in building envelope temperature will increase the indoor temperature. The indoor, outdoor relative humidity and wind speed were found to have negative contribution to indoor temperature. Therefore increase in the indoor, outdoor relative humidity and wind speed will reduce the indoor temperature. From Equation (6.2) the floor and the South walls were found to have negative contribution to the indoor temperature. Also, the indoor relative humidity and wind speed have negative contribution to the indoor temperature. Figures 6.11 and 6.12 show the measured and predicted indoor temperature for summer and winter, respectively. In winter the scaling value of the roof was zero, thus it was not included in the model.

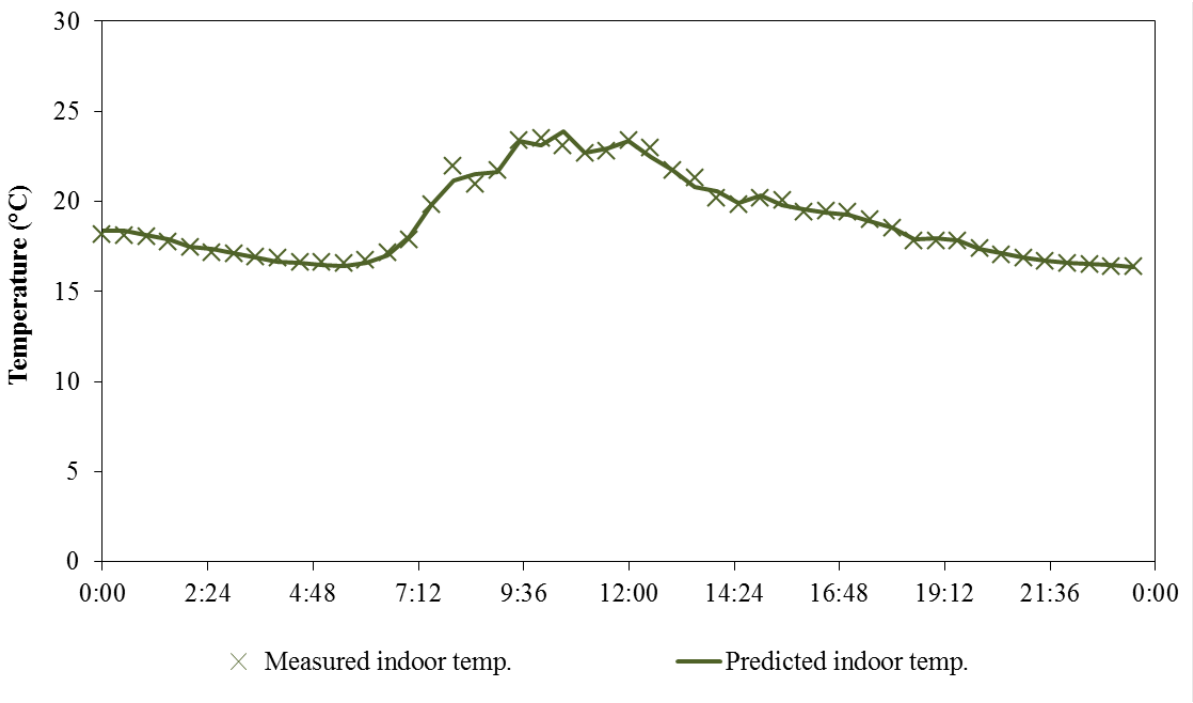

Figure 6.11: Measured and predicted indoor temperatures in summer period

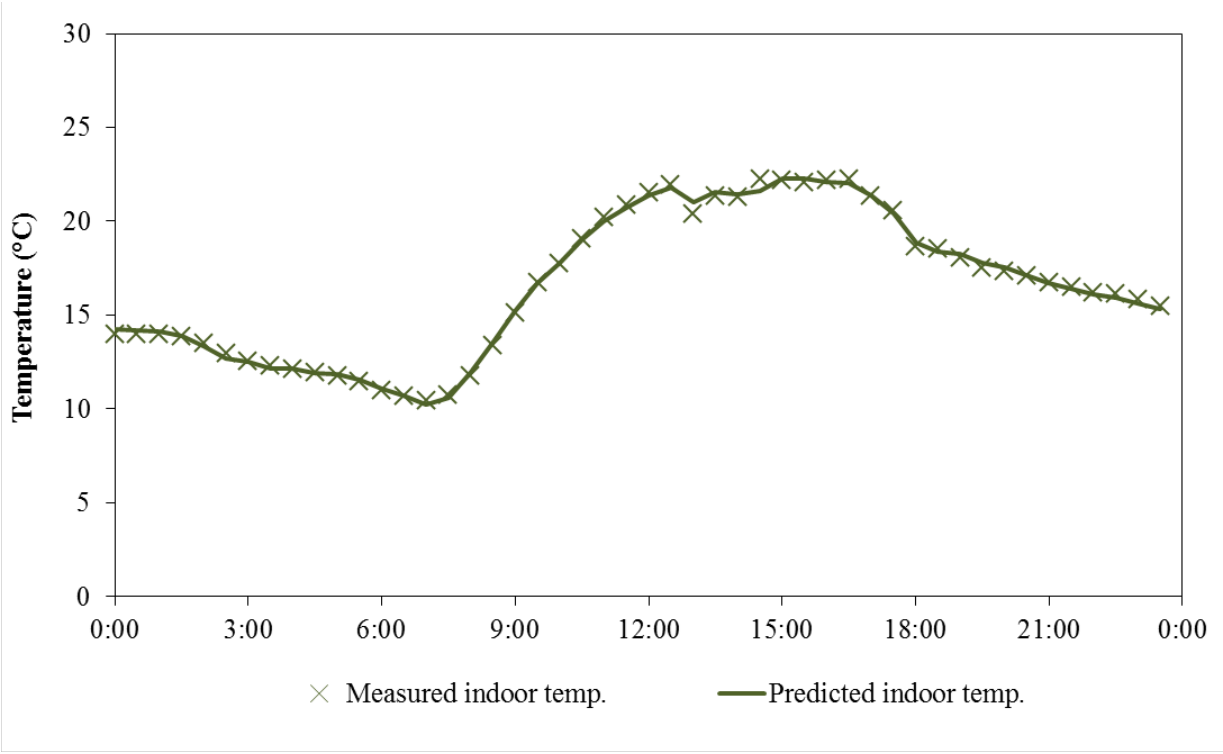

Figure 6.12: Measured and predicted indoor temperature in winter period

The relationship between the measured indoor temperature and predicted indoor temperature is shown graphically. Figure 6.13 show the relationship between the measured indoor temperature and predicted indoor temperature.

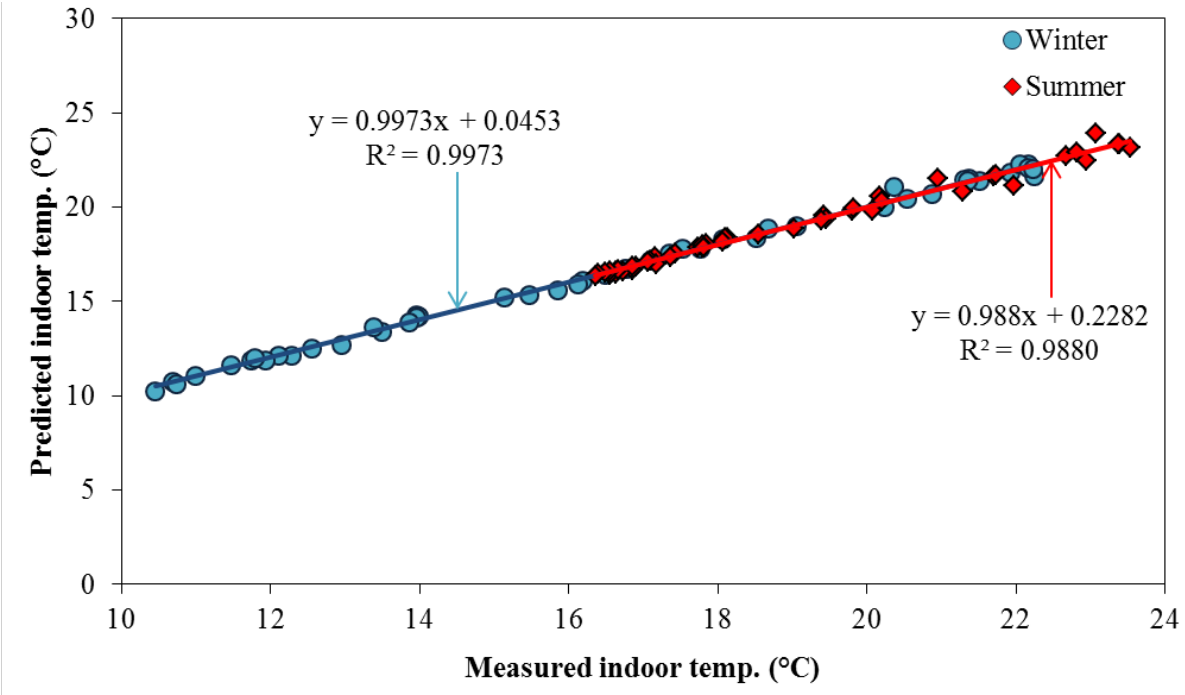

Figure 6.13: Relationship between measure and predicted indoor temperature

From Figure 6.13 in both seasons, the measured and predicted indoor temperatures show a best fit with approximately 99% of the response data set perfectly on the predicted temperature. The determination coefficients were 0.9973 and 0.9883 in summer and winter respectively. This proves that the predictors are the parameter that can serve as the basis for indoor temperature predictions for a low cost house, with the inner surface of the external wall coated with translucent water-based acrylic paint.

6.5 SUMMARY

After coating, the three external walls show significant increase in their heat resistance in both summer and winter season. This was depicted by the decrement factor and time lag of the walls. After coating, the time lags of the North wall increased by 1 hour in summer and winter. The time lag of the West and South wall increases by 1 hour and 1.5 hours walls each in summer and winter, respectively. The decrement factor of the North, West and South walls reduce by 21%, 22% and 13% in summer and 64%, 53% and 59% in winter, respectively. The thermal influence of the coated surface was also felt by the indoor temperature. Cooling degree hours (CDH) and heating degree hours (HDH) were used to determine the thermal influence of the coated surfaces on the indoor temperature. After coating, the amount of CDH and HDH required by the inner space of the house to maintain thermal comfort decreased by 42% and 46%, respectively in the winter period. In summer period, the CDH and HDH required also decreases by 58% and 36%, respectively. Finally, the house was found to save 41% of cooling energy demand and 32% of heating energy demand after coating.

From the model developed, it was found that all components of the building envelope contributed positively to the indoor temperature, in the summer. Indoor, outdoor relative humidity and winter speed contribute negatively to the indoor temperature. In the winter, it was seen that floor, and South wall contribute negatively to the indoor temperature, likewise the wind speed and indoor relative humidity. In both seasons, the measured and predicted indoor temperatures show a best fit with approximately 99% of the response data set perfectly on the predicted temperature. This proves that the predictors are the parameter that can serve as the basis for indoor temperature

predictions for a low cost house, with the inner surface of the external wall coated with translucent water-based acrylic paint.

CHAPTER 7

SUMMARY, CONCLUSIONS AND RECOMMENDATIONS

7.1 SUMMARY OF FINDINGS

The SEM image of TWAP shows that the paint is transparent to visible light. It was also revealed that coatings of TWAP greater than 127 microns (approximately 3 strokes of paint brush) results in peeling or flaking of the paint films. In the elemental composition of the paint, the EDX spectrum reveals the presence of Al; which is present as Al_2O_3. Due to the large percentage (36.41%) of Al in the paint, Al_2O_3 is considered as the major compound responsible for the thermal properties of TWAP. SiO_2 is another compound that also contributes to the thermal properties of the paint. Although, the EDX spectrum shows that Si is only 0.91% present in the paint. But the presence of Si that is also identified by the FTIR spectrum signifies that, there are considerable amount of Si in the paint. The thermography analysis reveals that, the surface coated with TWAP has high heat reduction capacity due to its smaller decrement factor compared to the other walls.

The indoor temperature was observed to be influenced by the temperature of the building envelope in both summer and winter seasons. In summer, it was observed that the indoor temperature variation closely follow the external wall temperature. Due to the large surface area (14.99 m^2) of the West wall, it was seen to influence the indoor temperature more than the North and South walls. On a typical summer hot day, the average maximum heating rate of the North, West and south walls were 5.93 W, 5,07 W and 2.24 W, respectively. It was found that the indoor temperature was mostly higher than that of the outdoor temperature, also that the indoor

temperature was within the comfort zone for only 46% of the time. The indoor relative humidity was within the comfort zone throughout the day.

In the winter season, it was found that the indoor temperature is more influenced by the middle and external walls temperature. Due to the locations of the walls, the middle-wall tends to contribute to stabilize the indoor temperature while the external walls reduce the indoor temperature. On a typical cold winter day, the average cooling rate for the North, West and South walls were found to be 0.89 W, 8.27 W and 0.30 W, respectively. The indoor and outdoor temperatures were seen completely out, below the comfort zone. On the other hand, the indoor relative humidity was found to be at the upper region of the comfort zone, ranging from 55% to 65%. It was also found that the wind speed experienced in winter was 12% higher than the maximum wind spend in the summer season.

Furthermore, during summer period before coating, it was observed that the inner space of the house requires an average of 0.59 HDH and 4.36 CDH in order to maintain thermal comfort. While in winter the inner space requires an average of 1.02 CDH and 2.74 HDH. After coating, in order to maintain thermal comfort the inner space of the house was found to require 46% HDH and 42% CDH less in winter and 58% CDH and 36% HDH less in summer. Either ways, the house was found to consume most of its energy in heating with an annual heating demand of 14.68 kWh/m^2. From the model developed, it was found that all components of the building envelope contribution positively to the indoor temperature, in the summer. Indoor, outdoor relative humidity and winter speed contributed negatively to the indoor temperature. In the winter, it found that the floor and South wall contributed negatively to the indoor temperature, as well as, the wind speed and indoor

relative humidity. In both season, the measured and predicted indoor temperatures show a best fit with approximately 99% of the response data set perfectly on the predicted temperature. This proves that the predictors are the parameter that can serve as the basis for indoor temperature predictions for a low cost house, with the inner surface of the external wall coated with translucent water-based acrylic paint.

7.2 CONTRIBUTION

The poor nature and thermal performance of the LCH has reached the attention of the department of housing and human settlement. This has led to the demolishing of several housing units over the years. The initiation of sustainable and efficient subsidy housing design by CSIR is aimed to improve thermal performance of the new LCH housing units. The major contribution of this work is the retrofitting of the already constructed housing units. The application of TWAP on the inner surface of building walls will improve thermal performance of the houses, by increasing the thermal resistance of the walls. Results from this study show that after the application of TWAP to the inner surface of a house; the house can save 40% of cooling energy and 32% of the heating energy per annum. Due to the transparent nature of TWAP in its dry state, it can be applied on an already painted wall surface and the initial appearance of the wall remains intact. Since TWAP do not rely on thickness as a function of its insulating ability, it does not reduce the inner space of the building like the traditional thermal insulation. Furthermore, it provides a healthy benefit by not harboring moisture, dust, mold, or dirt, which are some of the factors that reduce traditional thermal insulation's effectiveness over time and decrease in air quality. Most importantly, it is non-toxic (water-based) at prolong exposure neither in its dry nor wet state, and it is easy to install. In addition, the multiple linear regression models developed from the findings and results of the

thermal after coating, can be used to predict the indoor temperature of a low cost house with degree of confidence.

7.3 CONCLUSIONS

The thermal performance of the house shows significant improvement after coating with TWAP. After coating, the time lags of the North wall increased by 1 hour in summer and winter. The time lags of the West and South walls increased by 1 hour and 1.5 hours each in summer and winter, respectively. The decrement factor of the North, West and South walls reduce by 21%, 22% and 13% in summer and 64%, 53% and 59% in winter, respectively. The indoor thermal comfort also improved after coating. It was found that the cooling degree hours (CDH) which is used to estimate the amount of cooling hours required for the inner space of the house to maintain thermal comfort in warm season, decreases by 58% in summer. On the other hand, the heating degree hours (HDH) which is used to estimate the amount of heating hours required for the inner space of the house to maintain thermal comfort in cold season, decreases by 46%. After coating, the house was found to save 41% of cooling energy demand and 34% of heating energy demand per annual. From all investigations, translucent water-based acrylic paint was proven to have the insulating abilities of the convention insulation material and can be used to improve the thermal performance of a LCH.

7.4 RECOMMENDATIONS

Having evaluated the thermal influence of the building envelope (walls, roof and floor) on the indoor temperature at different seasons; a further investigation to determine the influence of

infiltration and exfiltration is necessary. This will give the thermal performance profile of the house with higher degree of confidence. These factors (infiltration and exfiltration) are responsible for the exchange of air between the inner and outer space of the building. The building inner space also gains and loses heat during the process of air exchange, resulting in the increase and decrease of the indoor temperature. This investigation (infiltration and exfiltration) will also account for heat transfer through the doors and windows.

REFERENCES

Alison, G., Nicholas, B. and Rajkovich (2010) *Addressing Climate Change in Comfort Standards*, Building and Environment; pp. 18–22

Al-Jabri, K. S., Hago, A. W., Al-Nuaimi, A. S., & Al Saidy A. H. (2004) *Concrete blocks for thermal insulation in hot climat*e, Cement and Concrete Research, Vol. 35, August, p. 1473

Agrement South Africa, (2002) *Assessment criteria: Building and walling system; Acoustics performance of buildings*, http://www.agrement.co.za/

Anapolskaya, L. E., and Gandin, L. S. (1990) *Environmental Factors in the heating of Buildings*, Keter publishing house Jerusalem Ltd, p. 113

ANSI/ASHRAE Standard 55. (2004) *Thermal Environmental Conditions for Human Occupancy*: ASHRAE, Atlanta

Asan, H. (2005) *Numerical Computation of Time Lags and Decrement Factors for Different Building Materials*, Trabzon, Turkey, February, p. 616

ASHRAE (1997) *Fundamentals Handbook: Nonresidential Cooling and Heating Load Calculations,* Atlanta, USA, pp. 28.5 – 28.7

Assawamartbunlue, K. (2013) *An Investigation of Cooling and Heating Degree-Hours in Thailand*, Journal of Clean Energy, Vol. 1, December, p.88

Avedelidis, N. P., and Moropoulau, A. (2002) *Emissivity Considerations in Building Thermography*, Athens, Greece, October, p. 663

Balaras, C. A., and Agrgiriou, A. A. (2002) *Infrared Thermography for Building Diagnostics*, Hellas, Greece, p. 172

Bagavathiappan, S. Lahiri, B., Saravanan, T., Philip, J. & Jayakumar, T. (2013) *Infrared Thermography for Condition Monitoring*, Tamil Nadu, India, March, p 38

Berdahl, P. H., (1996) *Pigments Which Reflect infrared Radiation from Fire*; University of California, Oakland. September, p7

Bolatturk, A., (2007) *Optimum Insulation Thicknesses for Building Walls with Respect to Cooling and Heating Degree-Hours in the Warmest Zone of Turkey*, Suleyman Demirel University, Turkey, February, p.1056

Brandemuehl, M. (2005) *Predicting Thermal Comfort*, AREN 3050 Environmental Systems for Buildings

Budaiwi, I. and Abdou, A. (2013) *The Impact of Thermal Conductivity Change of moist Fibrous Insulation on Energy performance of building under Hot-Humid Conditions*, January, p. 2

Butera, F. M (1998) *Principles of thermal comfort*, Renewable and Sustainable Energy Reviews, p. 45 – 49

Cengel, Y. A., and Boles, M. A. (1994) *Thermodynamics: An engineering approach*, 2nd edition, McGraw-Hill, Inc.

Clark, D. T. (2002) *X-Ploymers-D-Paints and Pigments;* NZ Institute of chemistry. July, pp. 10 – 15

Crolley, F. (2012) *Sustainable Buildings: New Solutions to increase100po energy efficiency in buildings*, March, p. 6

Day, T. (2006) *Degree-Days: Theory and Application*, Chartered Institution of Building Services Engineers (CIBS), London, UK, September

Datcu, S., Ibos L., Candau, Y. & Mattei, S. (2005) *Improvement of Building Wall Surface Temperature Measurements by Infrared Thermography*, France, March, p. 425

De Dear, R. (2004) RP-884 Project. Available from: http://aws.mq.edu.au/rp-884/ashrae_rp884_home.html

De Dear, R. (2007) *Adaptive Comfort Applications in Australia and Impacts on Building Energy Consumption*: Proceedings Of The 6th International Conference on Indoor Air Quality, Ventilation and Energy Conservation In Buildings (IAQVEC), Sendai, Japan, October, pp. 28 – 31

Dilavore, P. (1984) *Energy: Insight from Physics*, Canada: John Wiley & son, Inc

Djongyang, N. Tchinda, R. and Njomo, D. (2010) *Thermal Comfort: A Review Paper*, July, pp. 2627

Downton, P., Milne, G., McGee, C. & Reardon, C. (2010) *Your Home: Australia's Guide to Environmentally Sustainable Homes*, Sydney: Dept. of the Environment, water, Heritage and the Art

Duffie, J. A. and Beckman, W. A. (2006) *Solar Engineering of Thermal processes*, 3rd edition, John wiley & Sons, Inc

Ecotect, (2012) Viewed 13 September 2012 at www.ecotect.com

Ecotect WIKI, (2012) *Degree Days*, Viewed 13 September 2012 at http://squ1.org/wiki/

Ensminger, R. I. (1988) *Pigment Handbook*; Volume II, Edited by Temple C. Patton and John Wiley

Esds, L. G., Epperly, R. A. & Snell, J. R. (2000) *Thermography*, ASHRAE Journal 42, p. 55

Fanger, P. O. (1972) Thermal comfort Analysis and applications in environmental engineering, McGraw-Hill, New York, USA

Feist, P. (2002) *Infrared Spectroscopy*: Theory, Colorado, USA, July, p.157

Freire, R. C., Oliveira, G. H. & Mendes, N. (2007) *Predictive Controllers for Thermal Comfort Optimization and Energy Savings*, Curitiba, PR, Brazil, March, p.1354

Giancoli, D., C. (1998) *Physics, Principle with Applications*, 5th Edition, New Jersey: Prentice Hall, 276

Goldstein, J. I., Newbury, D. E., Echlin, P., Joy D.C., Fiori, C. and Lifshin E. (1981) *'Scanning Electron Microscopy and X-Ray Microanalysis: A Text for Biologists, Materials Scientists, & Geologists*, New York: Plenum Press

Gregory, K., Moghtaderi, B., Sugo, H. and Page, A. (2007) *Effect of Thermal mass on The Thermal Performance of Various Australian Constructions Systems*, April, p. 459-3

Halawaa, E. and Hoof, J. (2012) *The Adaptive Approach to Thermal Comfort: A Critical Overview*, Eindhoven, Netherlands, April

Hanlan, J. (1975) *The Scanning Electron Microscope and Microprobe: Application to Conservation and Historical Research*, Venedig: ICOM, 4th Triennal Meeting

Hart, J. M. (1991) *A practical guide to infra-red thermography for building surveys*, Garston, Watford, BRE

Hass, D., Prasad, B., Glass, E., and Wiedemann, E. (1997) *Reflective Coating on Fibrous Insulation for Reduced Heat Transfer*, NASA Contractor report, August, pp 4-5

Hinrichs, R. and Kleinbach, M. (2006) *Energy: Its Use and the Environment*, New York: Interactive Composition Corporation

Holm, et al (2008) *Assessment on the Impact of Retrofitted Insulation Technology on the Quality of Life of Low-income households*: Nova Institute, Pretoria

International Energy Agency (IEA), *(2011) Key World Energy: STATISTICS*, Paris

ISO 7730 (1984) *Moderate thermal environments: Determination of the PMV and PPD indices and Specifications of the conditions of thermal comfort*, International Standard, Switzerland

ISO 7730 (2005) *Ergonomics of the Thermal Environment: Analytical Determination and Interpretation of Thermal Comfort Using Calculation of the PMV and PPD Indices and Local Thermal Comfort Criteria*, International Standard, Switzerland

Kaszowskaa, Z., Malekb K., Panczyk M., and Mikołajskaa A. (2012) *A Joint Application of ATR-FTIR and SEM Imaging With High Spatial Resolution: Identification and Distribution of Painting Materials and Their Degradation Products in Paint Cross Sections*, Warszama, Poland, December, p.1

Kaynakli, and Kilic (2004) *Investigation of indoor thermal comfort under transient conditions*, Uludag University, TR-16059 Bursa, Turkey, May

Klunne, W. E. (2002) *Energy efficient housing to benefit South African households*, November, p. 27

Klunne, W. E. (2003) *Energy use for space heating in RDP houses*, January, p. 3

Knight, R. (2004) *A Decade of Democracy: Housing Services and Land in South Africa*, http://www.richardkinght.homestead. com/files/sihousing2004.htm

Kumar, A and Suman, B. M. (2012) *Experimental Evaluation of Insulations Materials for Walls and Roofs and Their Impact on Indoor Thermal Comfort Under Composite Climate*, September, p. 635

Lawrence, M. G., (2004) *The Relationship Between Relative Humidity and Dewpoint Temperature In Moist Air: A Simple Conversion and Application*, Mainz, Germany, July, pp.225–226

Leaman, A., Thomas, L. and Vandenberg, M. (2007) *Green Buildings: What Australian Users are Saying*? EcoLibrium, pp.22 – 30

Lin, Z. and Deng, S. (2008) *A Study on the Thermal Comfort in Sleeping Environments in the Subtropics: Developing a Thermal Comfort Model for Sleeping Environments*, Building and Environment, pp.70 – 80

Makaka, G. and Meyer E. (2006) *PhD Thesis*, University of Fort Hare

Maldague, X. (1993) *Nondestructive Evaluation of Materials by Infrared Thermography*, Springer-Verlag, Berlin

Mantler, M., Schrener, M. and Schweizer, F. (2000) *XRD in the Museum: Industrial Application of X-Ray Diffraction*, New York, Basel: Dekker, 621-658

Markov, D., (2006), *Practical Evaluation of Thermal Comfort Parameters*, Technical University of Sofia, Bulgaria

MIKRON (2006) *Mikroscan 7600PRO Operator's Manual: Principle of Thermal Imaging*, p. 275

Mlakar, J. and Strancar, J. (2012) *Temperature and Humidity Profile in Passive-house Building Blocks*, August, p. 185

Nansulate (2011) *Home protect Clear coat*, Data Sheet, January, p. 2

NEC San-EI Instruments, Ltd (1991) *TH1 101 thermo tracer*, Operation Manual, Japan

Nicol, J. F., and Humphreys, M. A. (2002) *Adaptive Thermal Comfort and Sustainable Thermal Standards for Buildings*, Energy and Buildings p. 563–572

Ozel, M. (2011) *Effect of wall orientation on the optimum insulation thickness by using a dynamic method*, p. 2429

Razumovskiy L. (2007) *Infrared Spectroscopy*, Medallion labs, May, p.1

Robnik-Sikonja, M., and Kononenko, I. (1997). *An adaptation of Relief for attribute estimation in regression*. Retrieved from CiteSeerX: http://citeseerx.ist.psu.edu/viewdoc/summary

Robnik-Sikonja, M., and Kononenko, I. (2003). *Theoretical and empirical analysis of ReliefF and RReliefF*. Machine Learning, 53, 23–69

Smith, D. (2004) '*AMP 16/32 Rely Multiplexer: Campbell Scientific Instruction Manual*, P. 1

Settle, A. F. (1997) *Handbook of Instrumental Techniques for Analytical Chemistry*: Mallinckrodt Baker Division

Thermal Insulation Association of South Africa (TIASA), (2010) *Thermal insulation-the invisible energy saver: The Guide to Energy Efficient Thermal Insulation Buildings*, Midrand: AAAMSA administered

Victoria (2005) *Sustainable Energy: Thermal Mass, Info sheet*, Victoria, Australia

Yao R, Li B, and Liu, J. A (2009) *Theoretical Adaptive Model of Thermal Comfort Adaptive Predicted Mean Vote (PMV)*. Building and Environment; pp. 2089 – 2096

Wan, J., W, Yang, K, Zhang, W., J., and Zhang, J., L. (2008) *A New Method of Determination of Indoor Temperature and Relative Humidity with Consideration of Human Thermal Comfort*, Guangzhou University, China, March, p. 412

Weismantel, G. E., ed. (1981) *The Paint Handbook*, McGraw Hill, Ohio, USA

Wolkoff, P. and Kjaergaard, S (2007) *The Dichotomy of relative Humidity on Indoor Air Quanlity*, May, p. 851-7

Zhang, Y., Barber A., and Smith Ray (2012) *The Depth Profiling of Tio_2 Pigment Coil Coatings Using Step Scan Phase Modulation Photoacoustic FTIR*, University of London, UK, September, p.131

APPENDIX A

DATA LOGGER PROGRAM

Wiring of sensors on the CR1000 data logger

HMP50 Temperature & Relative Humidity Sensor (1)

Ground: Blue

3H: Black

3L: White

G: Clear

12V: Brown

HMP50 Temperature & Relative Humidity Sensor (2)

Ground: Blue
4H: Black
4L: White
G: Clear
12V: Brown

LI200S Pyranometer

5H: Red

5L: Black

5L: Jumper to Ground

Ground: Jumper to 5L

G: Clear

03001 Wind Speed & Direction Sensor

Ground: Vane, White

EX1: Vane, Black

P1: Anemometer, Black

6H: Vane, Red

G: Anemometer, White

G: Anemometer, Clear

G: Vane, Clear

AM16/32 Multiplexer (2x32 mode)

7H: COM ODD H

7L: COM ODD L

G: Gnd

G: COM Ground

12V: 12V

C1: Res

C2: Clk

Wiring for AM16/32 Multiplexer (2x32 mode)-

Type K (chromel-alumel) Thermocouple (1)

1H: Yellow

1L: Red

Type K (chromel-alumel) Thermocouple (2)

2H: Yellow

2L: Red

Type K (chromel-alumel) Thermocouple (3)

3H: Yellow

3L: Red

Type K (chromel-alumel) Thermocouple (4)

4H: Yellow

4L: Red

Type K (chromel-alumel) Thermocouple (5)

5H: Yellow

5L: Red

Type K (chromel-alumel) Thermocouple (6)

6H: Yellow

6L: Red

Type K (chromel-alumel) Thermocouple (7)

7H: Yellow

7L: Red

Type K (chromel-alumel) Thermocouple (8)

8H: Yellow

8L: Red

Type K (chromel-alumel) Thermocouple (9)

9H: Yellow

9L: Red

Type K (chromel-alumel) Thermocouple (10)

10H: Yellow

10L: Red

Type K (chromel-alumel) Thermocouple (11)

11H: Yellow

11L: Red

Type K (chromel-alumel) Thermocouple (12)

12H: Yellow

12L: Red

Type K (chromel-alumel) Thermocouple (13)

13H: Yellow

13L: Red

APPENDIX B

RESEARCH OUTPUTS

B1. NATIONAL CONFERENCE

Overen O., K. Meyer, E. L., and Makaka, G., (July 2012) “Energy conservation in low cost house (LCH) in South Africa: thermal performance baseline”,SAIP Conference, Pretoria, South Africa.

B2. GENERAL PRESENTATIONS

Overen, O. K., Meyer, E. L., Makaka, G. and Ziuku, S. (September 2012) “Energy efficiency housing” Student mini conference, University of Fort Hare.